Interim Report No. 3

INTERNATIONAL COOPERATIVE RESEARCH PROGRAM ON TOOL WEAR

(Results on Carbide Tool Wear, Surface Finish, Built-Up-Edge, and Finish Machining)

L. V. Colwell, L. J. Quackenbush, J. C. Mazur, and J. M. Hardy

ABSTRACT

This is the third in a series of four reports scheduled for this contract. The first two (Interim Reports Nos. 1 and 2) presented the outline and objectives of the entire program along with detailed information on the properties of the tool materials and the XC45 work material (1045 steel).

This report presents the results of the cooperative program on the wear of European grades of sintered carbide tools in machining the controlled work material. An encouraging degree of agreement was found between the results of the nine participating laboratories located in eight different countries. Undoubtedly some causes for dispersion other than the workpiece and tool materials will be identified in later phases of the International Cooperative Program. Some results obtained at The University of Michigan for the later stages of tool wear point to the possibility that machine tool rigidity may be an influential factor. This and other identifiable factors will ultimately be investigated to greater depth in later phases of the CIRP/OECD program. The results to date are to be considered as essentially a progress report with final interpretation being withheld until the validity of results across international boundaries can be established within predictable probability limits as in "atomic weights" and similar physicochemical properties.

In addition to the results on wear of carbide tools, the report includes the extra work done by the University of Delft on the repeatability of wear measurements between laboratories and special studies on surface finish, built-up-edge, and finish machining. Initial results of a special study at Chalmers University on the plasticity of the work material also are presented.

TABLE OF CONTENTS

PART I

WEAR ON EUROPEAN CARBIDES IN MACHINING XC45 STEEL

The carbide tool portion of Phase 1 of the tool wear program with European carbides is completed. Progress reports on the work which began in 1963 have been issued by Professor Opitz from the Technical University of Aachen in Germany. The University of Michigan, the latest institution to join the program through the medium of this contract has also carried out tests on the European carbides. The results have been combined with those of the other participating countries to provide the first section or part of this report. The University of Michigan has also carried out some initial work on the XC45 steel with American carbide tools as a preliminary to a longer term program whose objective is to develop a workable "tie-in" between American grades of tools and work materials with those of the CIRP/OECD program. The latter results will be included in the last report of this series.

The following information on the wear of carbide tools is divided into two parts; the first part on "Typical Supporting Information" and the second on "Summary of Tool Wear Results." The total volume of information precludes presenting all of the supporting information in single report. Therefore, only some typical supporting information like that suggested in Interim Report No. 1 is included at this point to illustrate the basis for the final results given in the summary.

For the most part the supporting information is abstracted from a working report issued by the Technical University of Aachen in June, 1963. The summary of results includes all of the quantitative correlations derived from the main program. It includes the results obtained recently by The University of Michigan and those from the other participating laboratories as summarized in the report issued by Professor Opitz on December 23, 1964. Most of the quantitative information in Figs. 1-1 through 1-45 has been presented in the units of both the metric and English system for the convenience of those readers not normally accustomed to both and to encourage the development of greater familiarity with both systems.

TYPICAL SUPPORTING INFORMATION

Examples of the supporting information upon which the summary results are based are illustrated in Figs. 1-1 through 1-13. The first three of these are concerned directly with the wear criteria upon which tool life determinations are based. The second group of three deal with chip foreshortening known more commonly in the USA as cutting ratio. The remainder of the figures are concerned with the different tool life results arising out of the two heats of steel used for the Main Program.

Wear Criteria (Figs. 1-1 - 1-3)

Figure 1-1 shows a double logarithmic plot of flank wear as a function of elapsed cutting time. The test protocol suggests that limiting values of either 0.2 mm (.008 in.) or 0.4 mm (0.016 in.) be used as the end of useful tool life. It will be noted however that the large asterisks in four of the five tests included in this figure indicate that the tool was rendered unusable before a flank wear of 0.4 mm was reached; consequently the lower value must be used in this case.

All of the tests except for the highest speed show the familiar bend or "dog leg." The precise cause of this is not known as yet but it is suspected that it is related to the observation by Trigger and others that tool flank temperature actually decreases initially until a certain critical amount of wear is reached after which it increases. This would seem to be consistent with the observation that the bend occurs at lower values of wear at lower cutting speeds since a slower moving workpiece could sustain the same temperature on a smaller worn area. The fact that the rate of wear is more rapid after the bend could be due to the onset of diffusion as a wear mechanism on the flank. Takeyama in Japan suggested this several years ago.

Figure 1-2 is a Cartesian plot of crater depth versus elapsed cutting time. It is not used directly as a wear criterion. Instead it is used in combination with the distance from the cutting edge to the deepest point of the crater. This forms a dimensionless ratio such as that shown plotted on double logarithmic coordinates in Fig. 1-3 and permits using the same ratio as a criterion of failure for a large range of feed rates. Figure 1-2 is included only to illustrate the orderliness of crater depth as a wear parameter.

Figure 1-3 shows that the crater ratio (ratio of depth to distance of the deepest point from the cutting edge) also gives an orderly or consistent plot. These lines also exhibit a tendency to bend but the point of the bend appears to occur at a later time than the corresponding bend for flank wear. However, it is quite probable that the two are related through temperature although much further research on temperature phenomena and distribution will be needed before this can be established.

The test protocol suggests that a limiting crater ratio of either 0.1 or 0.2 be used as a criterion for determining the end of useful tool life. It can be seen that the larger of these values was nearly reached in all tests which was not true for the flank wear. Which criterion should be used obviously depends upon proximity to catastrophic failure and its significance to the job being done. More important, however, to the machinability of the work materials and the cutting ability of the tools is the shape which these two criteria give to the tool life curve. This is discussed later in connection with Figs. 1-7 through 1-13.

Cutting Ratio or Chip Foreshortening (Figs. 1-4 - 1-6)

This quantity is a sensitive measure of the friction between the chip and the cutting tool. By definition it is the ratio of the length of the chip to the length of the cut. As a measure of friction it is an average of a quantity which varies rapidly with time especially in the lower ranges of cutting speed. Furthermore, it is difficult and time consuming to measure accurately.

The three different methods suggested in the test protocol for measuring cutting ratio are compared in Fig. 1-4 for Test No. 2.1b. It is clear that even the average values vary by as much as 10% between the extremes. Consequently, it should not be surprising that cutting ratio has not provided any useful guide for predicting tool life differences in relation to cutting speed and work material. This is evident in Figs. 1-5 and 1-6 where typical values determined by the density method are plotted for a range of cutting speeds on both heats of the XC45 steel.

Despite the erratic nature of cutting ratio data it nevertheless indicates important trends. It will be noted that except for the one short test all of the data in Figs. 1-4 through 1-6 show an undeniable trend toward lower cutting ratios and higher friction at the longer tool lives. This means not only that frictional energy is higher but also that the shear-strain energy per unit volume has increased. Consequently, the power component of cutting force also must have increased despite the increases in crater depth.

It could be useful in future research to make an exhaustive analysis of the changes in at least eight quantities as the tool wears. These are

(1) flank wear,
(2) crater wear,
(3) cutting forces,
(4) cutting temperatures,
(5) cutting ratio,
(6) shape of the chip cross-section,
(7) shape of the crater, and
(8) degree and frequency of chip segmentation.

There is a pronounced lack of information of this type which could guide metallurgists in developing better tool materials for unique combinations of workpiece composition and microstructure.

Tool Life Plots (Figs. 1-7 - 1-13)

Typical tool life, cutting speed plots are shown inFigs. 1-7 through 1-13. These give a comparison of the two different wear criteria and different ways of representing them. They also emphasize the influence of the slight differences between the two heats of the program steel.

Figure 1-7 is a tool life plot based upon total tool travel rather than cutting time. The ordinate is the tool travel or rubbing distance. The volume of metal removed is simply the product of this distance and the cross-sectional area of the chip. When tool life is plotted in time units the amount of metal removed is the product of the time and the rate of removal which involves the cutting speed.

Figure 1-7 shows that using flank wear as the criterion for the end of useful tool life results in a straight line on the double logarithmic coordinates whereas the crater ratio produces an elliptically shaped curve. This is rather typical although flank wear also may show a tendency to curve in the same direction in the lower speed range.

It will be recalled from Fig. 1-1 that flank wear could be tolerated beyond the 0.2 mm limit at all but the highest test speeds. Consequently, the two criteria would have given more nearly the same result had the limiting flank wear been fixed at 0.3 or 0.25 mm. This phenomenon varies, however, with the different combinations of tool and work materials so that realistic limiting values cannot be based on a single combination.

The most important feature shown in Fig. 1-7 is the difference in shape of the two lines. This difference means that some cutting conditions will encounter catastrophic failure due to crater wear while others will be due to flank wear. This is the principal reason for different grades of carbide tools. The sensitivity of these parameters to cutting speed, size of cut, and tool geometry is not understood adequately at this time and will require a substantial amount of further study.

Figure 1-8 also is a plot of total tool travel versus cutting speed. Two curves each representing limiting crater wear as the criterian of tool life show the results for both heats of the OECD program steel. Heat No. Z0656 permits somewhat higher cutting speeds than the other heat when compared through this criterian. It is also notable that both lines are distinctly curved compared to the straight line shown for flank wear in Fig. 1-7.

Figures 1-9 through 1-13 are the familiar double logarithmic plots of tool life versus cutting speed. Figure 1-9 gives a comparison of the tool-life characteristics of both heats of the program steel based on a limiting flank wear of 0.2 mm. It is interesting that there is no significant difference between these two heats based on this criterian but there is an appreciable difference between them when the crater wear characteristics are compared as shown in Fig. 1-8. Figure 1-10 is a replot of the same data as Fig. 1-8 but with the tool life being expressed in minutes rather than in terms of the total rubbing distance. It will be noted that the curvature is not as evident in Fig. 1-10.

Figure 1-11 and 1-12 show a comparison of the tool life curves for the work material in the inner zone of the test bars versus that in the outer zone. Figure 1-11 makes a comparison for heat No. Z0656 based upon flank wear of 0.2 mm as a criterion. On the other hand Fig. 1-12 gives a similar comparison for heat No. Z0648 based on a crater ratio of 0.2. It will be noted that in both instances the work material in the outer zones of both heats permits higher cutting speed for the same tool life although it will be noted in Fig. 1-11 that the difference tended to disappear for a tool life of about one hour.

It was pointed out earlier in this section that differences in tool life depending upon whether one selects flank wear or crater wear as the limiting criterion is somewhat arbitrary depending upon the limiting values selected in each case. This is emphasized in Fig. 1-13 where two sets of tool-life lines are shown for heat No. Z0656. The set representing the higher cutting speeds and longer tool lives is based respectively upon a flank wear of 0.3 mm and a crater ratio of 0.2. The other set at lower cutting speed is based on flank wear of 0.2 mm and a crater ratio of 0.1. It will be noted in both cases that the results are nearly equal but that the crater wear becomes dominant at higher cutting speeds. Appropriate values of both of these criteria differ between work materials and vary with the type of operation. Consequently, it is inadvisable to specify any one set of limiting values as being best without much further information of this same type.

SUMMARY OF TOOL WEAR RESULTS (Figs. 1-14 - 1-45)

The results of both the Standard and Main Tool Wear Programs are summarized in Figs. 1-14 through 1-45. All test conditions are identified by test numbers shown in the figures with the corresponding test conditions described in detail in Tables II and III of Interim Report No. 1. Most of the tests in this Phase 1 program were carried out with the P30 tool material since the cutting speeds were not as high as those for the P10 material and therefore required less steel for carrying out the tests.

The first four figures give a summary comparison of the two different grades of tool materials. The next 22 figures give a more detailed analysis of the influence of tool geometry and other parameters. The next two figures (1-40 and 1-41) give an overall summary of the influence of chip breakers. The last four figures give a direct comparison of the results from the Standard Program which was carried out at the same test conditions by most of the participating laboratories. Obviously not all of the test conditions for the Standard Program were identical since the machine tools themselves were not measurable quantities.

Summary Comparison of Carbide Grades P10 and P30 (Figs. 1-14 through 1-17)

Figures 1-14 and 1-15 compare the two different grades of tool material over a range of side-cutting-edge angles. The numbers appearing on the abcissas of these two figures are in reality the setting angles as they are now defined by the ASA standard. These are also setting angles in the ISO standard used commonly in Europe. Consequently an angle of 90° as it appears in these figures corresponds to a zero side-cutting edge-angle in the ASA system while an angle of 50° corresponds to a side-cutting-edge angle of 40° in the same system.

It will be noted that when tool life is based on limiting flank wear the cutting speed for the grade P10 carbide is at least 60% higher than that for the grade P30 carbide. On the other hand when tool life is based on the crater ratio as shown in Fig. 1-15 the cutting speed for the same tool life appears to be nearly 100% higher. Thus it can be seen why economics dictated the study of most of the variables with the grade P30 tool material.

Figures 1-16 and 1-17 summarize the influence of feed rate upon the cutting speeds for 30- and 60-minute tool lives based respectively upon flank wear (Fig. 1-16) and crater ratio (Fig. 1-17). It will be noted from this summary that the percentage relationships of the cutting speeds for the two different tool materials are not as pronounced at the heavier feed rates.

Effect of Rake Angle

The effect of rake angle for both tool materials used for a variety of cutting conditions is summarized in Figs. 1-18 through 1-27. The rake angle, designated in these figures by the Greek letter gamma, is also properly described as the normal rake angle. This means that the rake angle is the inclination or slope away from the cutting edge. This does not correspond to either of the two terms or values used to express rake angles in the American standard. On the other hand it is being considered for a new American standard as well as for a uniform international standard. This practice has also been used in the United States since the mechanically clamped carbide tool tips became common. Consequently, it seemed proper to report the results of this study in units of "normal rake angle."

Results for the P30 carbide are summarized in Figs. 1-18 through 1-21 while those for the P10 grade are summarized in Figs. 1-22 through 1-27. The first two figures show the amount of flank wear after specified periods of cutting time at each of two cutting speeds. It will be noted that the amount of flank wear decreases with an increase of rake angle from -6° to about +6° after which it rises again rather rapidly. Similar information for three different cutting speeds is shown for a cutting time of 20 min in Fig. 1-20. Here again it will be noted that a positive normal rake of 6° appears to give an optimum or minimum of wear.

A similar comparison based on the cutting speed for a 30-min tool life is shown in Fig. 1-21. Here the results shown in the upper portion are based on a limiting flank wear of 0.2 mm whereas those shown in the lower portion are based on a crater ratio of 0.1. Again the results based on limiting flank wear seem to indicate that a normal rake angle of +6° is best not only for a feed rate of 0.010 ipr but probably also for a feed twice as great. On the other hand the cutting speeds based on limiting crater ratio as shown in the lower portion of Fig. 1-21 are not as sensitive to normal rake angle and in fact appear to favor a negative angle of -6°.

Obviously in the presence of such contradictory guide lines more research needs to be done not only to provide a broader base for making proper selections but also for determining the causes. A similar trend is shown later for the grade P10 carbide.

Flank wear information for the grade P10 carbide is shown for two normal rake angles in Figs. 1-22 and 1-23. These results show the same general trend as those for P30 tool material in the range from -6 to +6° of normal rake angle but unfortunately do not show corresponding information for the rake angle of +10°. On the other hand flank wear data for the P10 tool material run with chip breakers does show a tendency for an optimum to occur at +6° as shown in Figs. 1-24 and 1-25. Chip breakers were not used for the test results reported in Figs. 1-22 and 1-23.

Figures 1-26 and 1-27 once more demonstrate an opposite trend with regard to optimum or best normal rake angle depending upon whether flank wear or crater wear is used as the criteria for the end of useful tool life. As suggested earlier in this report this type of evidence justifies further study of these phenomena with the analysis being extended to include at least cutting temperature distribution, development of the crater profile, and changes in the shape of the cross section of the chips with all of these criteria being analyzed and documented during the entire useful life of the cutting tools.

Effect of Setting Angle (Side-Cutting-Edge Angle)

The influence of side-cutting-edge angle or setting angle of the side-cutting edge is summarized for the grade P30 tool material in Fig. 1-28. The cutting speeds for a 30-min tool life based both on limiting flank wear and crater ratio are plotted respectively in the upper and lower portions of the figure. It will be noted in the upper portion that increases of the side-cutting-edge angle from 0 (90° setting angle) permits higher and higher cutting speeds. On the other hand when the tool life is based on the crater ratio an increase in the side-cutting-edge angle first causes a reduction in cutting speed followed by an increase beyond the level which is valid for the 0 side cutting-edge angle. These conditions appear to be true for all three feed rates represented in the test conditions reported in this figure.

Consequently the analysis permitted by the results reported in the Fig. 1-29 are also interesting. Here the side-cutting-edge angle was held constant at 20° (70° setting angle) as the rake angle was changed. In the upper portion of the figure representing results based on limiting flank wear a rake angle of +6° was best while -6° was poorest. On the other hand the data in the lower portion of the figure based on crater ratio as a tool life criterion show a rake angle of -6° as best and 0° as poorest. The latter data appeared to be somewhat erratic although when one recalls that these are the averages from more than one laboratory there must be some consistent causes that are not yet understood. Detailed supporting information for Figs. 1-28 and 1-29 are shown cross plotted in Figs. 1-30 through 1-38.

Similar information for the grade P10 tool material at a constant feed rate of 0.010 ipr is summarized in Fig. 1-39. These results are for only one feed rate but they show the same tendencies as were revealed for the grade P30 tool material so it may be concluded tentatively that the same unknown factors are operative here as well.

Effect of Chip Breakers

Several of the tests in the cooperative program were made with chip breakers and the results are reported in several places elsewhere in this report. However the group of similar tests made both with and without chip breakers are summarized here in Figs. 1-40 and 1-41. Those in the first figure compare the cutting speed for 30-min tool life based upon a limiting flank wear of 0.2 mm whereas those in the second figure present similar information based upon a limiting crater ratio of 0.1. In all cases that were directly comparable those tests made with a chip breaker resulted in speeds at least equal to or slightly higher than for those tests made without a chip breaker.

The chip breaker settings were as specified in Table IV of Interim Report No. 1 and presumably all of the results are valid only for these settings. Consequently there remains a question as to the influence of the chip breaker setting itself. It probably exerts some influence analogous to that of the rake angle and the side-cutting-edge angle.

Comparison of Results Between Participating Laboratories

All of the laboratories who participated in the cooperative program carried out tests in both the Standard and the Main Programs as outlined in Tables II and III of Interim Report No. 1. Only those tests in the Standard Program were common to all laboratories. The results are summarized in Figs. 1-42 through 1-45. Only the cutting-speed, tool-life results based on limiting flank wear and limiting crater ratio are plotted in these figures. Some of the test points are the result of extrapolation and are so indicated by being contained within parentheses.

The results for the grade P30 carbide are shown first in Figs. 1-42 and 1-43. The first of these is based upon limiting flank wear equal to 0.2 mm while the second is based upon a crater ratio of 0.1. There is a scatter of the order of two to one in most of the data but this is considerably better than that for the high-speed steel where the scatter was from 10 to 20 times as great. Straight lines have been drawn through the data in both of these figures although the original line submitted in the working report for Fig. 1-43 was drawn curved concave toward the left in the figure or in other words with a bulge toward higher speeds in the tool-life range of 20 to 50 min.

Similar information for the grade P10 carbide is shown in Figs. 1-44 and 1-45. The cutting-speed, tool-life line shown in Fig. 1-44 is based on limiting crater wear and gave the most consistent results with relatively little scatter. On the other hand similar information based on limiting flank wear of 0.2 mm resulted in the greatest scatter as shown in Fig. 1-45. Here the range is appreciably more than 2 to 1 but yet substantially better than the corresponding information obtained for high-speed steel.

The tool-life results obtained at The University of Michigan and based upon crater ratio compared very favorably with those obtained from other laboratories. On the other hand the results based upon flank wear were generally somewhat poorer especially with the grade P10 carbide as shown in Fig. 1-45. The lathe used for these tests was the only one in participating laboratories mounted upon vibration isolators. This was suspected as a possible cause along with the shuck mounting and the live center in the tail stock. Attempts at changing the shuck mounting conditions and the tail stock center produced some improvement but not in any consistent pattern. Therefore, it might be concluded tentatively that loss of torsional rigidity through the lathe not being fastened to the floor is a contributing factor to a faster rate of flank wear.

CONCLUSIONS

The following conclusions are those of the authors of this report and not necessarily those of the CIRP/OECD committee.

1. It is possible to obtain reasonable agreement across international boundaries as to the machining characteristics of tools and work materials when both are adequately defined and analytical procedures are specified and controlled and test equipment is carefully compared.

2. The American practice of basing the life of carbide tools only upon flank wear is suspect for many applications.

3. Tool geometry may be a more important factor in influencing the wear of carbide tools than is generally understood.

For these and other reasons which might be drawn from these results it is recommended that the cooperative program be extended to other work materials and microstructures as is contemplated in Phase 2. It is recommended further that efforts be made to explore a broader range of tool properties and to make more exhaustive analysis of the changes in the eight quantities listed earlier in this section. These are:

1. flank wear;
2. crater wear;
3. cutting forces;
4. cutting temperatures and their distribution;
5. cutting ratio;
6. shape of the chip cross section;
7. shape of the crater; and
8. degree and frequency of chip segmentation.

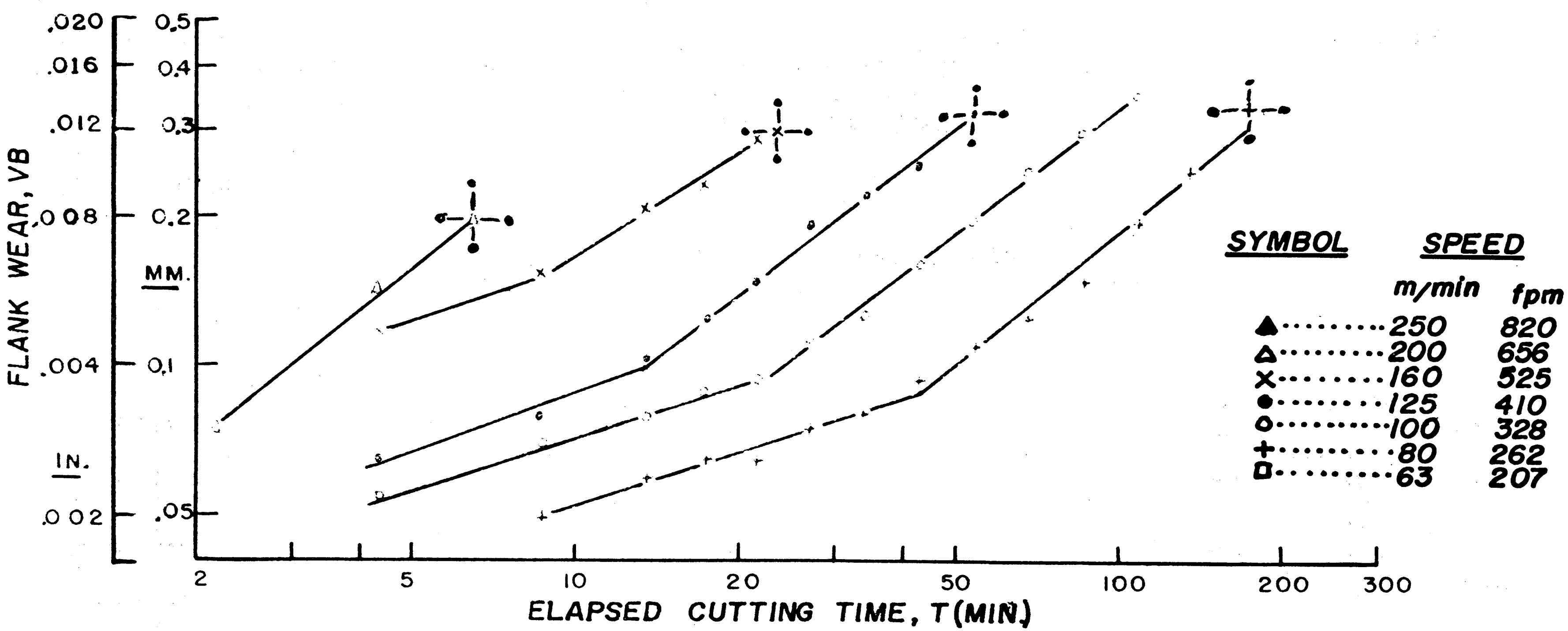

WORK MATERIAL: XC 45

HEAT ZC656

WORKING DIA.: 96-48 mm
4 - 2 in

TOOL MATERIAL: CARBIDE P30

SIZE OF CUT:
$b \times s = 3 \times 0.25\ mm^2$
$= 0.12 \times 0.01\ in^2$

TEST NO. 2.1b

TOOL GEOMETRY

α	γ	λ	χ	ε	r
6°	6°	0°	70°	90°	0.8 mm 0.032 in

VB vs T

FIG. NO. 1-1

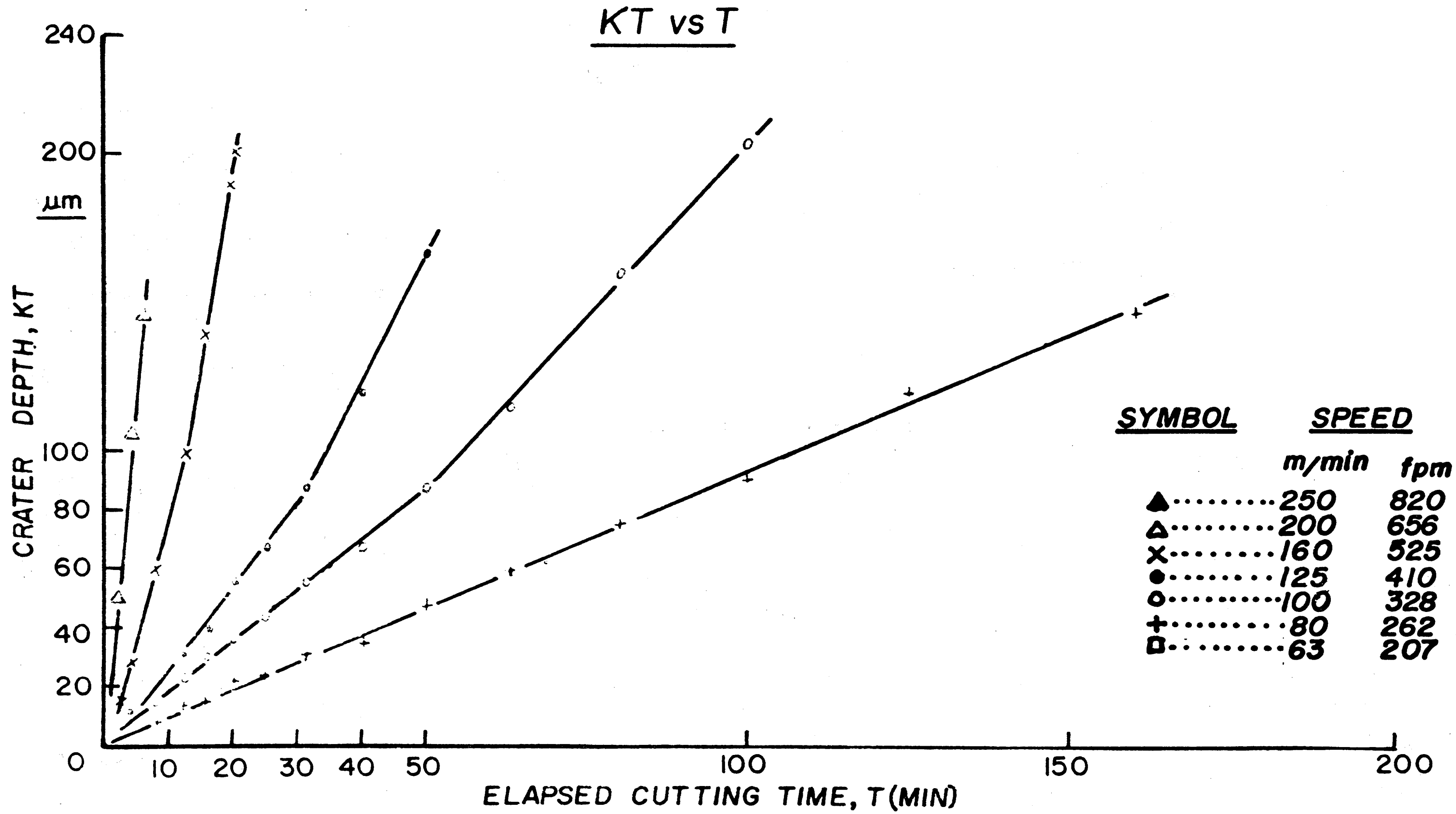

WORK MATERIAL: XC 45
HEAT: Z0656
WORKING DIAMETERS:
96–48 mm 2–4 in
TOOL MATERIAL: CARBIDE P 30
TEST NO. 2.1b
SIZE OF CUT: $3 \times .25\ mm^2$
$0.12 \times 0.01\ in^2$

TOOL GEOMETRY

α	γ	λ	ϰ	ε	r
6	6	0	70	90	08 mm 0.032 in

FIG. NO. 1–2

K vs T

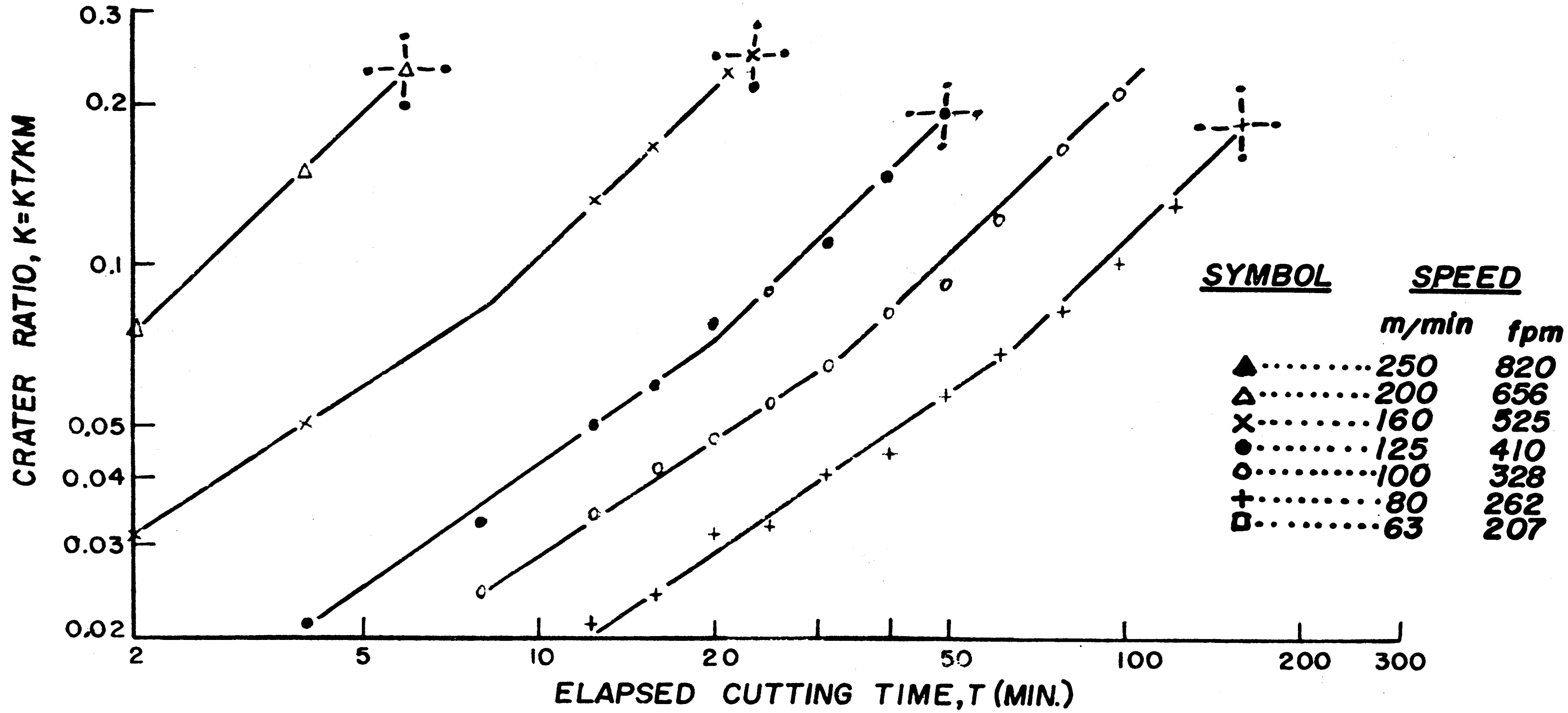

WORK MATERIAL: XC45
HEAT: Z0656
WORKING DIAMETERS
96-46 mm or 4-2 in
TOOL MATERIAL: CARBIDE P30
TEST NO. 2.1b
SIZE OF CUT: 3 x 0.25 mm
0.12 x 0.01 in

TOOL GEOMETRY

α	γ	λ	χ	ε	r
6	6	0	70	90	0.8 mm 0.032 in

FIG. NO. 1-3

CHIP FORESHORTENING
VS
ELAPSED CUTTING TIME

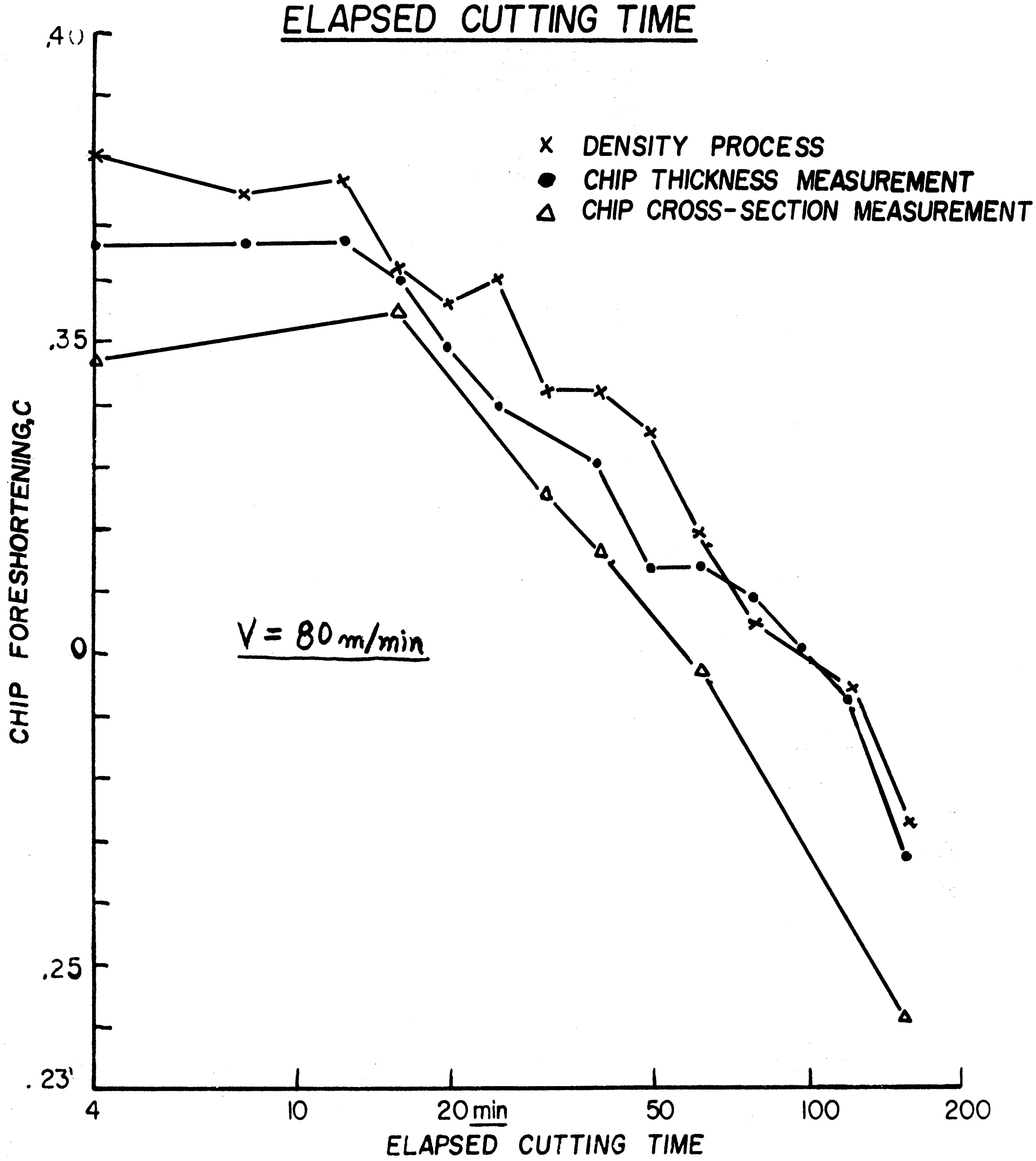

WORK MATERIAL: XC45
HEAT: Z0648
WORKING DIAMETER:
96–48 mm or 4–2 in.
TOOL MATERIAL: CARBIDE P30
TEST NO. 2.1a
SIZE OF CUT: 3 x .25 mm
0.12 x 0.01 in.

TOOL GEOMETRY

α	γ	λ	χ	ε	r
6	6	0	70	90	0.8 mm 0.032 in

FIG. NO. 1-4

CHIP FORESHORTENING
VS
ELAPSED CUTTING TIME

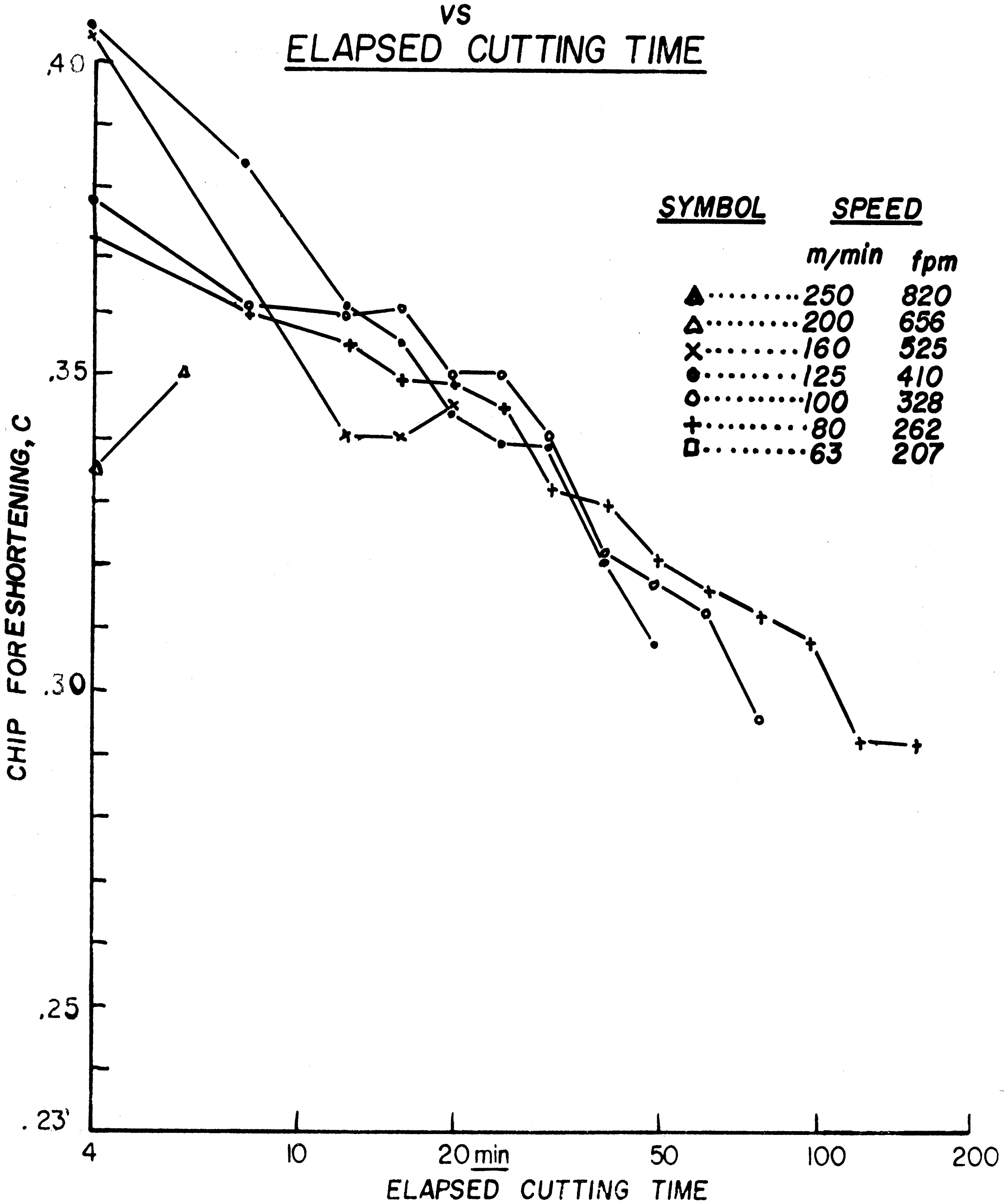

WORK MATERIAL: XC45

HEAT: Z0656

WORKING DIAMETER:
96–48mm or 4–2 in.

TOOL MATERIAL: CARBIDE P30

TEST NO. 2.1b

SIZE OF CUT: 3 x .25mm
0.12 x 0.01 in.

TOOL GEOMETRY

α	γ	λ	κ	ε	r
6	6	0	70	90	0.8mm 0.032 in

FIG. NO. 1-5

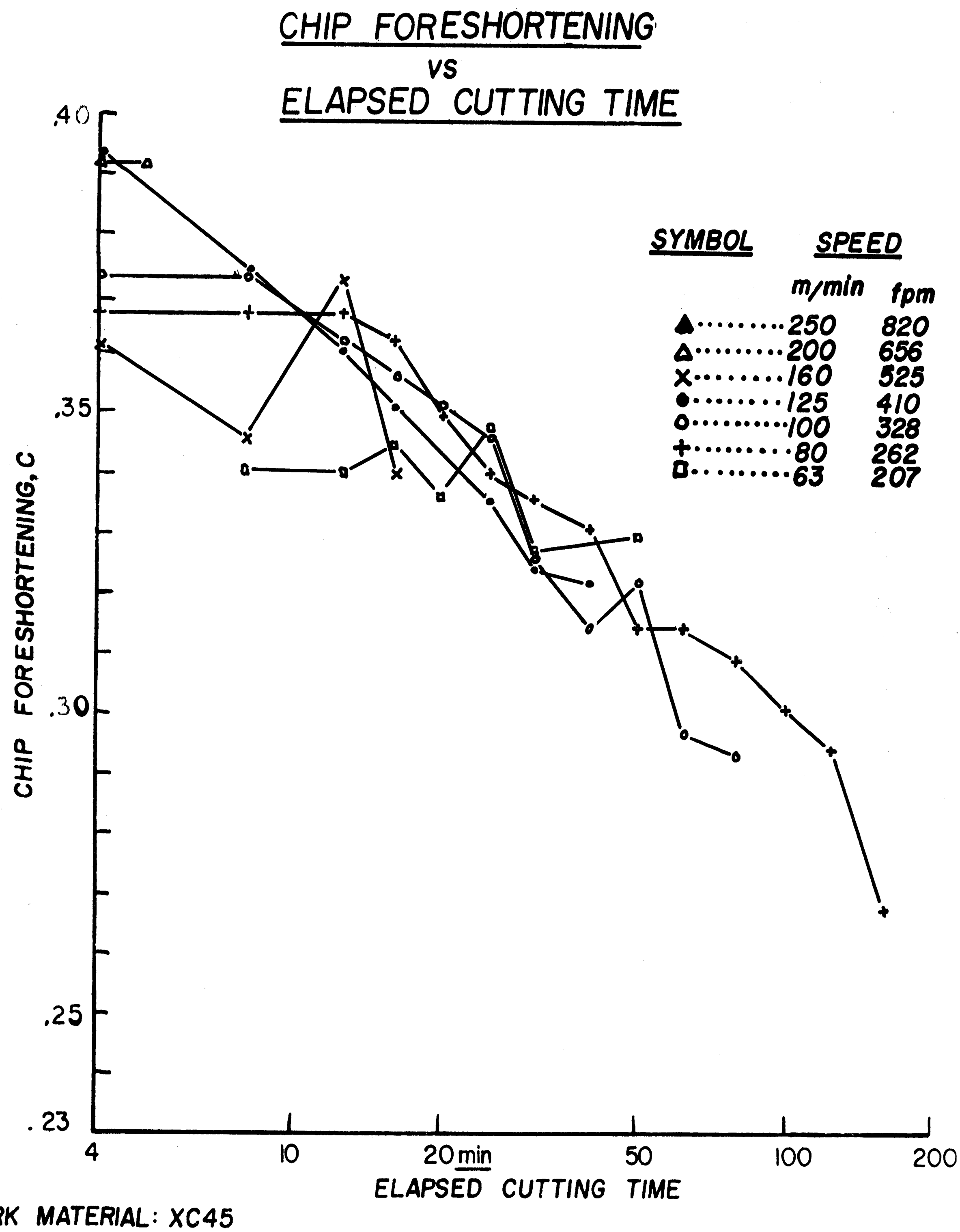

WORK MATERIAL: XC45

HEAT: Z 0648

WORKING DIAMETER:
96–48 mm or 4–2 in.

TOOL MATERIAL: CARBIDE P30

TEST NO. 2.1a

SIZE OF CUT: 3 x .25 mm
0.12 x 0.01 in.

TOOL GEOMETRY

α	γ	λ	χ	ε	r
6	6	0	70	90	0.8 mm 0.032 in

FIG. NO. 1-6

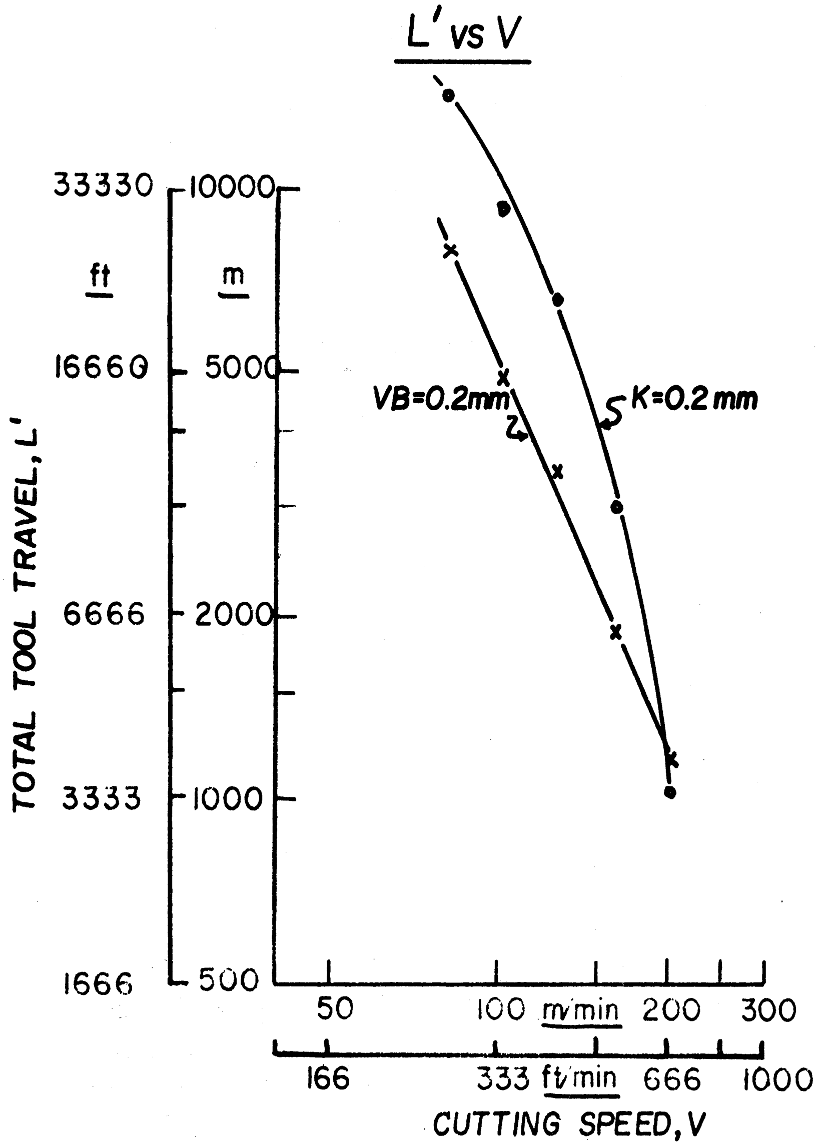

TOOL MATERIAL: CARBIDE P 30

HEAT: Z0656

WORKING DIAMETER:
96–48 mm or 4–2 in

WORK MATERIAL: XC45

TEST NO. 2.1b

SIZE OF CUT: $3 \times .25\ mm^2$
$0.12 \times 0.01\ in^2$

TOOL GEOMETRY

α	γ	λ	χ	ε	r
6	6	0	70	90	0.8 mm 0.032 in

FIG. NO. 1-7

L' vs V

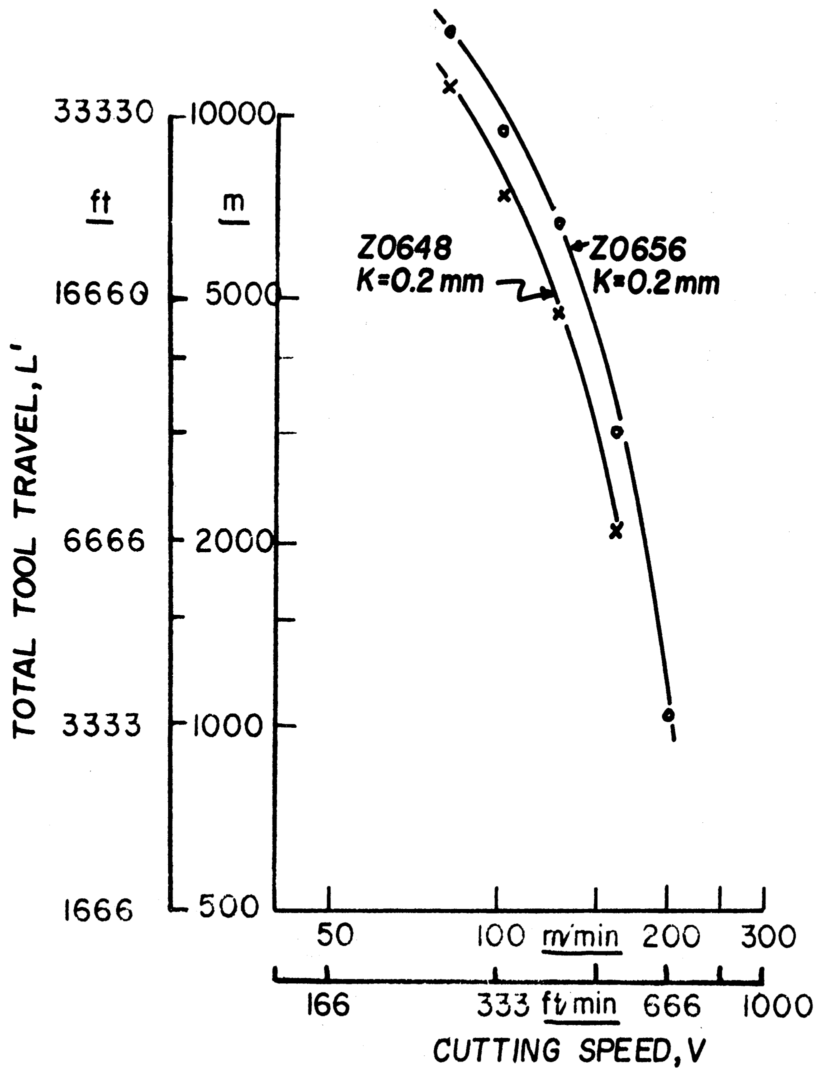

TOOL MATERIAL: CARBIDE P 30

HEAT: Z0648/Z0656

WORKING DIAMETER:
96–48 mm or 4–2 in

WORK MATERIAL: XC45

TEST NO. 2.1 a/b

SIZE OF CUT: 3 x .25 mm²
0.12 x 0.01 in²

TOOL GEOMETRY

α	γ	λ	$\varkappa$	ε	r
6	6	0	70	90	08 mm 0.032 in

FIG. NO. 1-8

T' vs V

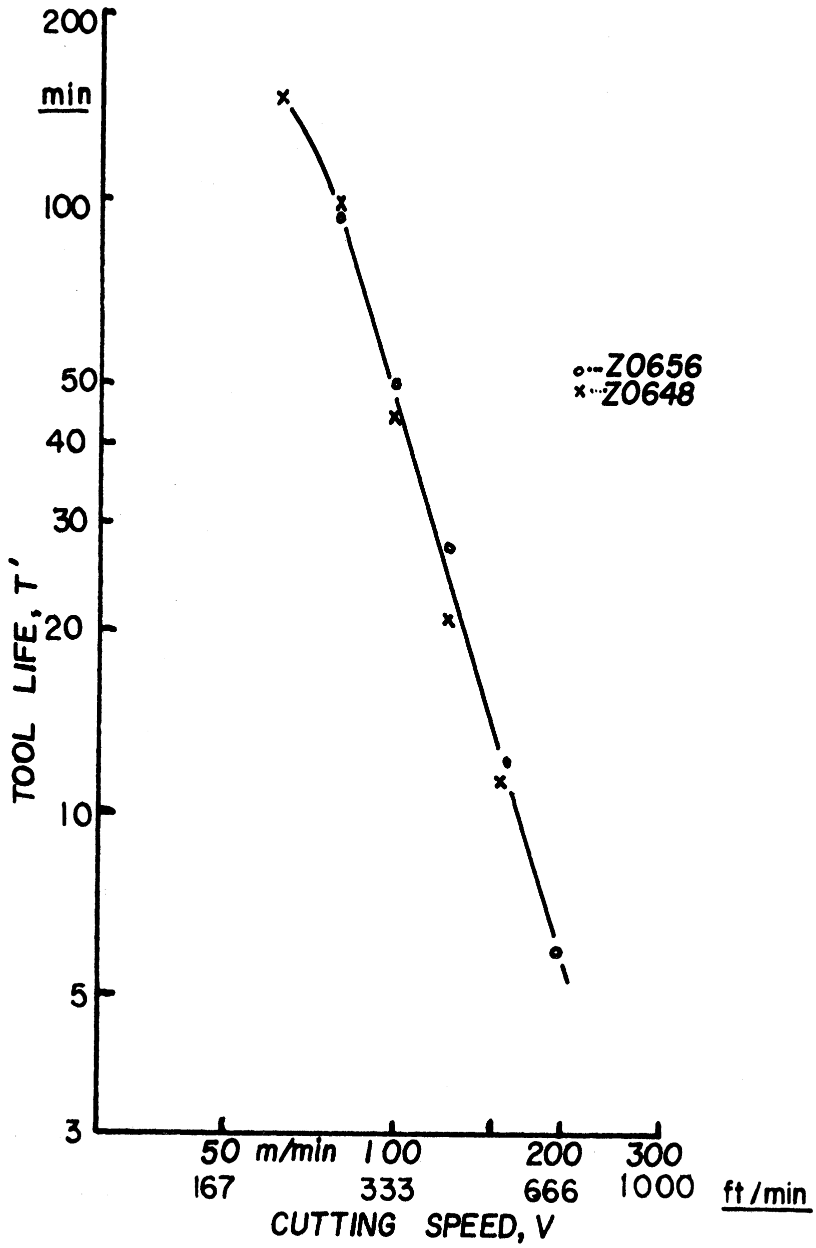

WORK MATERIAL: XC 45

HEAT: Z0648/Z0656

WORKING DIAMETER

96–48 mm or 4–2 in

TOOL MATERIAL: CARBIDE P 30

TEST NO 2.1 a/b

SIZE OF CUT: $3 \times 0.25 \, mm^2$

$= 0{\cdot}120 \times 0{\cdot}010 \, in^2$

TOOL GEOMETRY

α	γ	λ	$\varkappa$	ε	r
6	6	0	70	90	0.8 mm 0.032 in

FIG. NO. 1-9

T' vs V

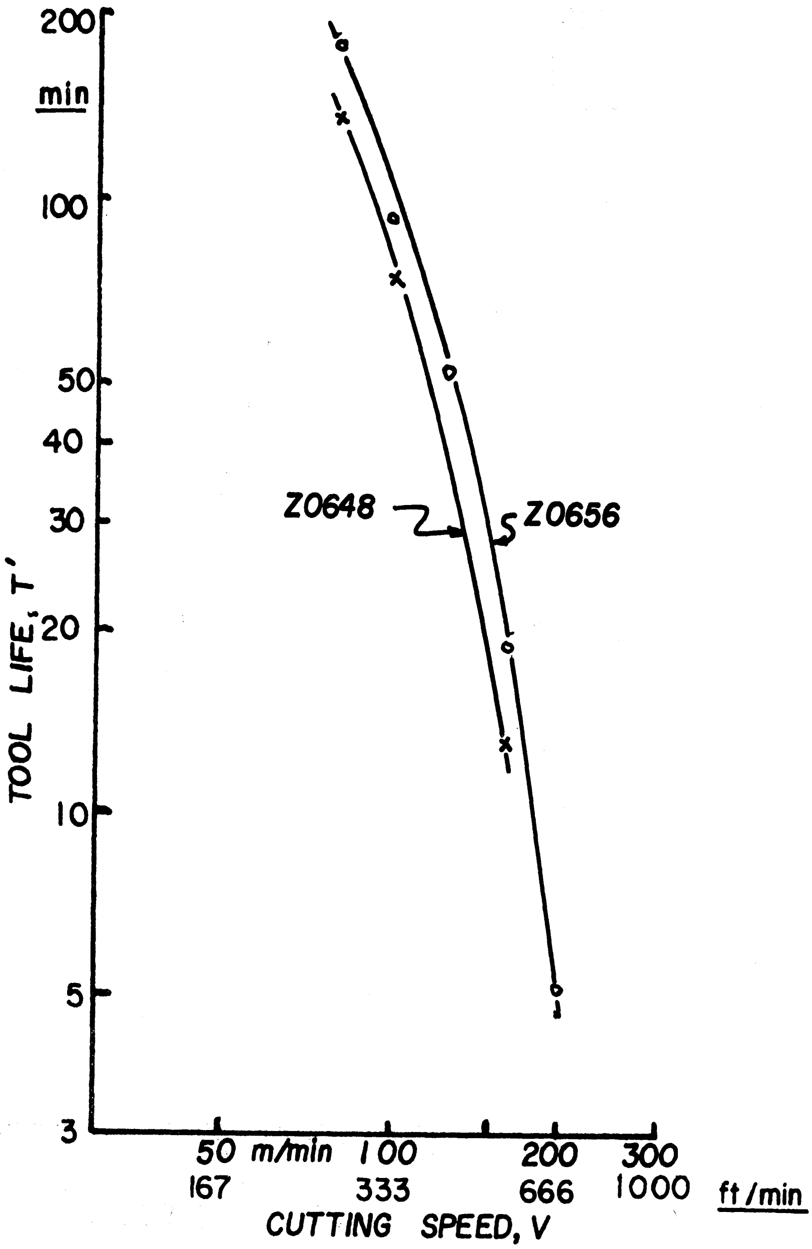

WORK MATERIAL: XC 45

HEAT: Z0648/Z0656

WORKING DIAMETER
96–48 mm or 4–2 in

TOOL MATERIAL: CARBIDE P 30

TEST NO 2.1 a/b

SIZE OF CUT: 3x0.25 mm^2
= 0·120 x 0·010 in^2

TOOL GEOMETRY

α	γ	λ	ϰ	ε	r
6	6	0	70	90	0.8 mm 0.032 in

FIG. NO. 1-10

T' vs V

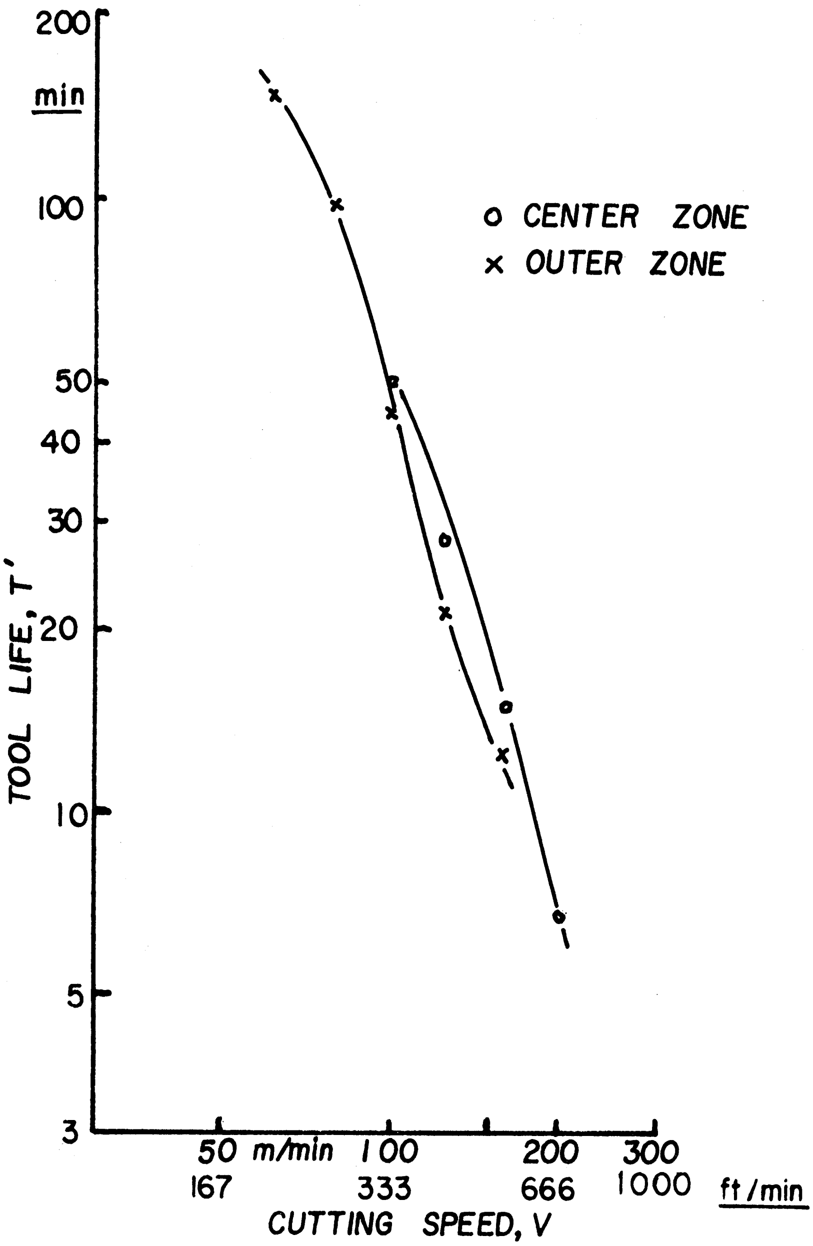

WORK MATERIAL: XC 45

HEAT: Z0656

WORKING DIAMETER

96–48 mm or 4–2 in

TOOL MATERIAL: CARBIDE P 30

TEST NO 2.1a/b

SIZE OF CUT: $\cdot 3 \times 0.25\ mm^2$

$= 0{\cdot}120 \times 0{\cdot}010\ in^2$

TOOL GEOMETRY

α	γ	λ	$\varkappa$	ε	r
6	6	0	70	90	0.8 mm 0.032 in

FIG. NO. I-11

T′ vs V

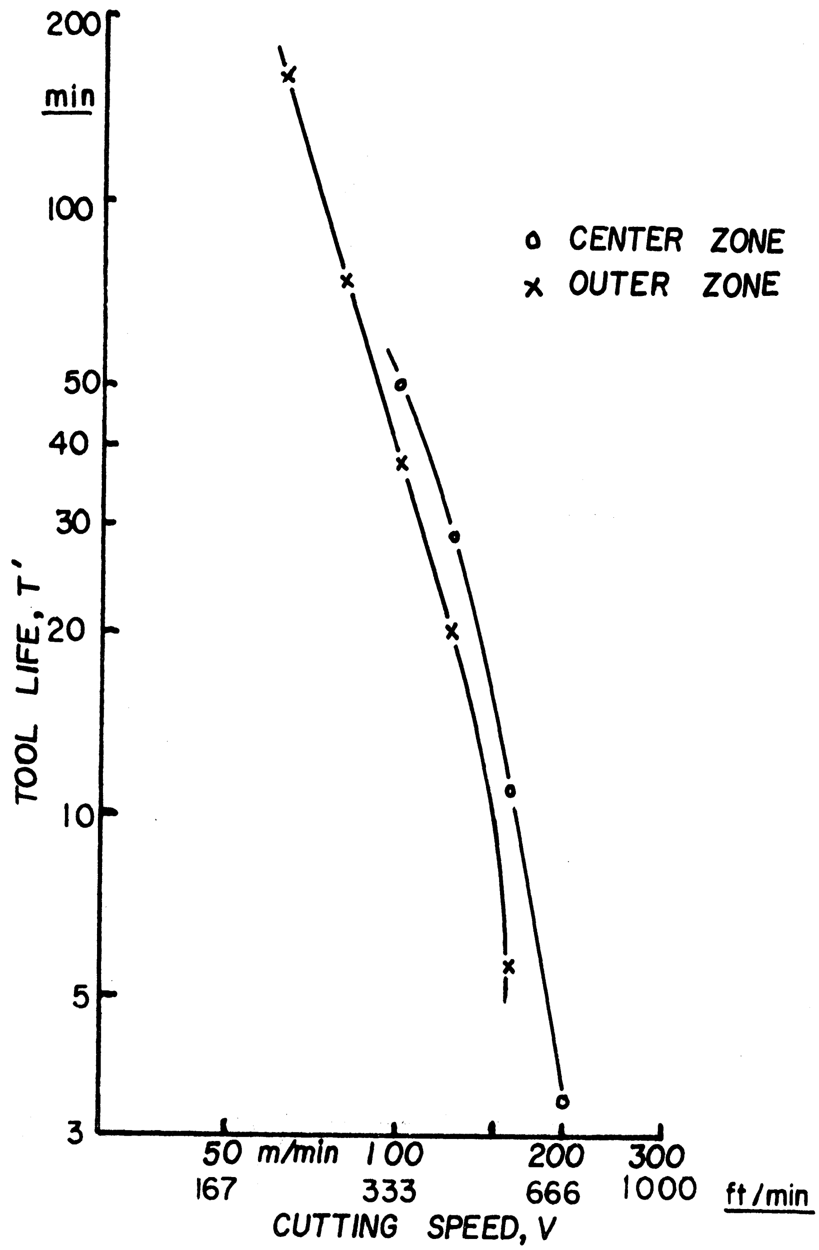

WORK MATERIAL: XC 45

HEAT: Z0648

WORKING DIAMETER

96–48 mm or 4–2 in

TOOL MATERIAL: CARBIDE P 30

TEST NO 2.1a/c

SIZE OF CUT: $3 \times 0.25\ mm^2$

$= 0.120 \times 0.010\ in^2$

TOOL GEOMETRY

α	γ	λ	$\varkappa$	ε	r
6	6	0	70	90	0.8 mm 0.032 in

FIG. NO. 1-12

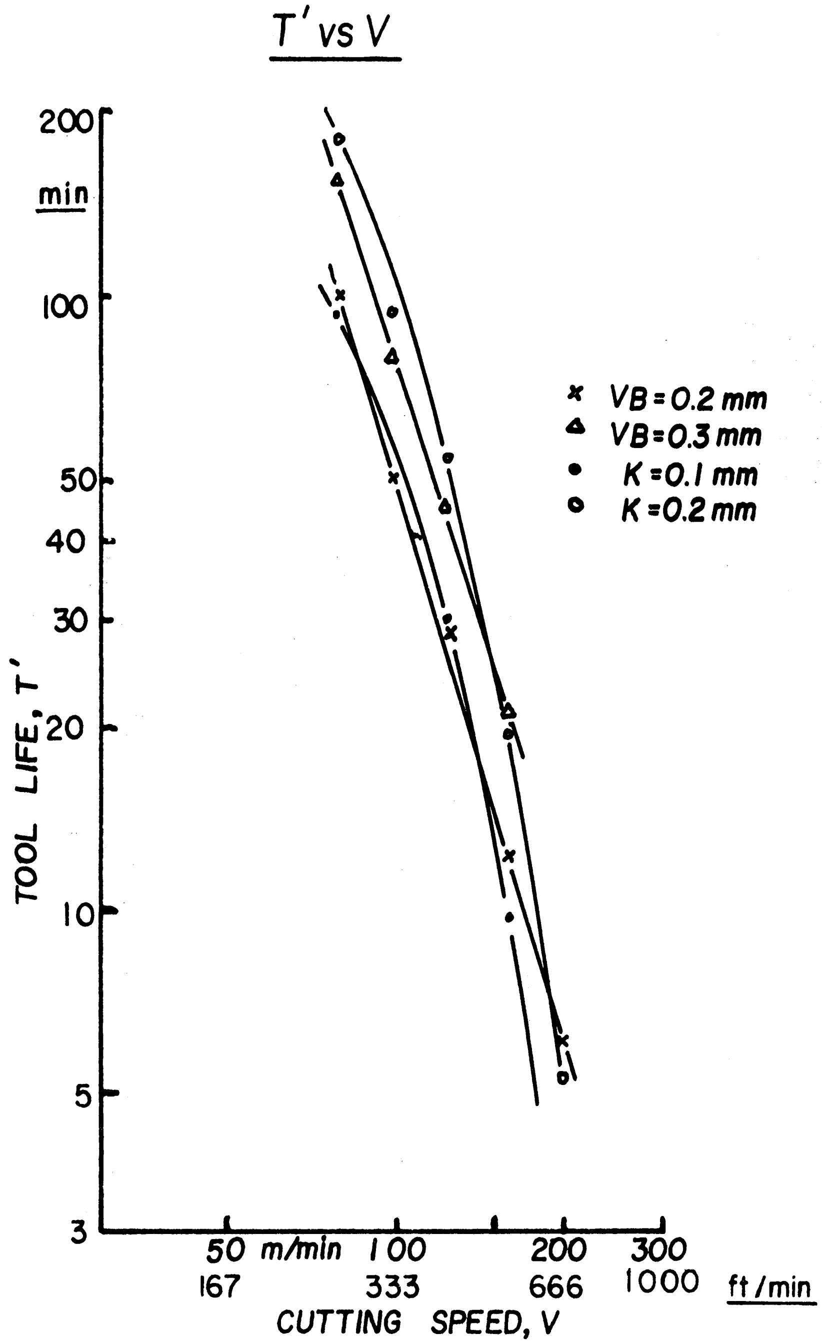

WORK MATERIAL: XC 45

HEAT: Z0656

WORKING DIAMETER

96–48 mm or 4–2 in

TOOL MATERIAL: CARBIDE P 30

TEST NO 2.1b

SIZE OF CUT: 3x0.25 mm^2

=0.120 x 0.010 in^2

TOOL GEOMETRY

α	γ	λ	χ	ε	r
6	6	0	70	90	0.8 mm 0.032 in

FIG. NO. 1-13

V vs $\varkappa$

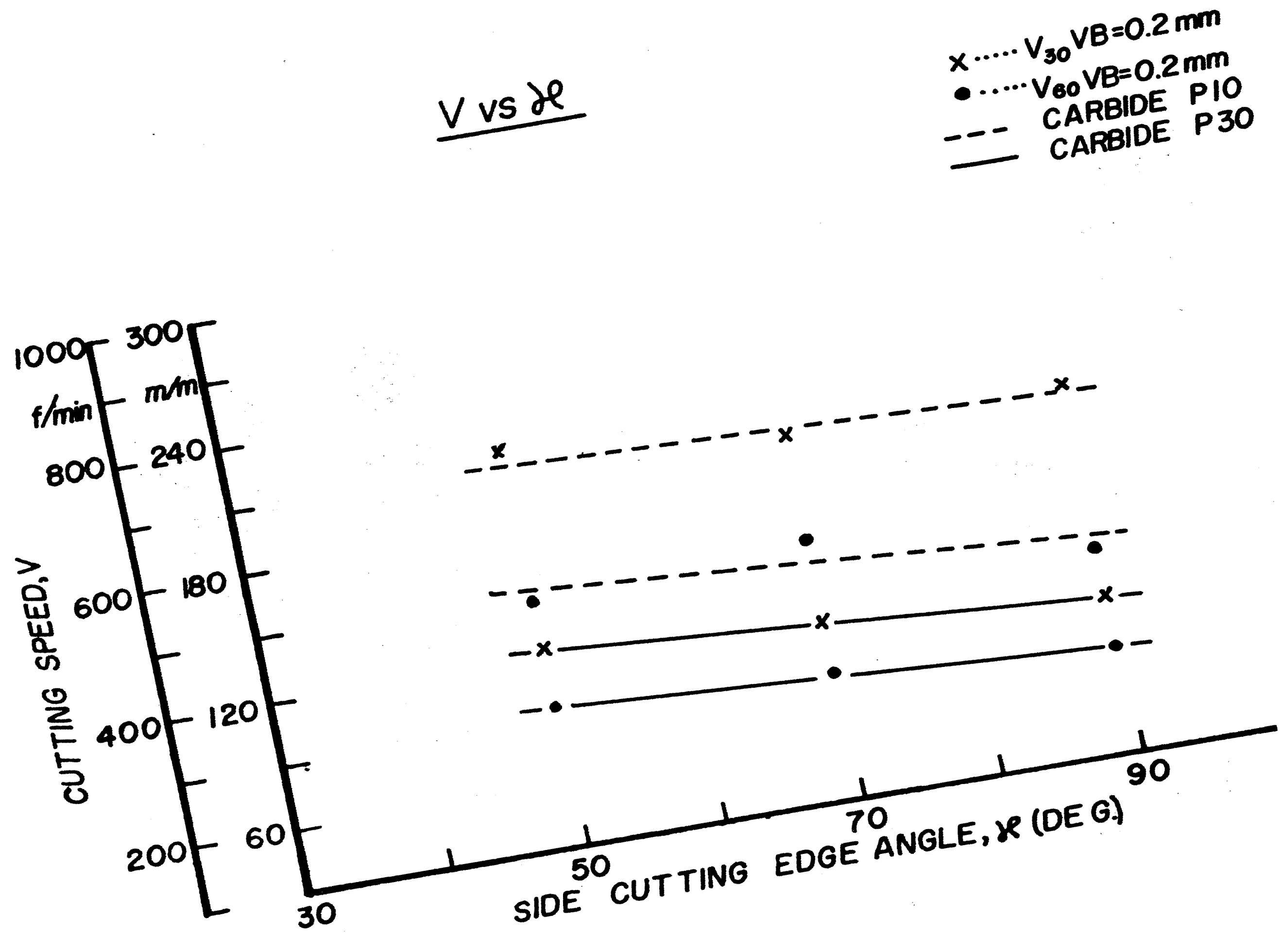

WORK MATERIAL: XC 45
HEAT:
WORKING DIAMETER
96-48 mm or 4-2 in
TOOL MATERIAL: CARBIDE P10 / P30
TEST NO. 2.1/4.1/5.1 | 10.1 | 12.1 | 13.1
SIZE OF CUT: 3 x 0.25 mm^2 = 0.12 x 0.010 in^2

α	γ	λ	$\varkappa$	ε	r
6	6	0		90	0.8 mm 0.032 in

FIG. NO. 1-14

V vs $\varkappa$

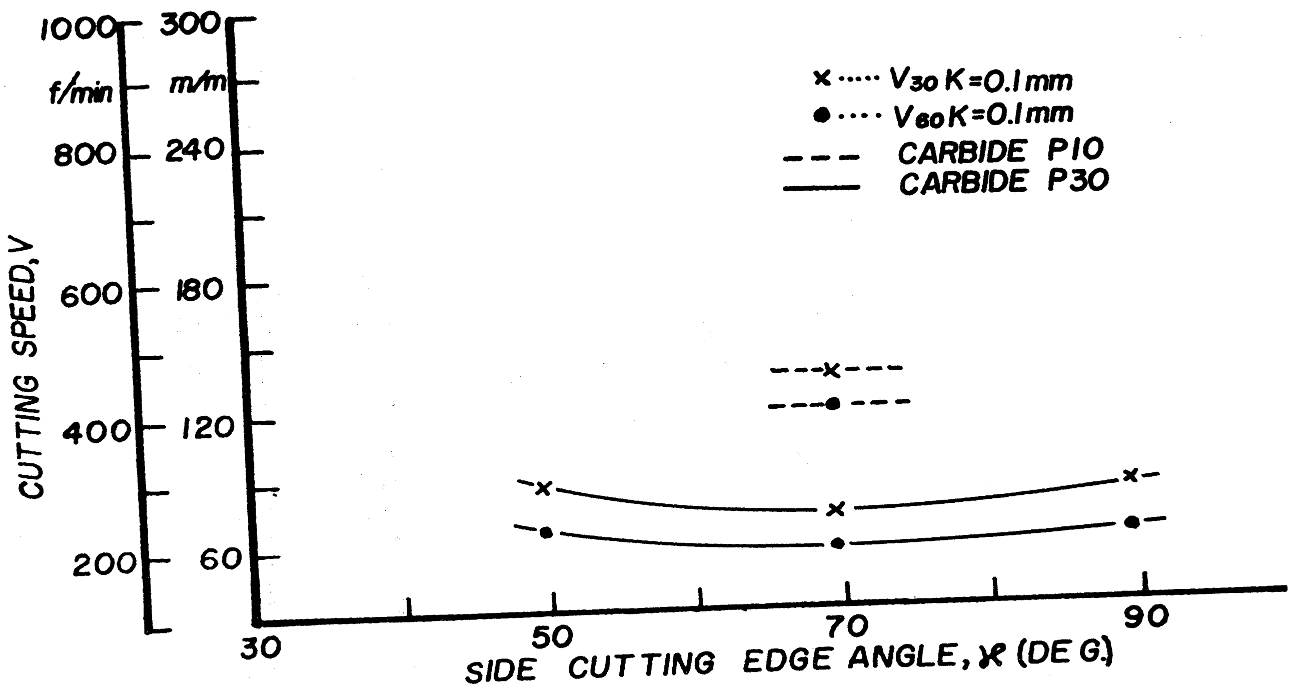

WORK MATERIAL: XC 45

HEAT:

WORKING DIAMETER
96-48 mm or 4-2 in

TOOL MATERIAL: CARBIDE P10 / P30

TEST NO. 2.1 | 4.1 | 5.1 | 10.1 | 12.1 | 13.1

SIZE OF CUT: $3 \times 0.25 mm^2 = 0.12 \times 0.010 in^2$

α	γ	λ	$\varkappa$	ε	r
6	6	0		90	0.8 mm 0.032 in

FIG. NO. 1-15

V vs S

WORKING MATERIAL: XC 45
WORKING DIAMETER
96-48 mm or 4-2 in.
TOOL MATERIAL: CARBIDE P10/P30
TEST NO. 2.1,2,3 10.1,2
SIZE OF CUT: 3 x Var. mm^2
= 0.12 x 0.01 in^2

α	γ	λ	$\varkappa$	ε	r
6	6	0	70	90	0.8 mm 0.3

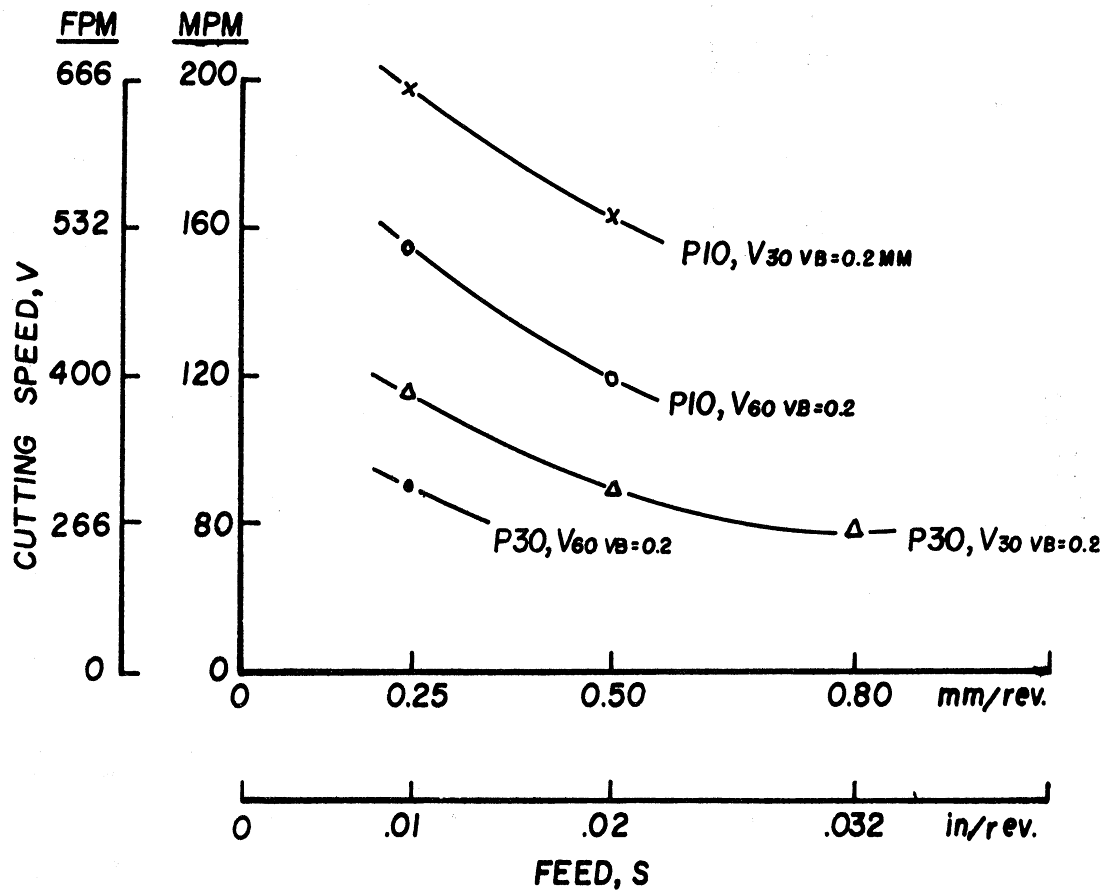

FIG. NO. 1-16

V vs S

WORKING MATERIAL: XC 45
WORKING DIAMETER
96–48 mm or 4–2 in.
TOOL MATERIAL: CARBIDE P10/P30
TEST NO. 2.1, 2, 3 10.1, 2
SIZE OF CUT: 3 x Var mm^2
=0.12 x 0.01 in.^{2}

α	γ	λ	χ	ε	r
6	6	0	70	90	0.8 mm 0.3

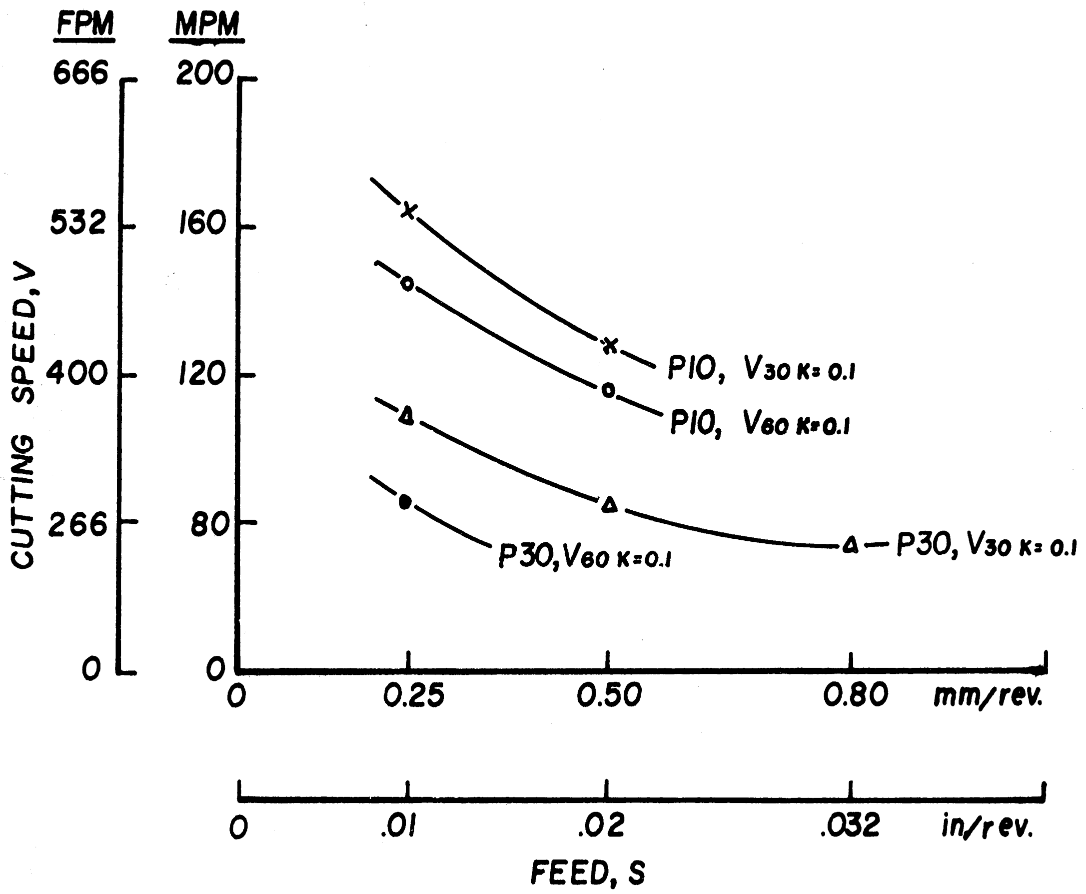

FIG. NO. 1-17

TOOL GEOMETRY

α	γ	λ	χ	ε	r
6		0	70	90	0.8 mm
		−6			0.032 in

WORK MATERIAL: XC 45
HEAT: Z0648/Z0656
WORKING DIAMETER
96−48 mm or 4−2 in
TOOL MATERIAL: CARBIDE P 30
TEST NO. 1.1/2.1/3.1/7.1
SIZE OF CUT: 3 x 0.25 mm^2
= 0.12 x 0.01 in^2
CUTTING SPEED, V = 80 m/min.

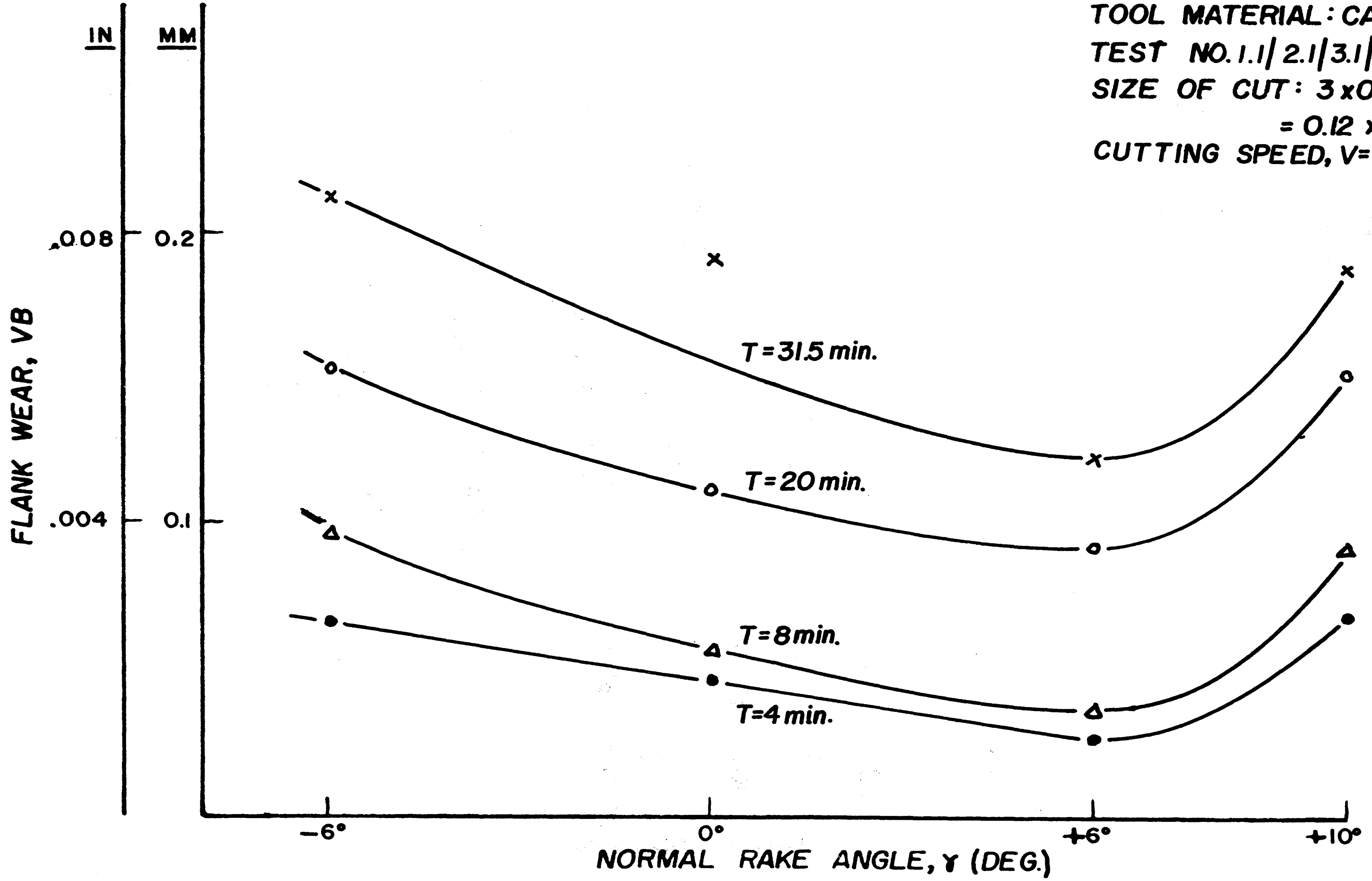

VB vs γ

FIG. NO. 1-18

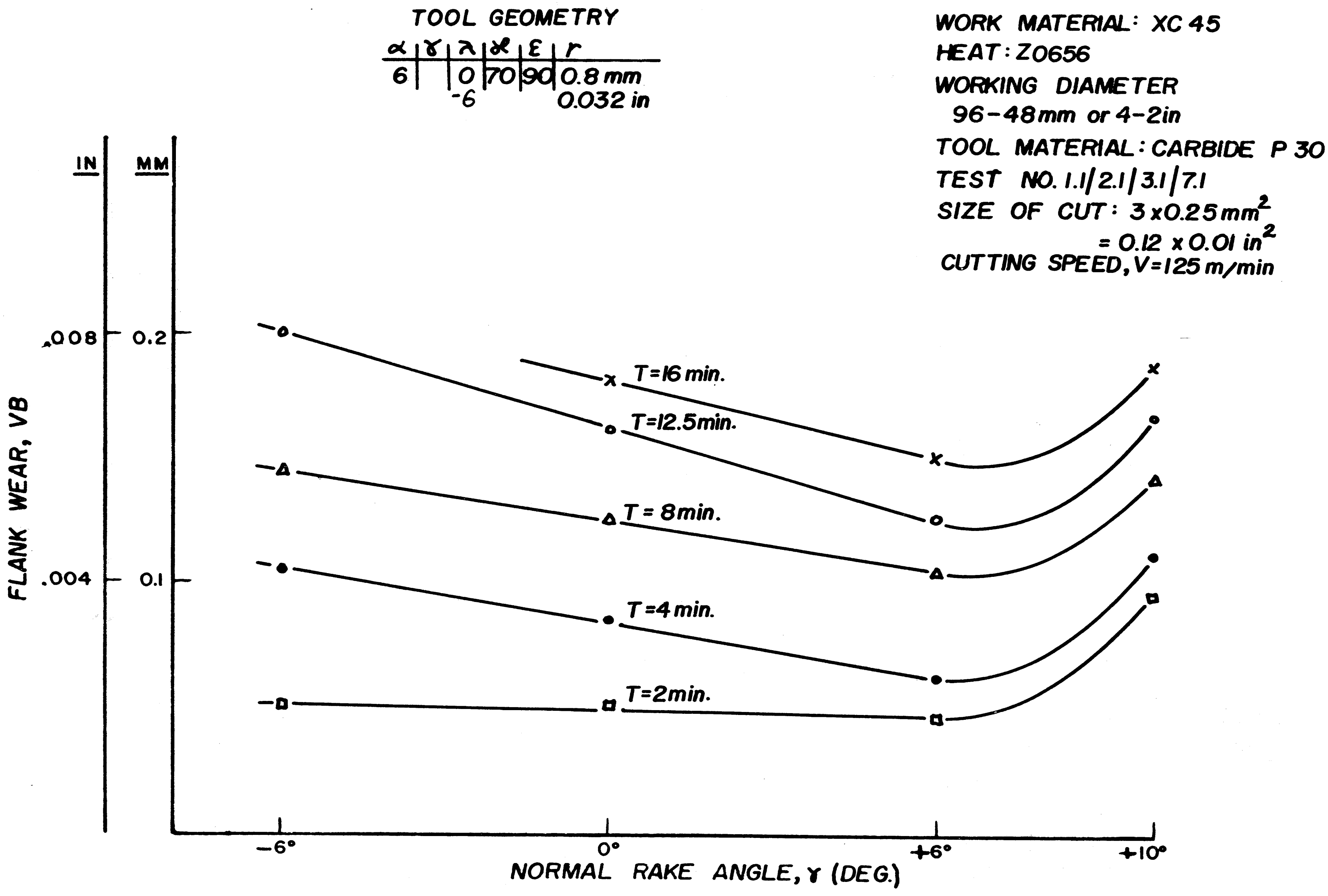

VB vs γ

FIG. NO.1-19

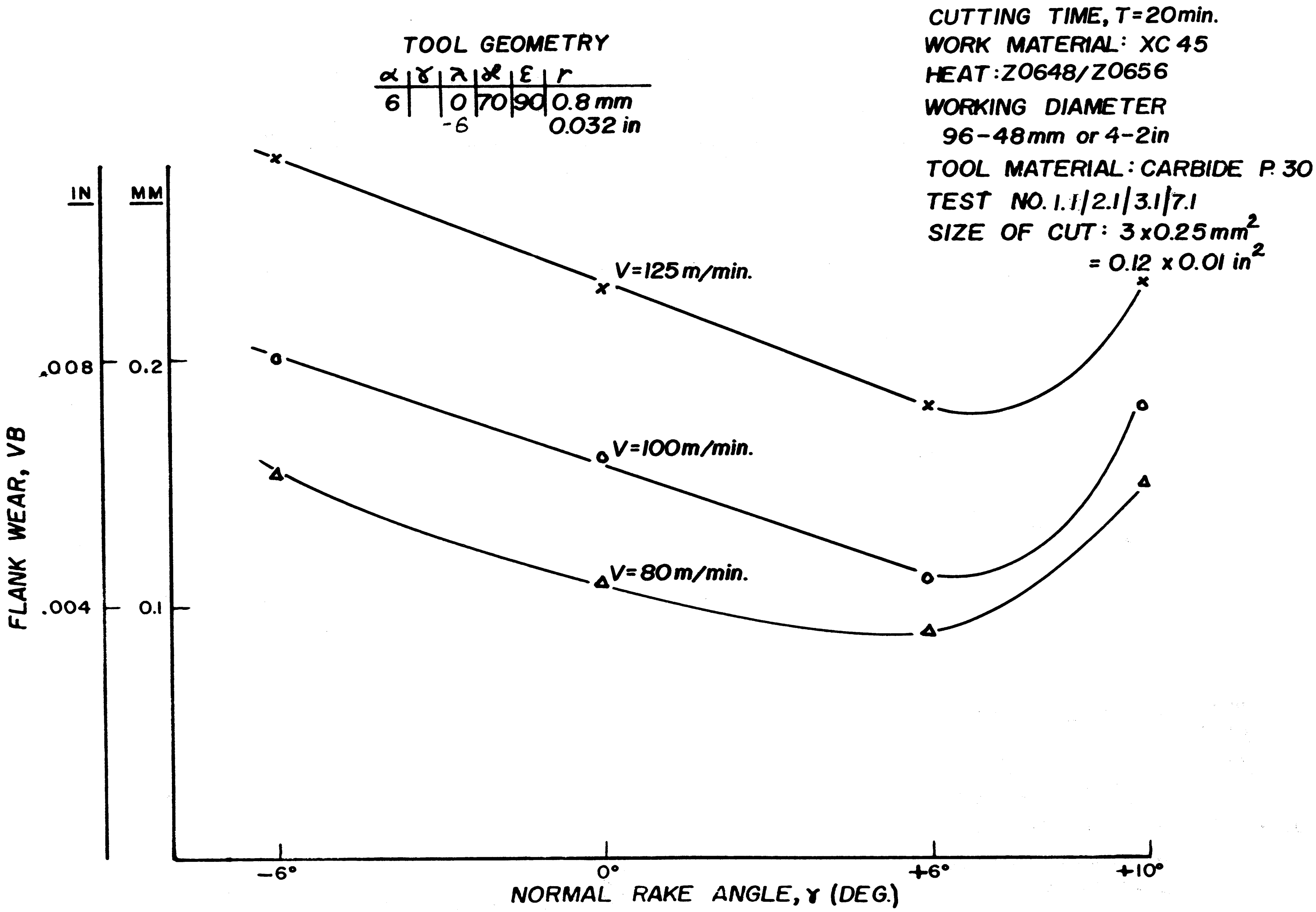

VB vs γ

FIG. NO. 1-20

TOOL GEOMETRY

α	γ	λ	χ	ε	r
6		0	70	90	0.8mm
		-6			0.032 in

WORK MATERIAL: XC 45
TOOL MATERIAL: CARBIDE P 30
SIZE OF CUT: 3 x Var. mm²
= 0.12 x 0.01 in²
TEST NOS.: 1.1/2.1,2.3/3.1/7.1

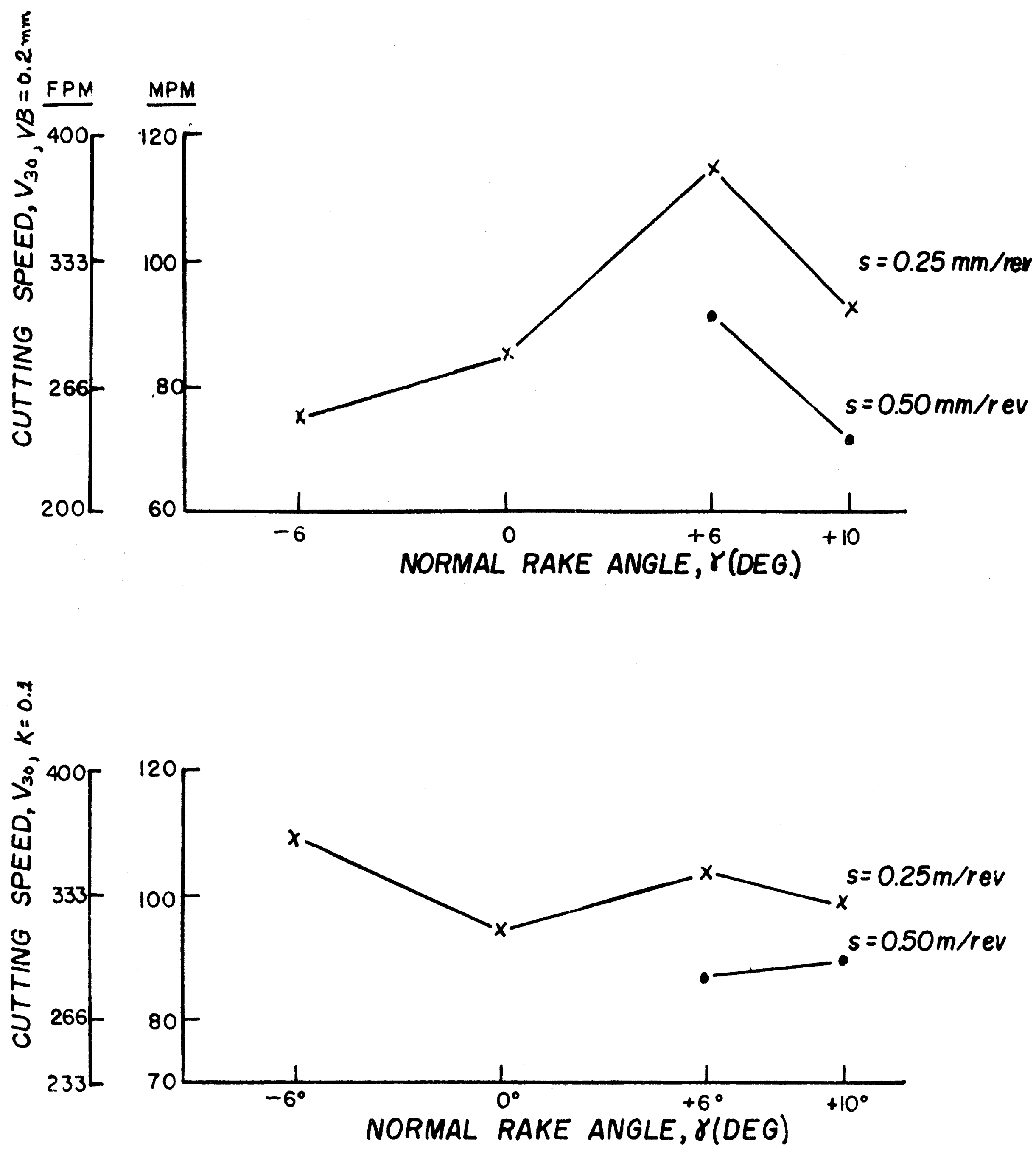

V vs γ

FIG. NO. 1.21

TOOL GEOMETRY

α	γ	λ	χ	ε	r
6		0 -6	70	90	0.8 mm 0.032 in

WORK MATERIAL: XC 45
HEAT: Z 0648
WORKING DIAMETER
96–48 mm or 4–2 in
TOOL MATERIAL: CARBIDE P 10
TEST NO. 10.1 15.1
SIZE OF CUT: 3 x 0.25 mm^2
= 0.12 x 0.01 in^2
CUTTING SPEED, V=125 m/min.

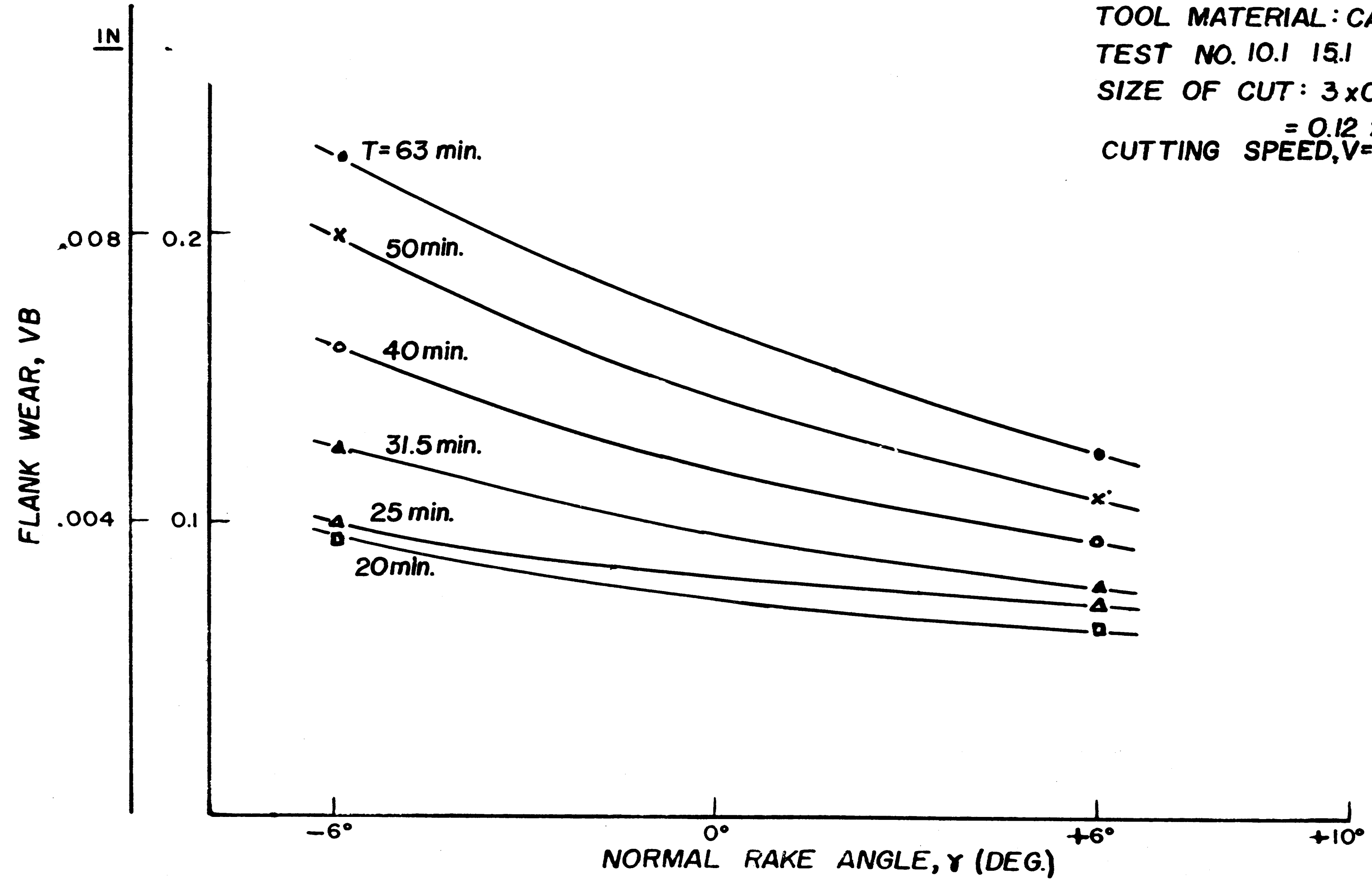

VB vs γ

FIG. NO. 1-22

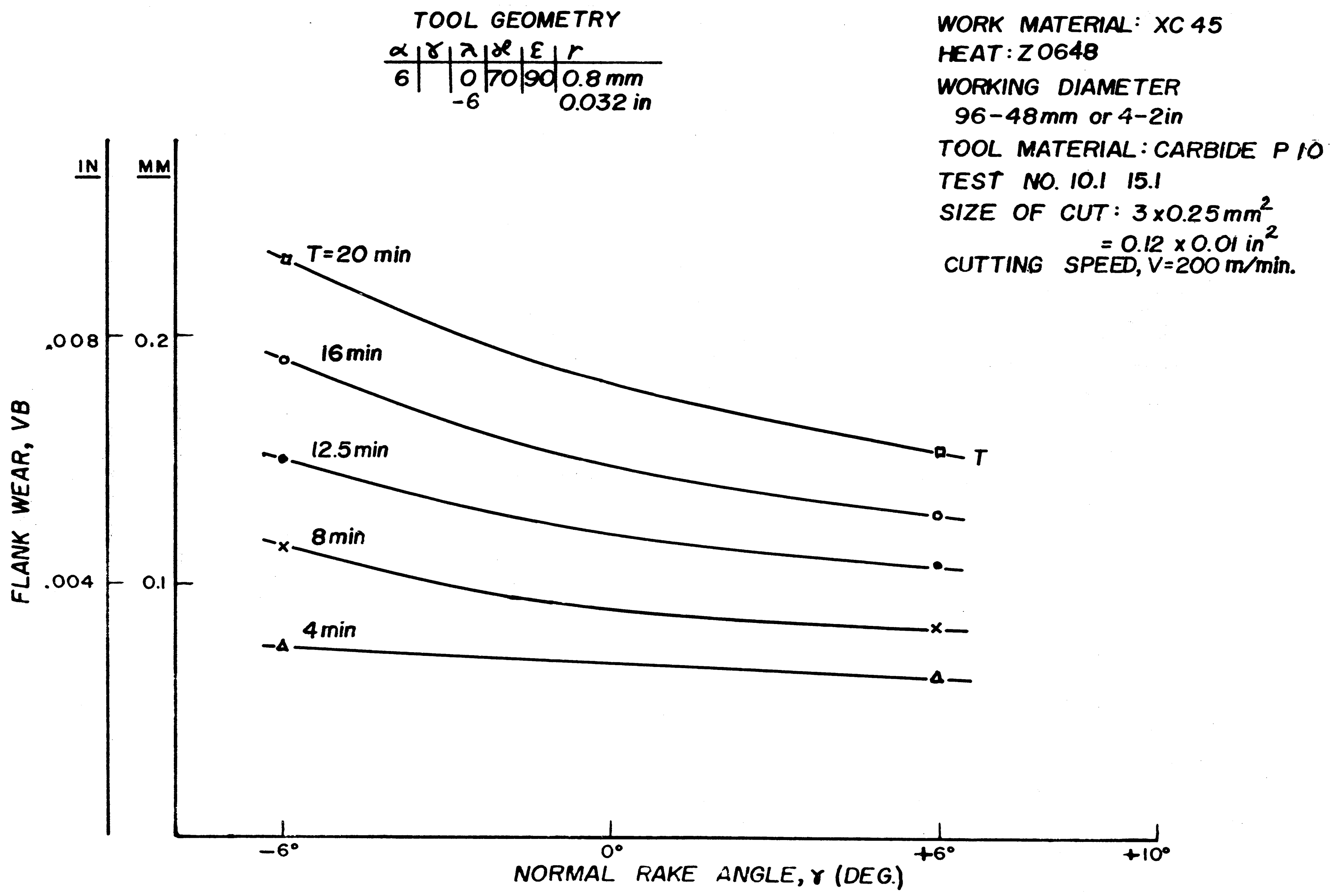

VB vs γ

FIG. NO. 1-23

TOOL GEOMETRY

α	γ	λ	ϰ	ε	r
6		0	70	90	0.8 mm 0.032 in

WORK MATERIAL: XC 45
HEAT: Z0656
WORKING DIAMETER
96–48 mm or 4–2 in
TOOL MATERIAL: CARBIDE P 10
TEST NO. 14.1,2,3 *
SIZE OF CUT: $3 \times 0.25\ mm^2$
$= 0.12 \times 0.01\ in^2$
CUTTING SPEED, V=125 m/min

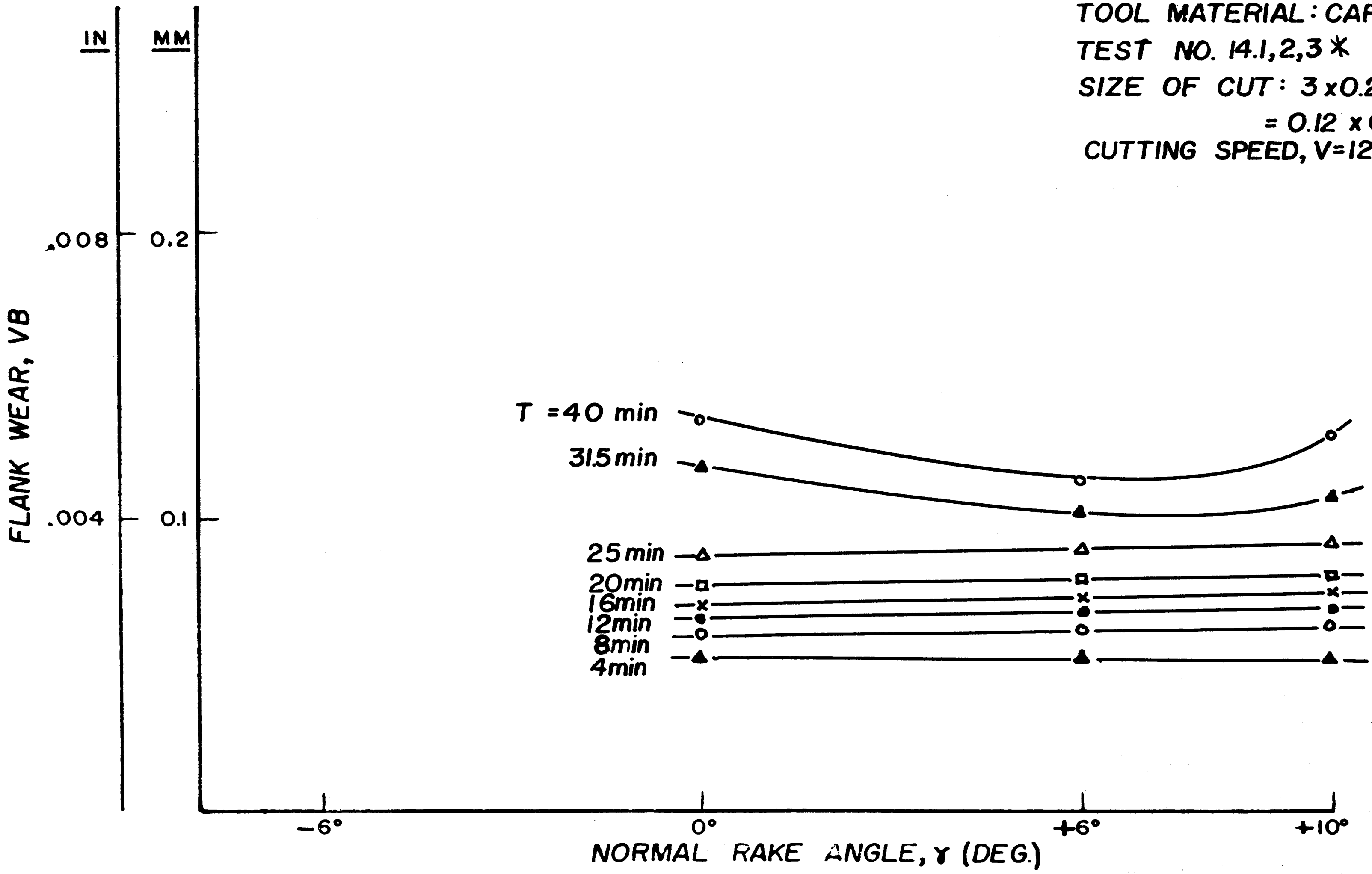

VB vs γ

FIG. NO. I-24

TOOL GEOMETRY

α	γ	λ	χ	ε	r
6		0	70	90	0.8 mm 0.032 in

WORK MATERIAL: XC 45
HEAT: Z0656
WORKING DIAMETER
96–48 mm or 4–2 in
TOOL MATERIAL: CARBIDE P 10
TEST NO. 14.1,2,3 *
SIZE OF CUT: $3 \times 0.25\ mm^2$
$= 0.12 \times 0.01\ in^2$
CUTTING SPEED, V=200 m/min

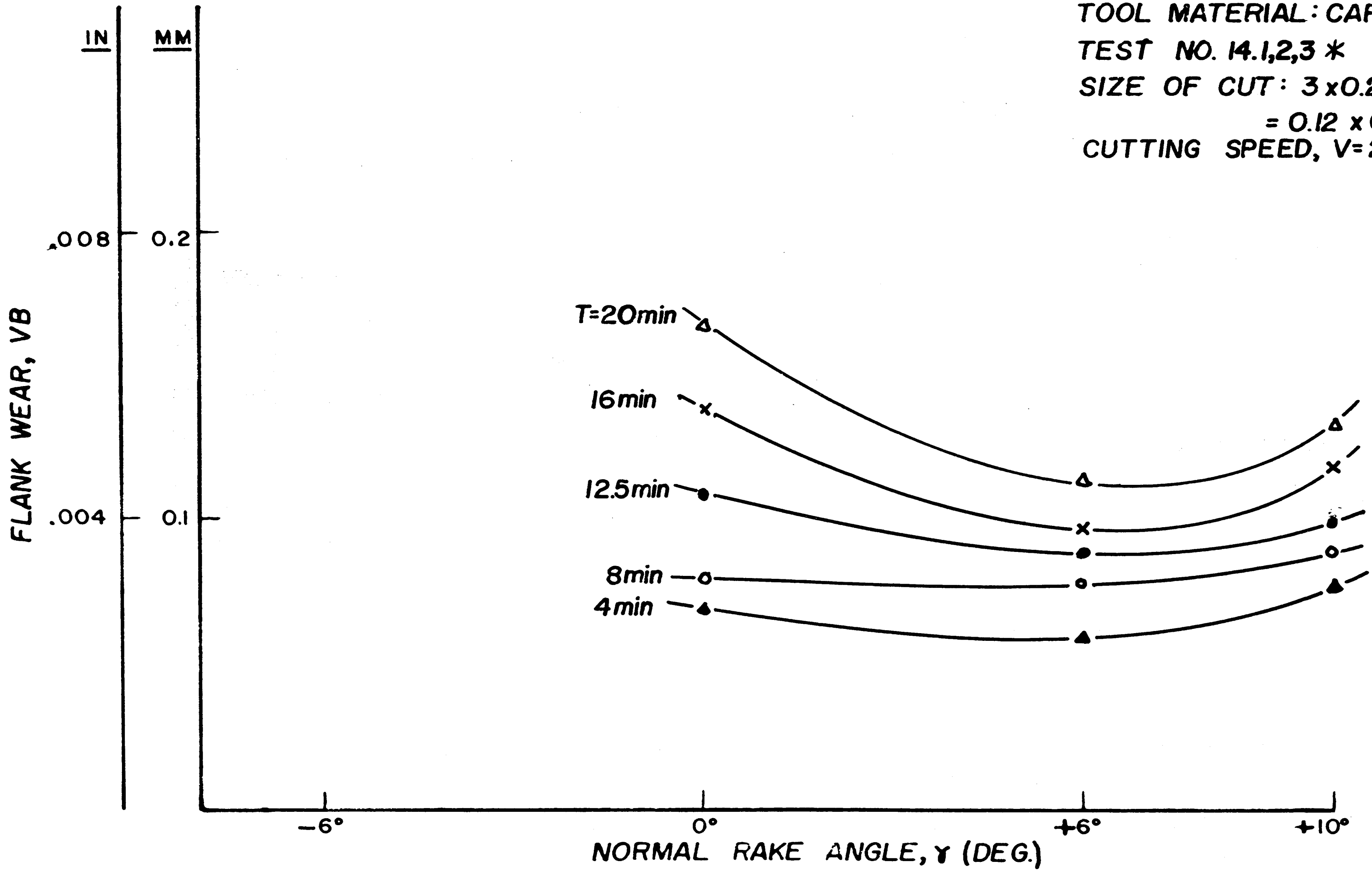

VB vs γ

FIG. NO. 1–25

TOOL GEOMETRY

α	γ	λ	χ	ε	r
6		0	70	90	0.8 mm 0.032 in

WORK MATERIAL: XC 45
TOOL MATERIAL: CARBIDE P10
SIZE OF CUT: $3 \times 0.25\ mm^2$
$= 0.12 \times 0.01\ in^2$
TEST NO.: 14.1, 14.2, 14.3 *

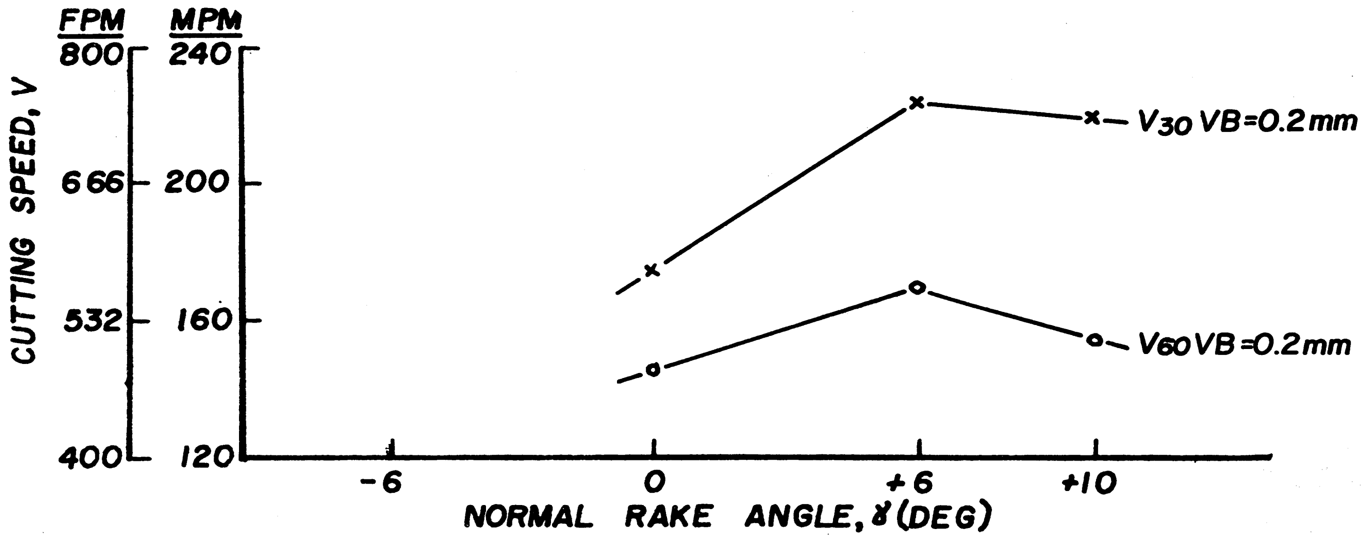

V vs γ

FIG. NO. 1-26

TOOL GEOMETRY

α	γ	λ	$\varkappa$	ε	r
6		0	70	90	0.8 mm 0.032 in

WORK MATERIAL: XC 45
TOOL MATERIAL: CARBIDE P10
SIZE OF CUT: $3 \times 0.25\ mm^2$
$= 0.12 \times 0.01\ in^2$
TEST NO.: 14.1, 14.2, 14.3 *

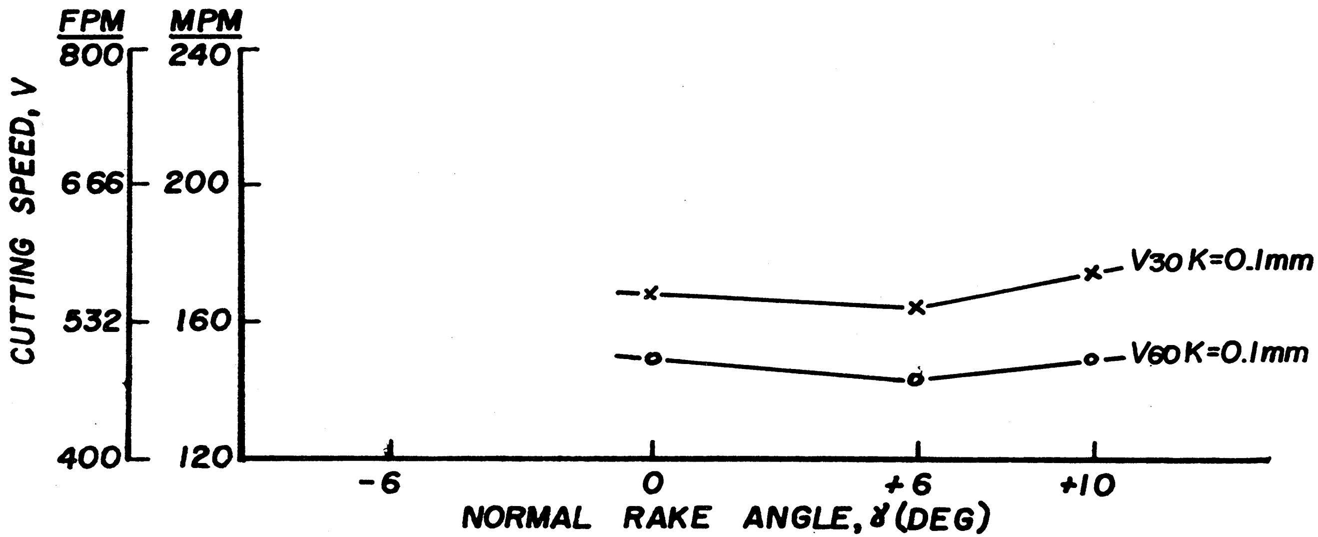

V vs γ

FIG. NO. 1-27

V vs S

α	γ	λ	ϰ	ε	r
6	6	0		90	0.8mm 0.032 in

WORK MATERIAL: XC 45
TOOL MATERIAL: CARBIDE P30
SIZE OF CUT: 3 x (Var. mm^2
=0.12 x 0.01 in^2
TEST NO 2.1,2,3/4.1,2,3/5.1,2

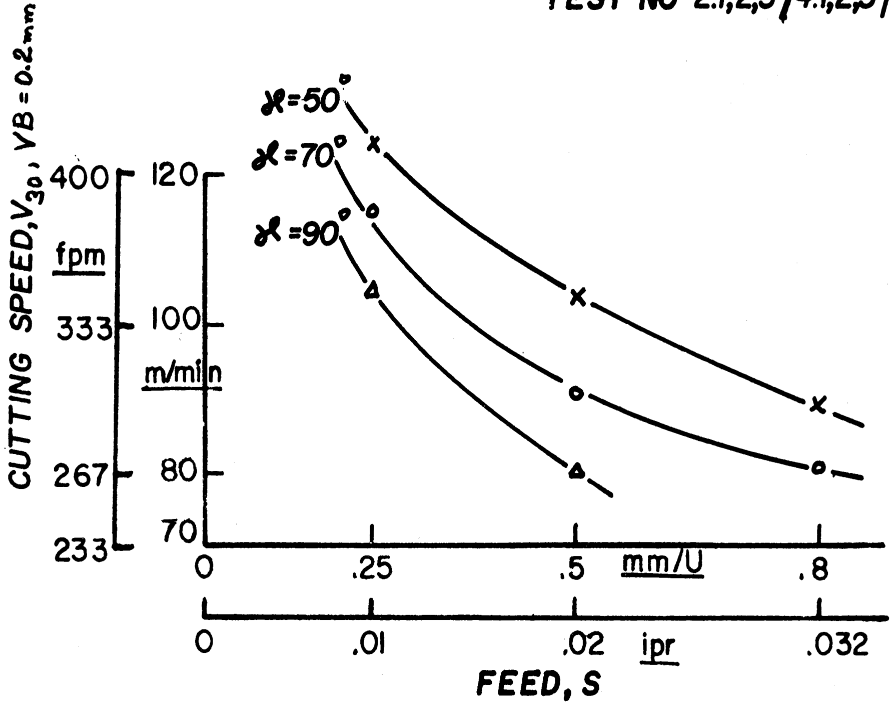

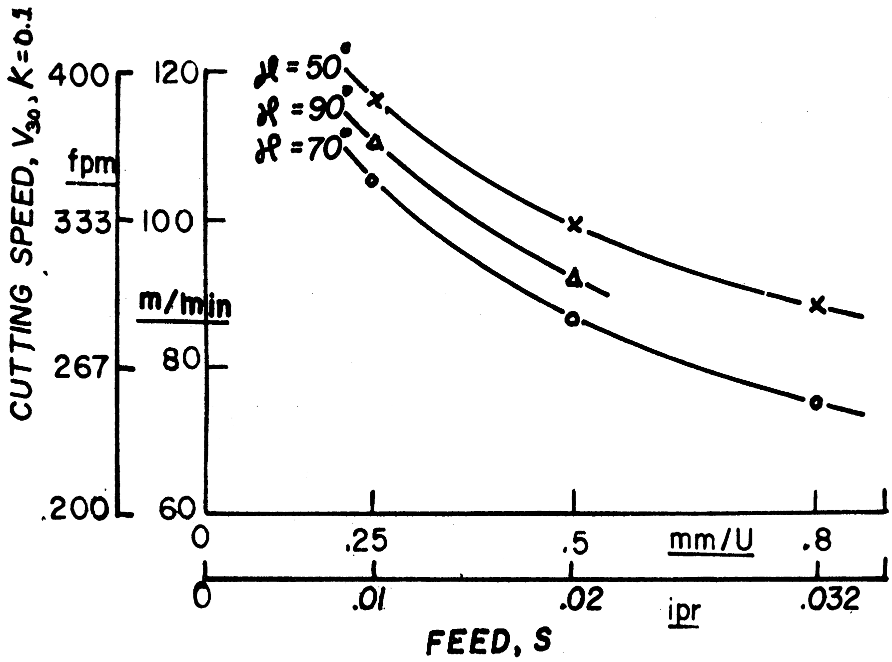

FIG. NO. 1-28

V vs S

α	γ	λ	χ	ε	r
6		0	70	90	0.8mm 0.032 in

WORK MATERIAL: XC 45
TOOL MATERIAL: CARBIDE P30
SIZE OF CUT: 3 x (Var mm^2
= 0.12 x 0.01 in^2
TEST NO 2.1,2,3 3.1,2

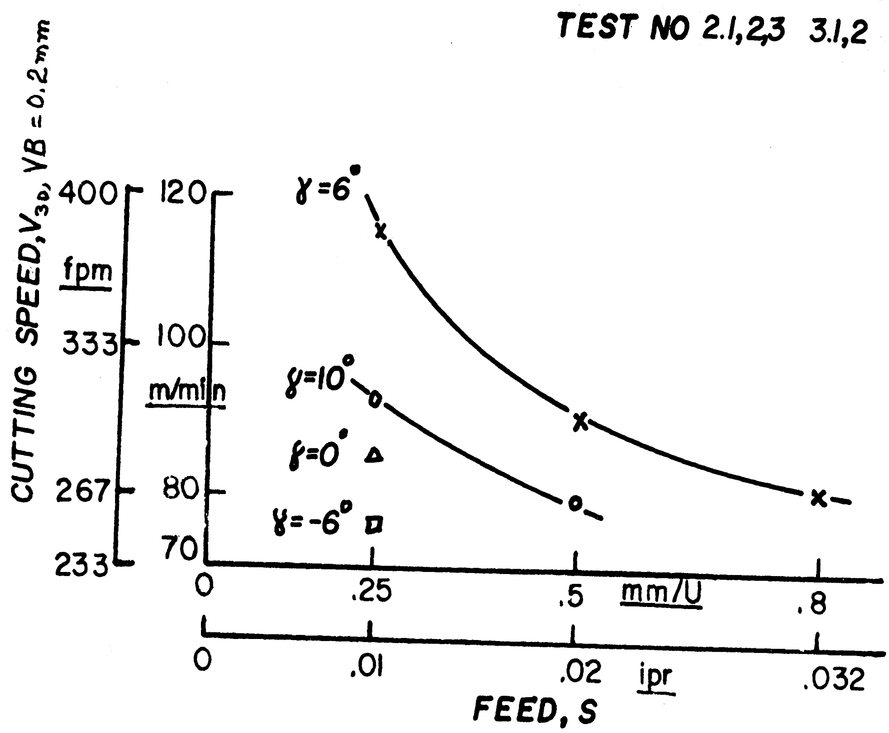

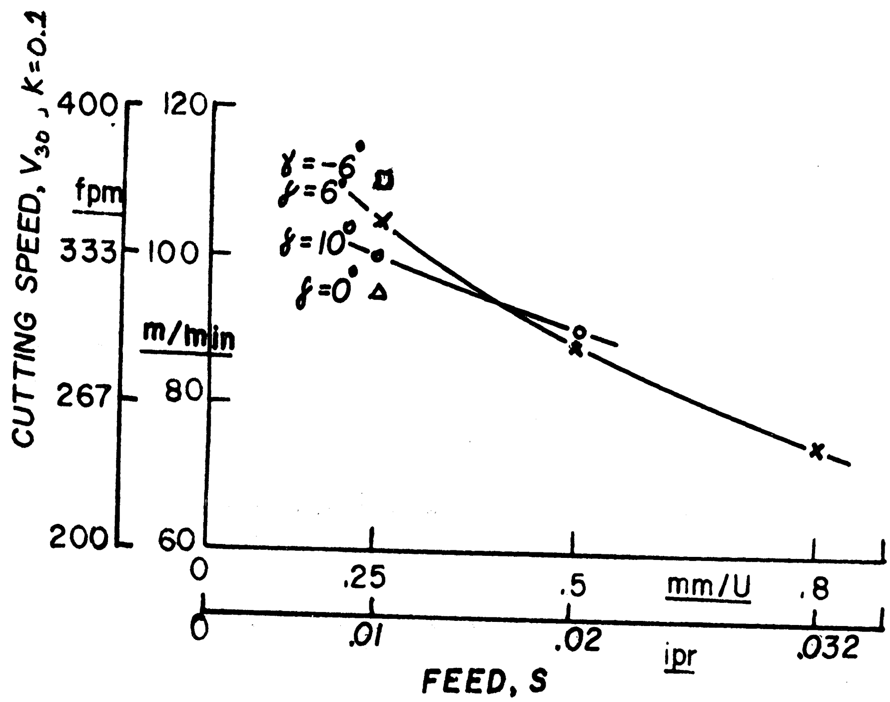

FIG. NO. 1-29

VB vs ϰ

CUTTING SPEED, V=80 m/min
WORK MATERIAL: XC 45
HEAT: Z0648
WORKING DIAMETER:
96–48 mm or 4–2 in
TOOL MATERIAL: CARBIDE P30
TEST NO. 2.1 4.1 5.1
SIZE OF CUT: 3 x 0.25 mm^2
= 0.12 x 0.01 in^2

TOOL GEOMETRY

α	γ	λ	ϰ	ε	r
6	6	0		90 88	0.8 mm 0.032 in

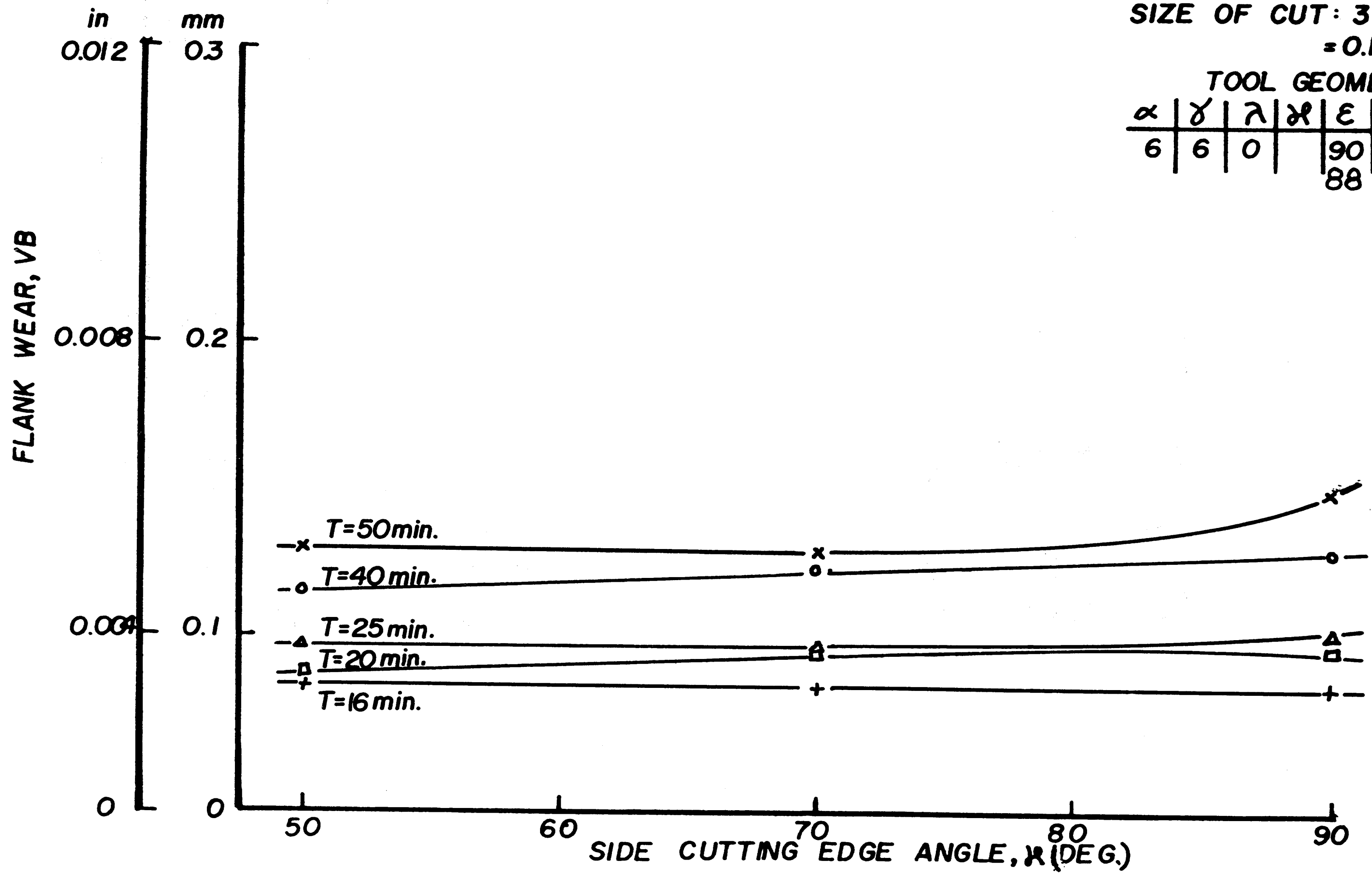

FIG. NO. 1–30

VB vs ϰ

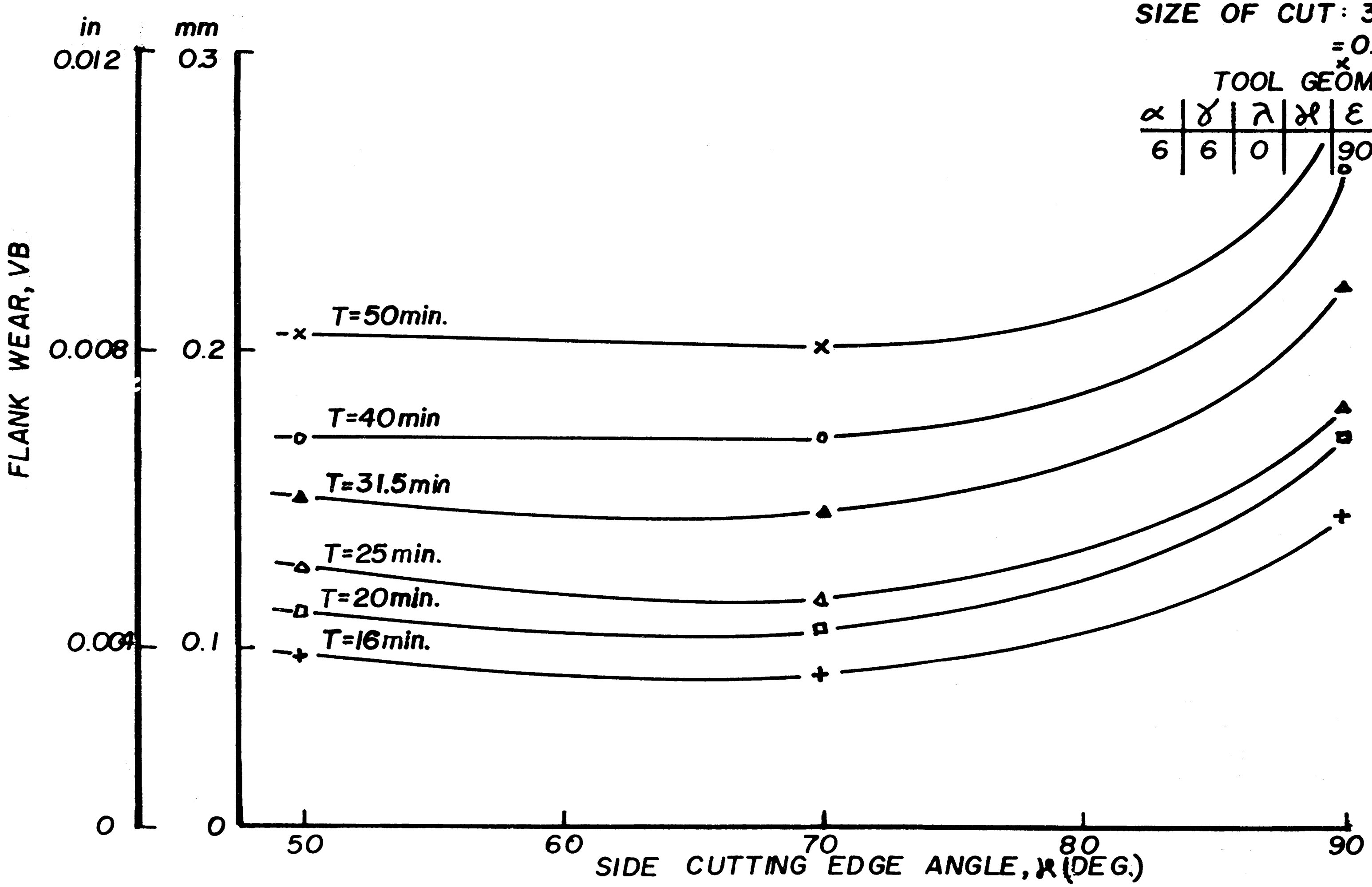

CUTTING SPEED, V=100 m/min.
WORK MATERIAL: XC 45
HEAT: Z0648
WORKING DIAMETER:
96–48 mm or 4–2 in
TOOL MATERIAL: CARBIDE P30
TEST NO. 2.1 4.1 5.1
SIZE OF CUT: 3 x 0.25 mm^2
= 0.12 x 0.01 in^2

TOOL GEOMETRY

α	γ	λ	ϰ	ε	r
6	6	0		90	0.8 mm 0.032 in

FIG. NO. 1-31

VB vs ϰ

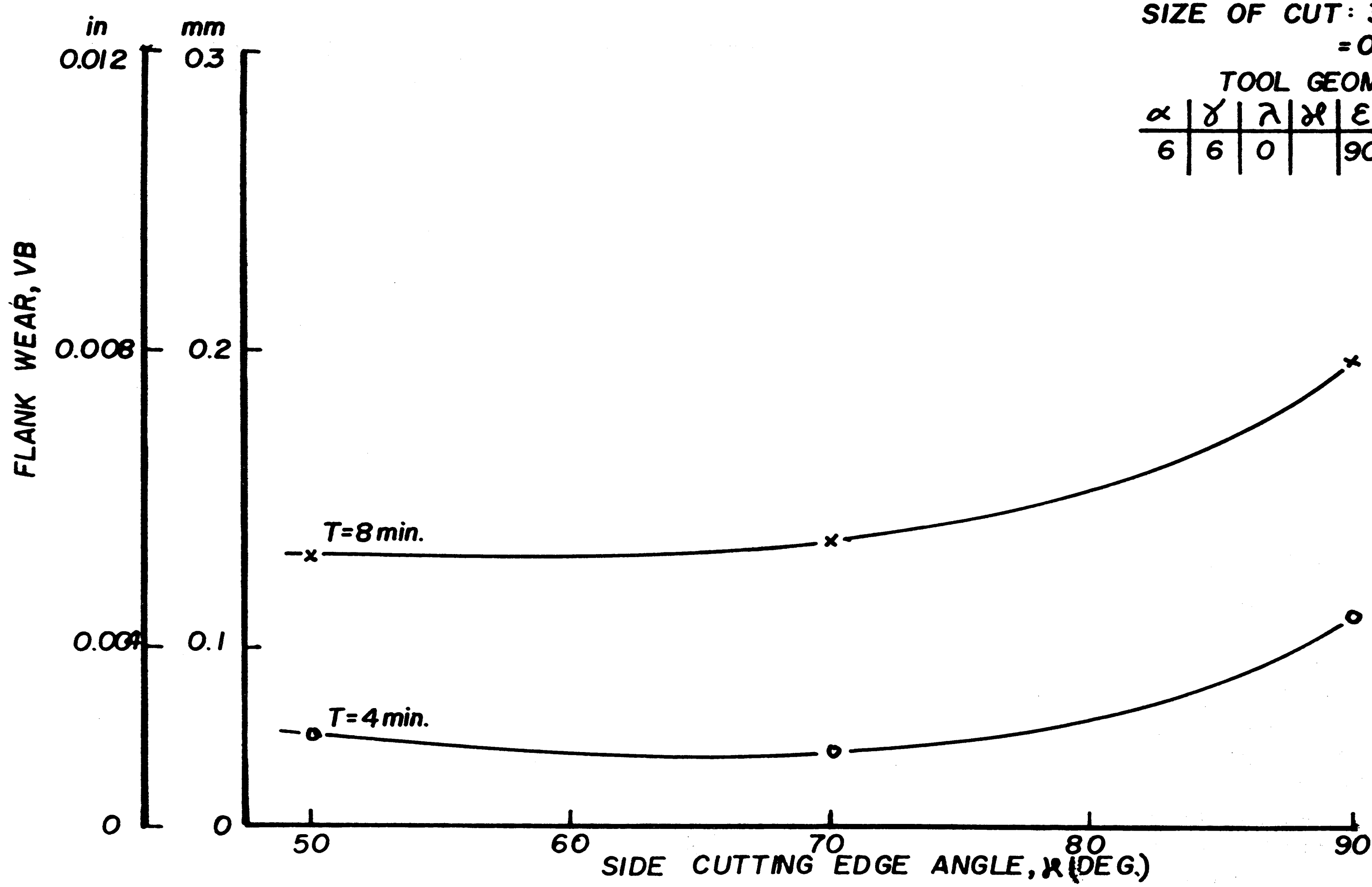

CUTTING SPEED, V=160 m/min.
WORK MATERIAL: XC 45
HEAT: Z0648
WORKING DIAMETER:
96–48 mm or 4–2 in
TOOL MATERIAL: CARBIDE P30
TEST NO. 2.1 4.1 5.1
SIZE OF CUT: $3 \times 0.25\ mm^2$
$= 0.12 \times 0.01\ in^2$

TOOL GEOMETRY

α	γ	λ	$\varkappa$	ε	r
6	6	0		90	0.8 mm 0.032 in

FIG. NO. 1–32

VB vs $\varkappa$

CUTTING TIME, T=8 min.
WORK MATERIAL: XC 45
HEAT: Z0648
WORKING DIAMETER:
96-48 mm or 4-2 in
TOOL MATERIAL: CARBIDE P30
TEST NO. 2.2 4.2 5.2
SIZE OF CUT: 3 x 0.5 mm^2
= 0.12 x 0.01 in^2

TOOL GEOMETRY

α	γ	λ	$\varkappa$	ε	r
6	6	0		90 88	0.8 mm 0.032 in

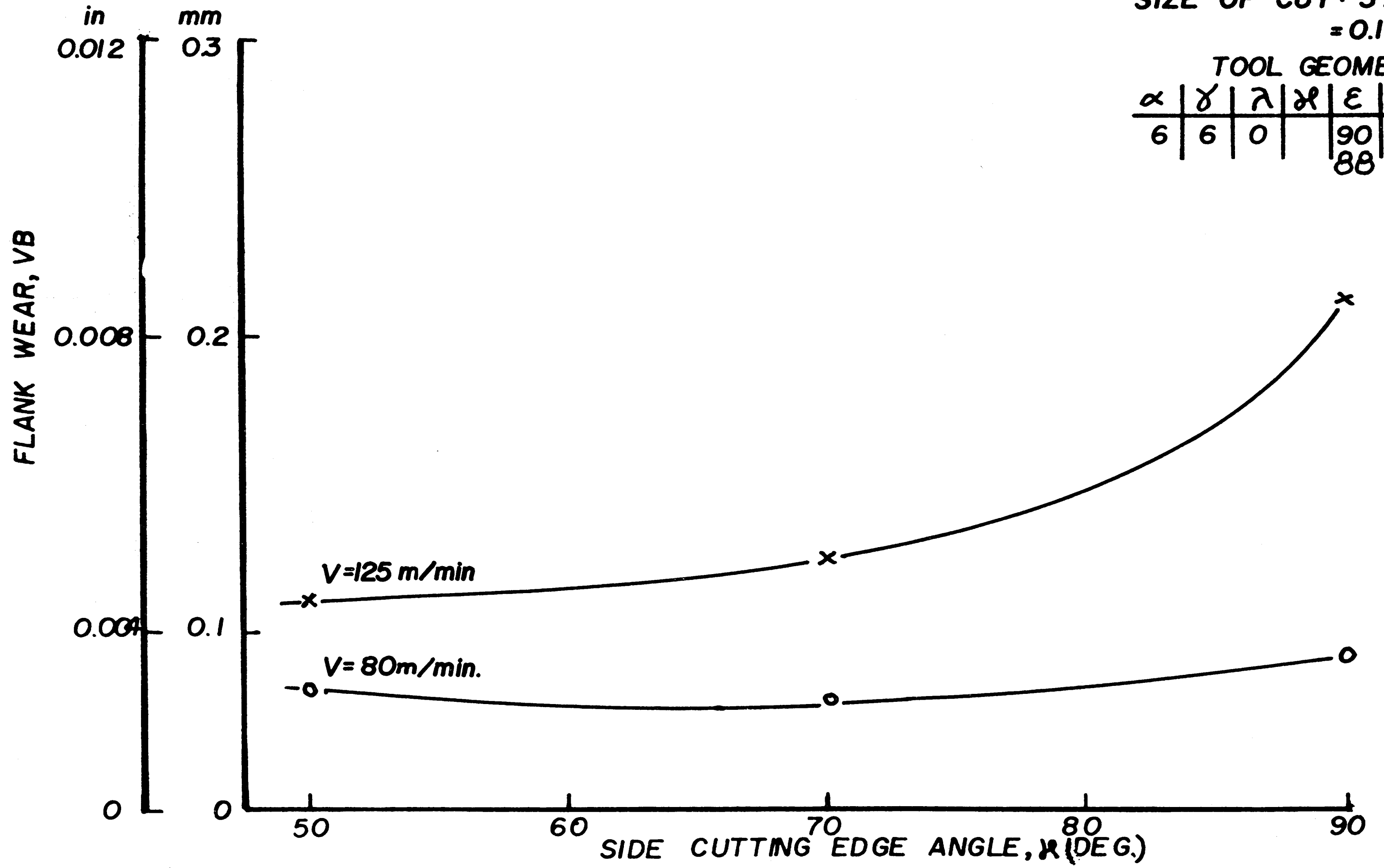

FIG. NO. 1-33

VB vs χ

CUTTING SPEED, V=80 m/min.
WORK MATERIAL: XC 45
HEAT: Z0648
WORKING DIAMETER:
96-48 mm or 4-2 in
TOOL MATERIAL: CARBIDE P30
TEST NO.2.3 4.3
SIZE OF CUT: 3 x 0.8 mm^2
= 0.12 x 0.01 in^2

TOOL GEOMETRY

α	γ	λ	χ	ε	r
6	6	0		90 88	0.8 mm 0.032 in

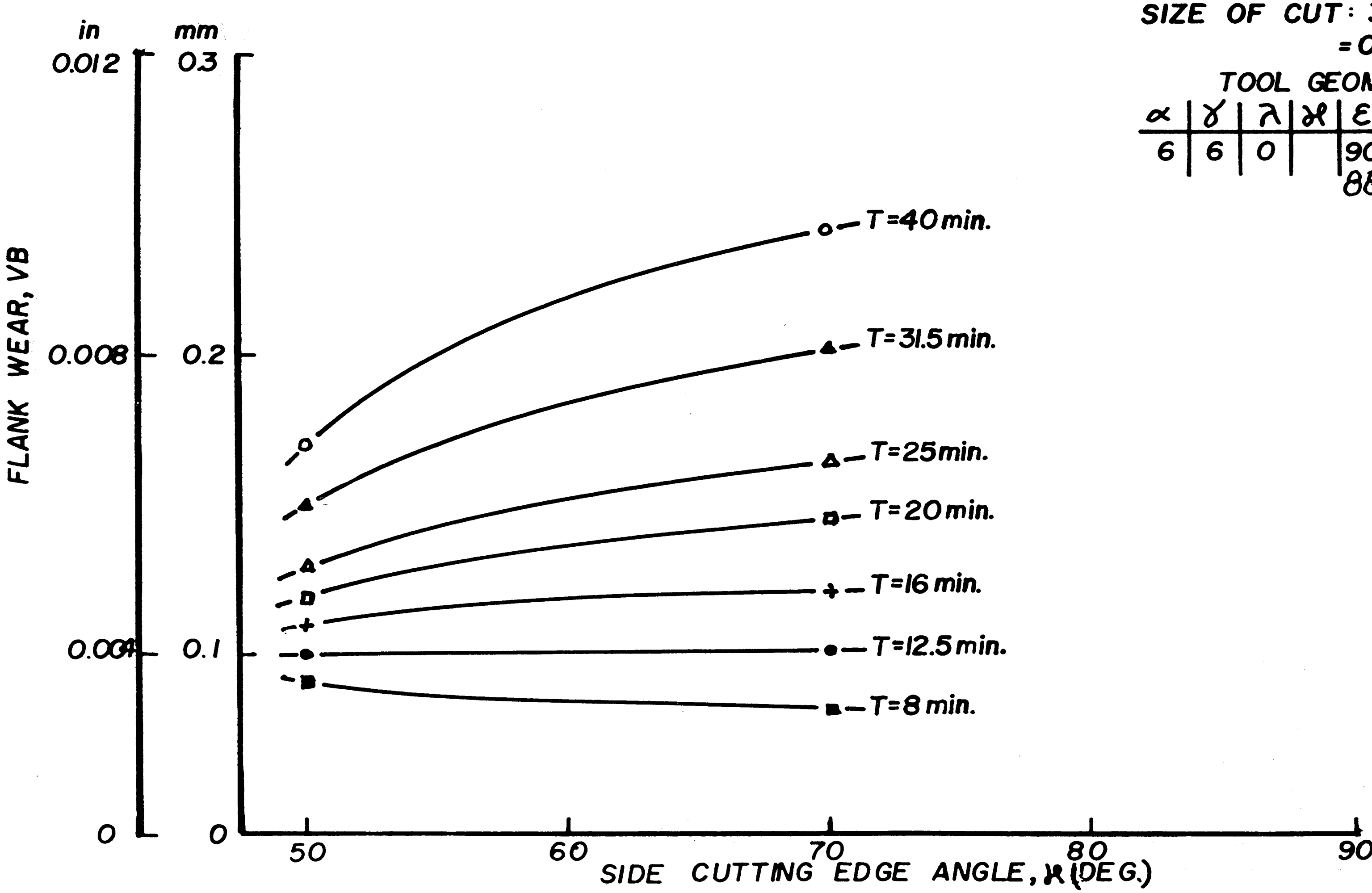

FIG. NO. 1-34

WORK MATERIAL: XC 45
TOOL MATERIAL: CARBIDE P30
TEST NO. 2.1 4.1 5.1
SIZE OF CUT: $3 \times 0.25\ mm^2$
$= 0.12 \times 0.01\ in^2$

TOOL GEOMETRY

α	γ	λ	ϰ	ε	r
6	6	0		90 88	0.8mm 0.032in

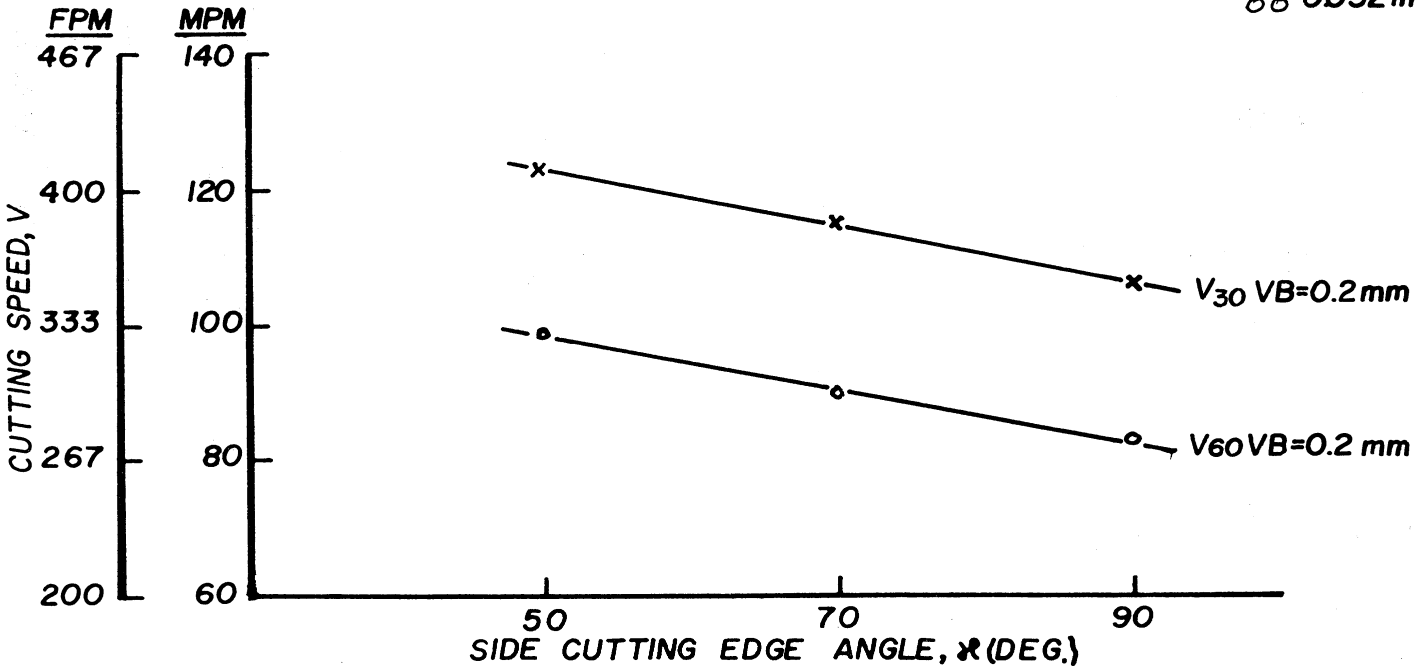

FIG NO. 1-35

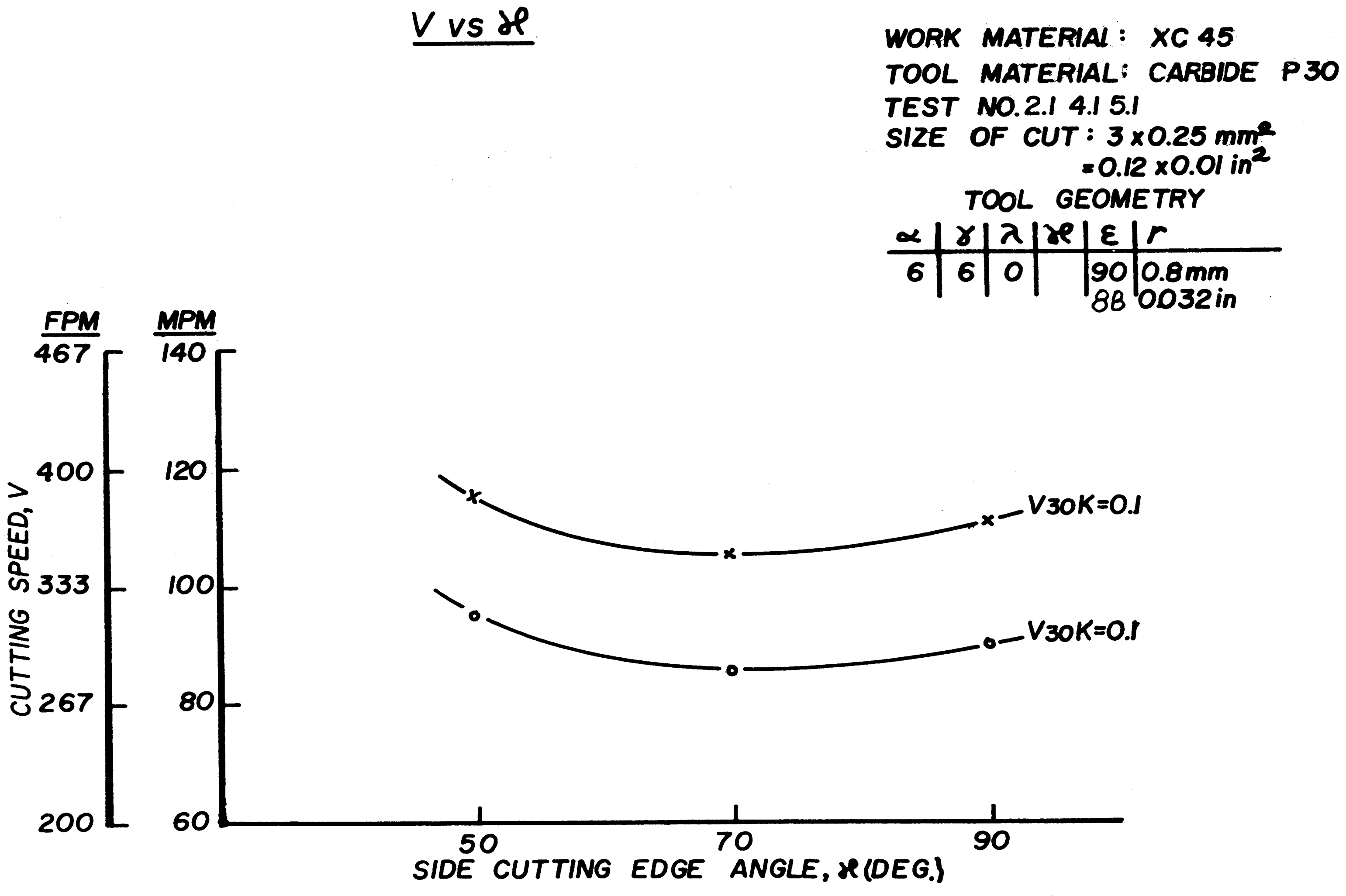
V vs ϰ
WORK MATERIAL : XC 45
TOOL MATERIAL: CARBIDE P30
TEST NO. 2.1 4.1 5.1
SIZE OF CUT : 3 x 0.25 mm²
= 0.12 x 0.01 in²
TOOL GEOMETRY
α | γ | λ | ϰ | ε | r
6 | 6 | 0 | | 90 | 0.8 mm
88 | 0.032 in
FPM
MPM
467
140
400
120
333
100
267
80
200
60
CUTTING SPEED, V
V30K=0.1
V30K=0.1
50
70
90
SIDE CUTTING EDGE ANGLE, ϰ (DEG.)

FIG NO. 1-36

V vs ϰ

WORK MATERIAL: XC 45
TOOL MATERIAL: CARBIDE P30
TEST NO. 2.1,2,3 4.1.2.3 5.1,2
SIZE OF CUT : 3 x Var. mm^2
= 0.12 x 0.01 in^2

TOOL GEOMETRY

α	γ	λ	ϰ	ε	r
6	6	0		90	0.8mm 0.032in

FIG NO. 1-37

V vs ϰ

WORK MATERIAL: XC 45
TOOL MATERIAL: CARBIDE P30
TEST NO. 2.1,2,3 4.1,2,3 5.1,2
SIZE OF CUT: 3 x Var. mm^2
= 0.12 x 0.01 in^2

TOOL GEOMETRY

α	γ	λ	ϰ	ε	r
6	6	0		90	0.8mm 0.032in

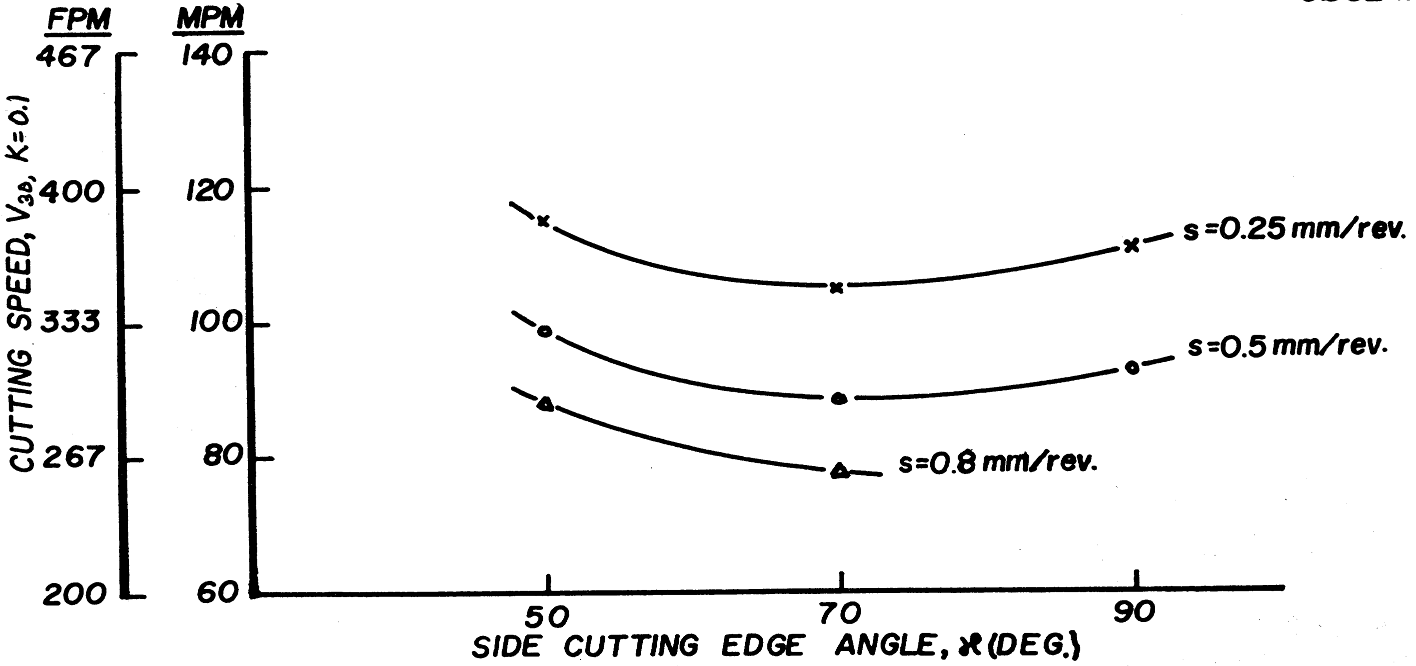

FIG NO.1-38

VB vs $\varkappa$

CUTTING SPEED, V=160 m/min.
WORK MATERIAL: XC 45
HEAT: Z0648
WORKING DIAMETER:
96–48 mm or 4–2 in
TOOL MATERIAL: CARBIDE P10
TEST NO. 10.1 12.1 13.1
SIZE OF CUT: 3 x 0.25 mm^2
= 0.12 x 0.01 in^2

TOOL GEOMETRY

α	γ	λ	$\varkappa$	ε	r
6	6	0		90	0.8 mm 0.032 in

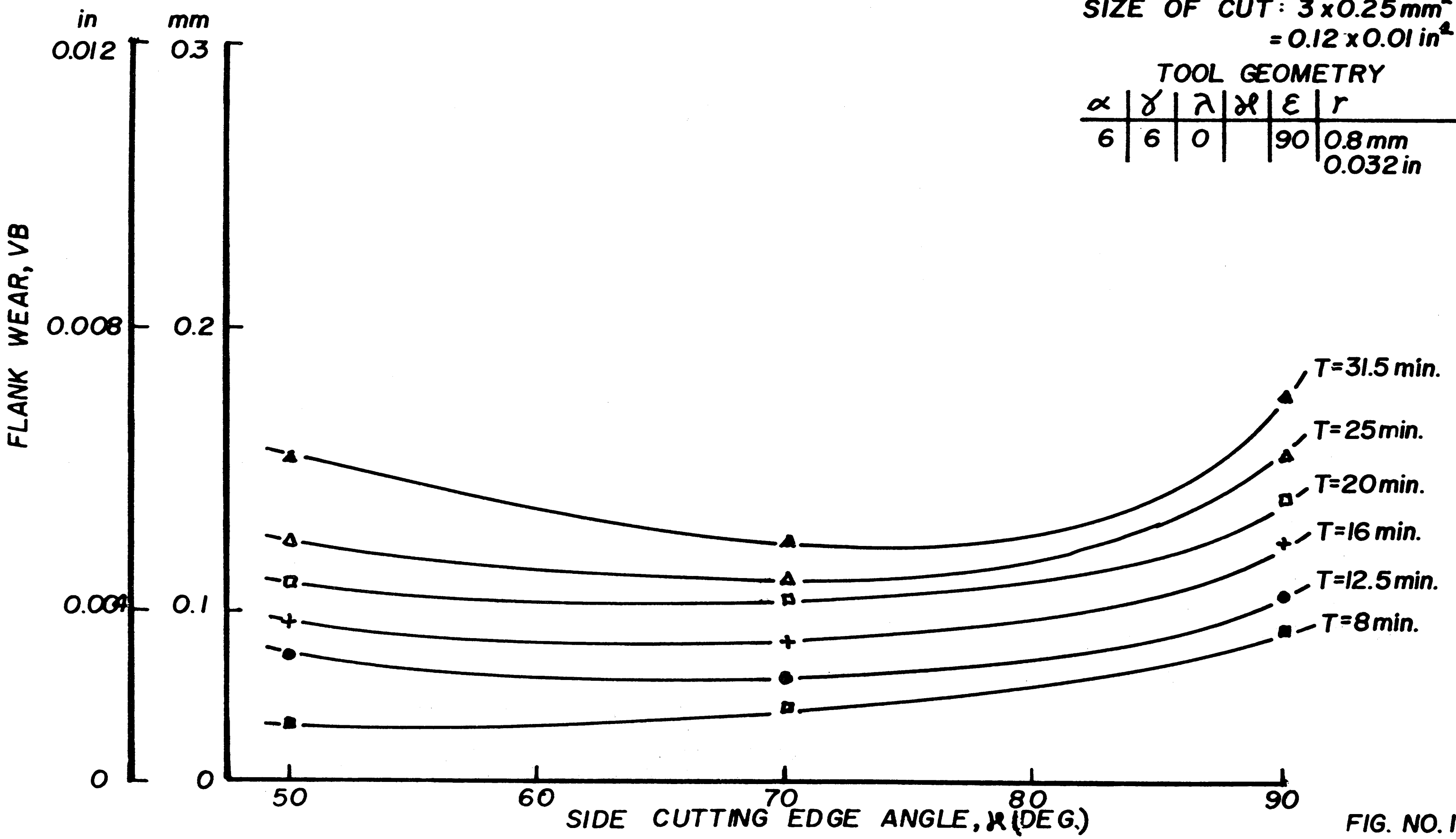

FIG. NO. 1-39

CUTTING SPEEDS FOR 30min. TOOL LIFE

WORK MATERIAL: XC 45

TOOL MATERIAL: CARBIDE P10/P30

SIZE OF CUT : 3x0.25 mm^2 = 0.12x0.01 in^2

TEST NO. 1.1 2.1 3.1 6.1,2,3 7.1 10.1 12.1 14.1,2,3 15.1

TOOL GEOMETRY

α	γ	λ	$\varkappa$	ε	r
6		0 -6	70	90	0.8 mm .0 32 in

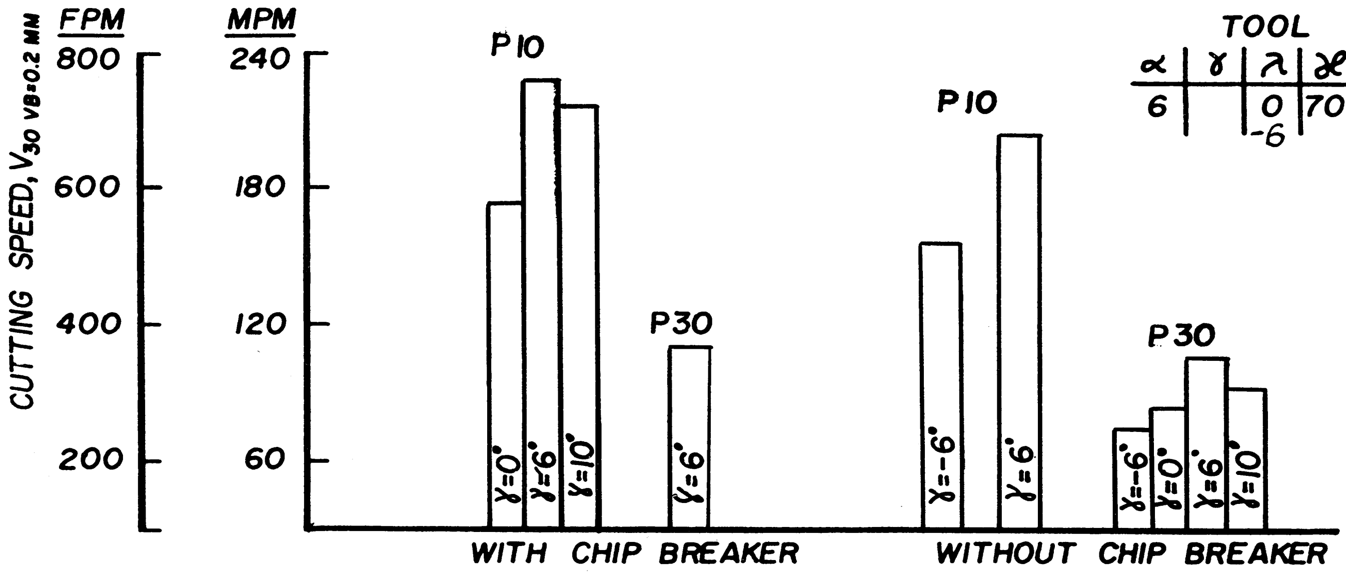

FIG. NO. 1-40

CUTTING SPEEDS FOR 30min. TOOL LIFE

WORK MATERIAL: XC 45

TOOL MATERIAL: CARBIDE P10/P30

SIZE OF CUT: $3 \times 0.25\ mm^2 = 0.12 \times 0.01\ in^2$

TEST NO. 1.1 2.1 3.1 6.1,2,3 7.1 10.1 12.1 14.1,2,3 15.1

TOOL GEOMETRY

α	γ	λ	$\varkappa$	ε	r
6		0 -6	70	90	0.8 mm .032 in

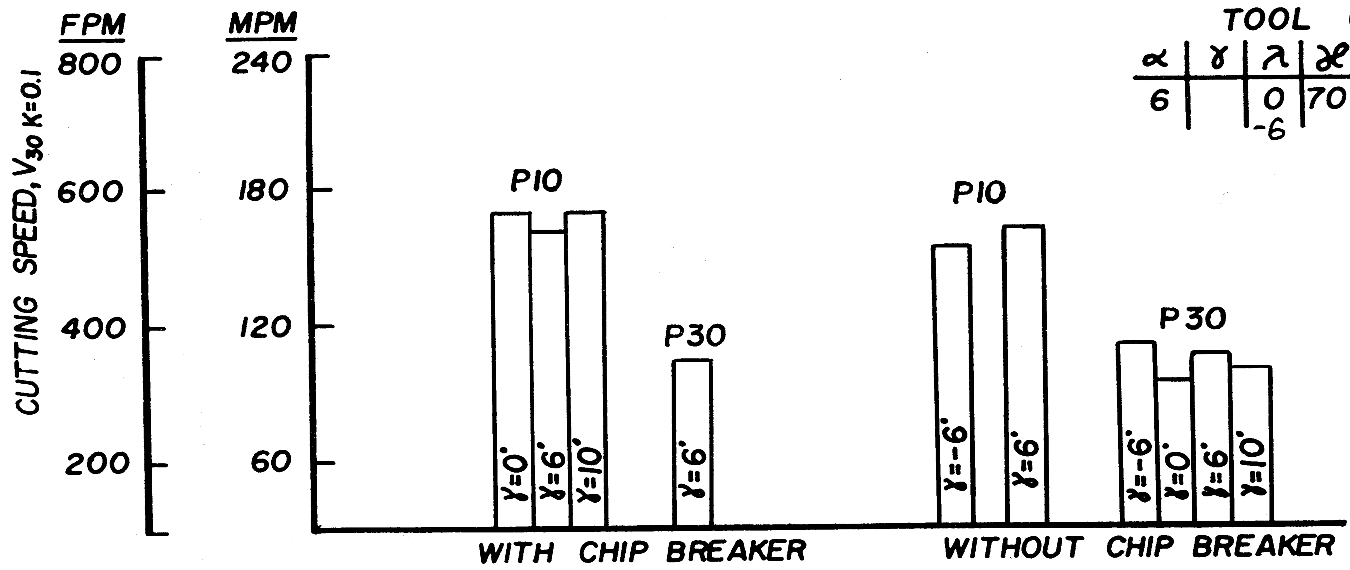

FIG. NO.1-41

TOOL LIFE vs CUTTING SPEED

WORK MATERIAL: XC 45
TOOL MATERIAL: CARBIDE P 30
SIZE OF CUT: $3 \times 0.25 mm^2$
$= 0.12 \times 0.01 in^2$
TEST NO. 6.2

TOOL GEOMETRY

α	γ	λ	ϰ	ε	r
6	6	0	70	90	0.8 m .032 in

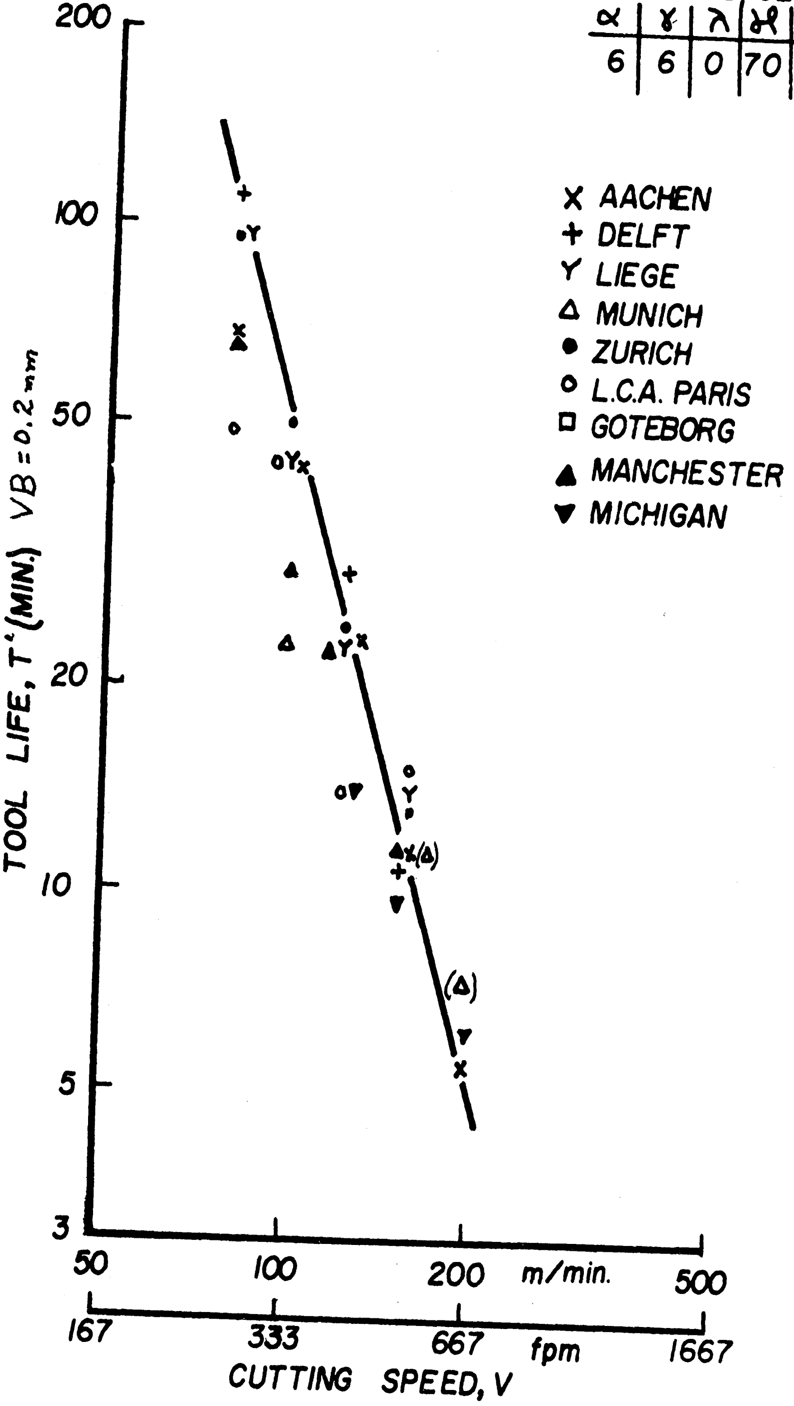

FIG. NO. 1-42

TOOL LIFE vs CUTTING SPEED

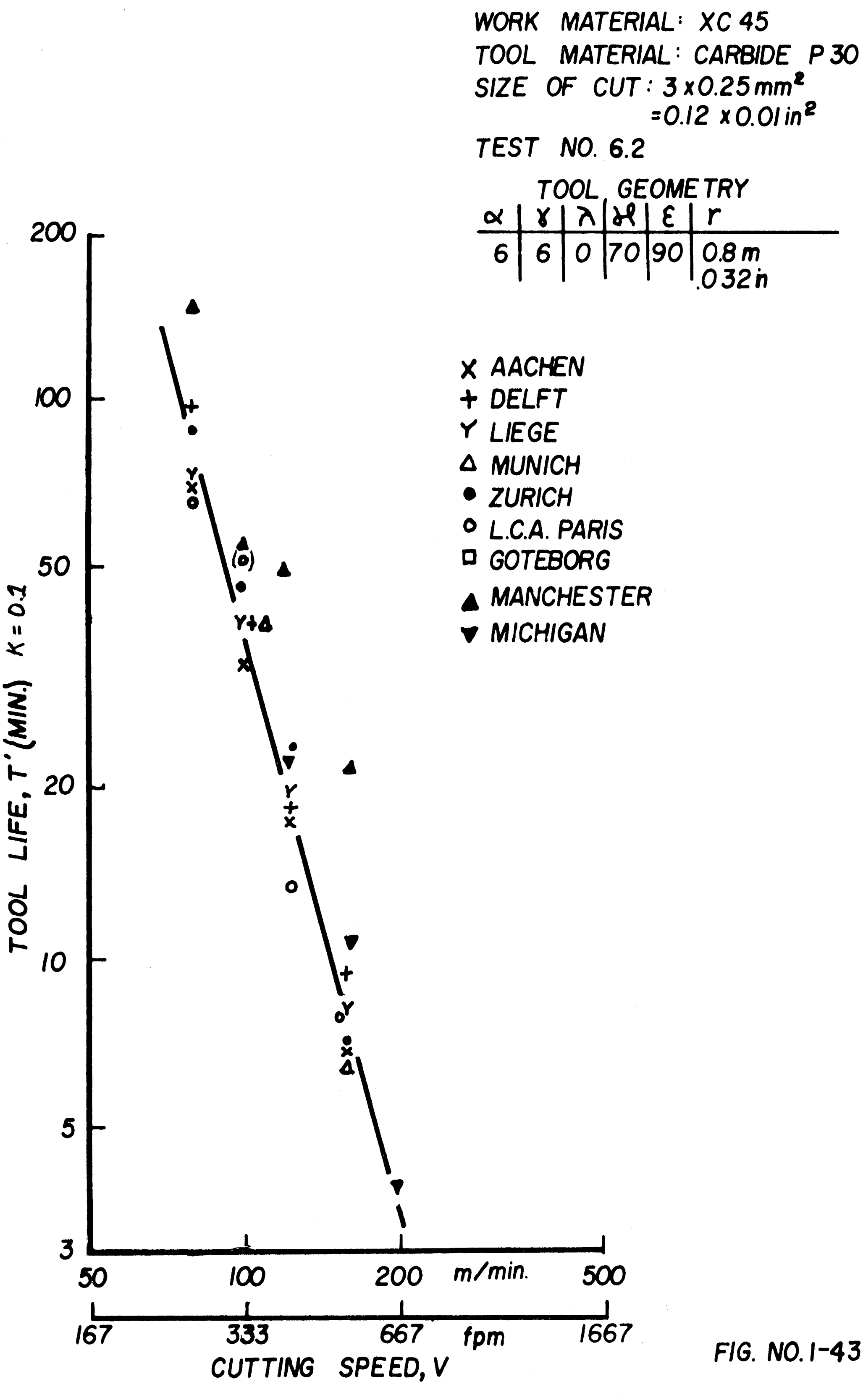

FIG. NO. 1-43

TOOL LIFE vs CUTTING SPEED

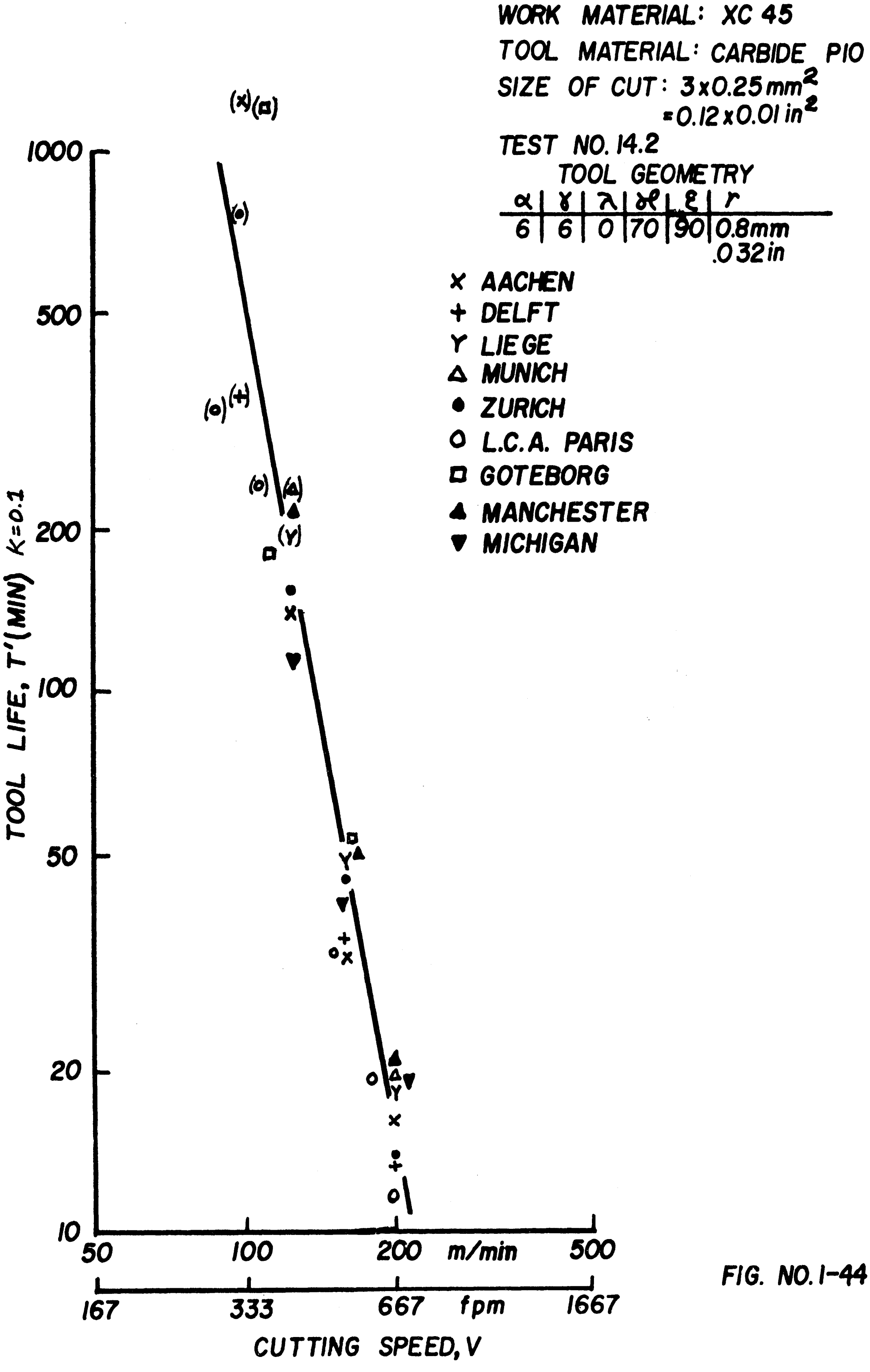

FIG. NO. 1-44

TOOL LIFE vs CUTTING SPEED

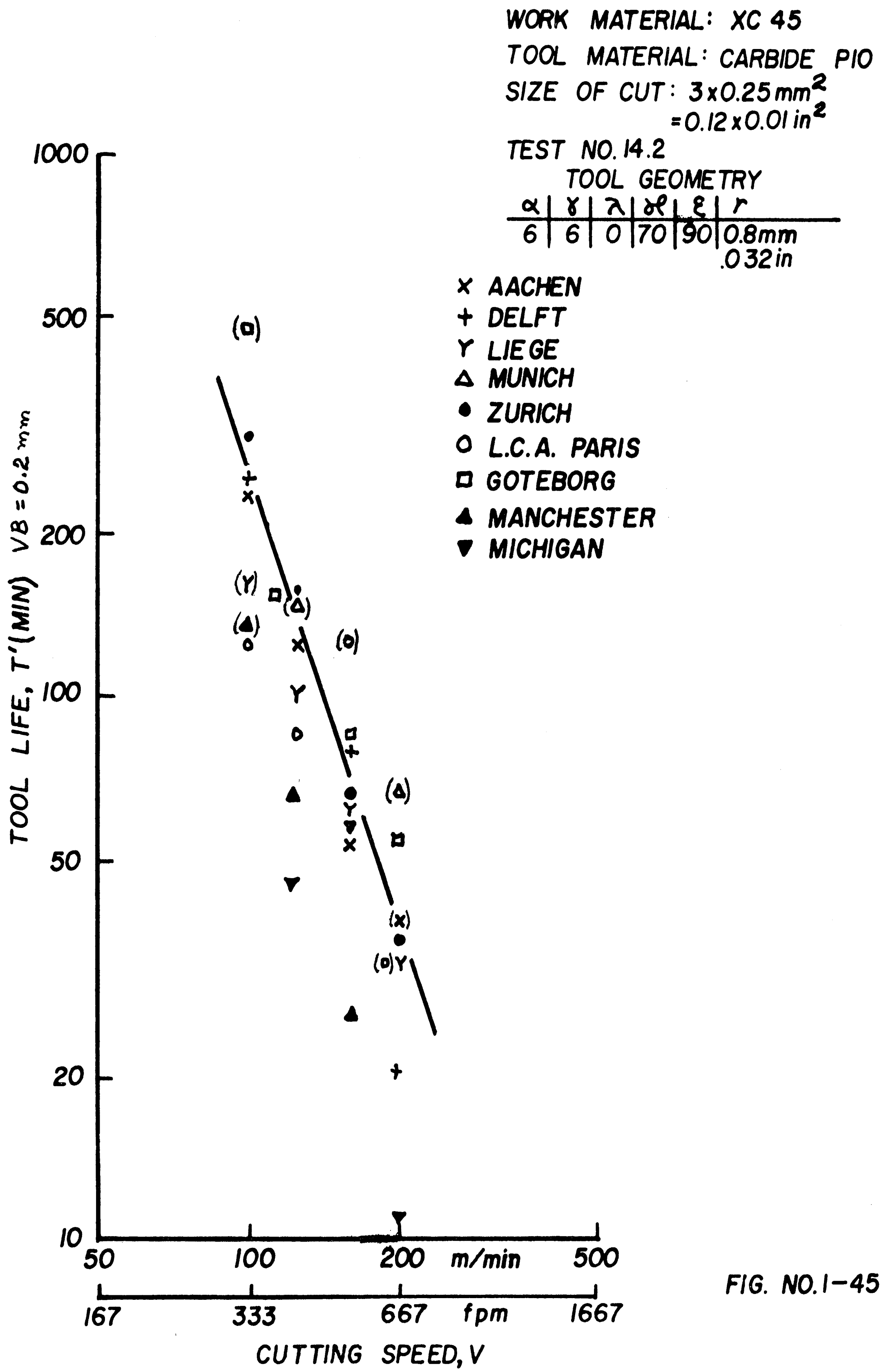

FIG. NO. 1-45

PART II

REPEATABILITY OF WEAR MEASUREMENTS BETWEEN LABORATORIES

Up to this time two formal attempts have been made to ascertain the degree of reliability or repeatability of tool-wear measurements between the participating laboratories. Both investigations have been coordinated by Professor Pekelharing at the University of Delft and the results were reported out, respectively, in 1963 and 1965.

The first study involved only five laboratories all of which measured all eight of the same group of eight worn carbide tools. The results are summarized in Table 2.1. The figures within parentheses in the left-hand column refer to the desired resolution of measuring instruments and to the units reported. The tool "edge code numbers" refer to the system illustrated in Fig. 9 of Interim Report No. 1 while the dimensions measured are shown in Fig. 11 of the same report.

It is suggested that some of the dispersion or scatter shown in Table 2.1 is due to human judgement in making measurements. Such judgment as must be exercised in the measuring of actual tools tends to mask errors arising out of the equipment itself. Consequently a second series of tests was carried out with simulated tools prepared at the University of Delft.

SIMULATED TOOLS (2nd Series)

Sixteen slices of hardened steel were bolted together and the contours of the artificial wear marks were ground (see Fig. 2.1). Inspection revealed that the dimensions of the wear marks were uniform to an accuracy of within 0.01 mm. The bolts were then loosened and the slices numbered from 1 to 16 inclusive and the edges marked A and B (see Fig. 2.1).

Some laboratories used different devices to measure the dimensions and some tools were measured by more than one institute. Therefore, the cutting surface was given a number and a letter if more than one institute used it. Table 2.2 lists the institutions and identifies the type of measuring devices used by them.

RESULTS (2nd Series)

The results of the data obtained by the respective institutes are compiled in Table 2.3 and graphically presented in Figs. 2.2 through 2.4. Important deviations are summarized in Table 2.4.

A further analysis leads to the tentative conclusion that equipment using physical contact with diamonds or similar devices may be responsible for some of the larger deviations. At least two of the tools (those measured in London and Michigan) had grinding burrs which confuse some of the measurements. It is easier to avoid the influence of burrs and similar hazards by optical techniques where they can be recognized. It is possible also that the included angles of tracer styli tend to mask boundaries such as the edges of tools.

The simulated tools will be retained by the various laboratories as reference standards since the deviations from the averages shown in Table 2.3 seem to be under control. Some institutions, especially those using tracer equipment, will have to be especially careful in interpreting certain measurements.

TABLE 2.1

TOOL WEAR MEASUREMENTS

(Average, minimum, and maximum values of tool wear measurements obtained by Aachen (A), Kapfenberg (K), Zurich (Z), Torino (T), and Delft (D) on 8 worn carbide tool edges from Delft are given below.)

Dimension	Edge 5-1					Edge 5-3					Edge 6-1					Edge 6-3				
	Average	Minimum	By	Maximum	By	Average	Minimum	By	Maximum	By	Average	Minimum	By	Maximum	By	Average	Minimum	By	Maximum	By
VB (0.01 mm)	17.2	15.3	T	18.86	K	20.8	15.6	T	23.5	A	22.1	20.8	T	23.0	A	20.8	16.8	T	22.4	D
VB max. (0.01 mm)	23.0	20.6	T	24.5	Z	36.6	26.0	A	36.0	Z	29.4	26.5	T	31.0	A	27.6	25.8	T	28.9	D
KS (0.001 mm)	3.4	1.0	D	5.5	Z	2.9	2.0	A-Z	3.7	T	2.8	1.5	A	3.8	T	1.9	1.0	D-Z	3.0	T
KT (0.001 mm)	421.0	384.0	T	460.0	Z	319.0	296.0	T	350.0	Z	463.0	408.0	T	490.0	D-T	311.0	279.0	T	350.0	Z
KM (0.001 mm)	754.0	619.0	Z	800.0	A	867.0	673.0	K	940.0	Z	903.0	738.0	K	955.0	T	1104.0	803.4	K	1210.0	Z
KT/KM	0.576	0.504	T	0.648	K	0.373	0.328	T	0.456	K	0.503	0.437	T	0.533	K	0.288	0.235	T	0.3696	K
KB (0.01 mm)	128.0	121.1	T	144.0	D	131.1	126.0	A	134.6	Z	145.7	142.0	D	147.5	K	159.0	157.8	T	160.68	K

Dimension	Edge 7-1					Edge 7-3					Edge 8-1					Edge 8-3				
	Average	Minimum	By	Maximum	By	Average	Minimum	By	Maximum	By	Average	Minimum	By	Maximum	By	Average	Minimum	By	Maximum	By
VB (0.01 mm)	24.1	22.3	D	26.0	T	22.7	20.8	T	24.0	A	21.0	18.0	T	23.0	A	19.3	16.2	T	21.0	A
VB max. (0.01 mm)	31.7	29.4	T	33.4	D	29.6	27.8	K	32.0	D	25.0	19.2	T	28.0	D	30.0	25.0	T	33.6	D
KS (0.001 mm)	2.8	2.0	D	3.4	Z	4.1	3.0	D-A	5.2	Z	3.5	1.0	D	5.5	Z	4.0	3.0	D-A	6.3	T
KT (0.001 mm)	525.0	473.0	T	560.0	A	351.3	318.0	T	380.0	Z	460.0	407.0	T	490.0	Z	333.0	305.0	T	370.0	Z
KM (0.001 mm)	889.0	743.7	K	960.0	Z	1043.0	792.1	K	1157.0	Z	781.0	635.0	K	840.0	D	881.0	666.9	K	956.0	T
KT/KM	0.594	0.509	T	0.6862	K	0.345	0.286	T	0.4276	K	0.568	0.499	T	0.6493	K	0.385	0.319	T	0.4828	K
KB (0.01 mm)	145.5	142.0	D	150.0	A	157.0	155.0	D	160.0	A	126.9	125.0	D	129.0	A	133.4	133.0	D-A	134.0	Z

TABLE 2.2

PARTICIPATING LABORATORIES AND EQUIPMENT USED

Tool No.	Laboratory	Equipment
1	Delft (Netherlands)	A, B, VB', KB, KL: toolmakers' microscope amplification 30x KM, KT; Talysurf amplification: vertical 200x; horizontal 20x
2a	Aachen (Germany)	A, B, VG', KB, KL: toolmakers' microscope A, KB, KM, KL, KT: Leitz-Forster
2b	London	First reading
2c	London	One day later
3a	Kapfenberg (Austria)	KT: Leitz-Forster all other sizes: Stereo microscope with ocular micrometer magnification rx and for KL 100x
3b	Aachen	Same as 2b
4	Zurich	Schmaltz-lightsection microscope on a SIP universal measuring machine MU 214 B
5a	Chippendale (Austria)	Light section microscope of own design
5b	Chippendale	Profile projection method
7	Goteborg (Sweden)	Talysurf and toolmakers' microscope
8	Leige	A, B, VB', KB, KL: toolmakers' microscope KT: Forster-Leitz
9a	Manchester (England)	Microscope
9b	Manchester	Talysurf
9c	Manchester	Talysurf and microscope, readings one month later
10	Saint-Ouen	B, VB': SIP measuring machine MU 214 B other sizes: Perthometer
11a	Arcueil (France)	SIP measuring machine MU 214 B
11b	Arcueil	A, B, VB', KB, KL: toolmakers' microscope magnification 13x; KT, KM: Schmaltz light section microscope
12a	Torino (Italy)	SIP measuring machine MU 214 B
12b	(Torino	A, B: optical comparator Microtechnica magnification 50x; VB', KB, KM, KL, KT: optical micrometer (Galileo) magnification 50x
12c	Michigan (U of M)	Toolmakers' microscope
12d	Michigan	Proficorder
15	Kapfenberg	Same as 3
16a	Delft	Same as 1
16b	Pittsburgh (Carnegie Tech.)	Profile recorder and measuring microscope

TABLE 2.3

MEASUREMENTS ON SIMULATED TOOLS

Tool No.	Edge A (see Fig. 2.1) A Size	A Dev.	B Size	B Dev.	VB' Size	VB' Dev.	KB Size	KB Dev.	KM Size	KM Dev.	KL Size	KL Dev.	KT Size	KT Dev.
1	3.14	+15	2.02	+10	1.63	+38	1.46	+13	0.75	- 7	0.19	+ 7	0.224	- 6
2a	3.2	++	2.0	-10	1.59	- 2	1.53	++	0.84	++	0.2	+17	0.26	++
2b	3.125	0	2.017	+ 7	1.610	+18	1.447	0	0.767	+10	0.175	- 8	0.231	+ 1
2c	3.121	- 4	2.020	+10	1.607	+15	1.444	- 3	0.757	0	0.178	- 5	0.233	+ 3
3a	3.110	-15	1.990	-20	1.579	-13	1.442	- 5	0.815	++	0.187	+ 4	0.231	+ 1
3b	3.115	-10	1.995	-15	1.555	-37	1.458	- 8	0.730	-27	0.185	+ 2	0.229	- 1
4	3.124	- 1	2.016	+ 6	1.601	+11	1.444	- 1	0.76	+ 3	0.185	+ 2	0.227	- 3
5a	3.124	- 1	2.012	+ 2	1.570	-22	1.450	+ 3	0.759	+ 2	0.180	- 3	0.236	+ 6
5b	3.129	+ 4	2.012	+ 2	1.567	- 25	1.450	+ 3	0.750	+ 2	0.180	- 3	0.236	+ 6
7	3.12	- 5	0.01	0	1.58	-12	1.44	- 7	0.76	+ 3	0.18	- 3	0.225	- 5
8	3.128	+ 3	2.018	+ 8	1.595	+ 3	1.458	+11	0.783	+26	0.170	-13	0.224	- 6
9a	3.136	+11	2.019	+ 9	1.585	- 7	1.435	-12	-	-	0.162	-21	-	-
9b	3.161	+36	-	-	-	-	1.445	- 2	0.744	-13	0.225	+42	0.208	-
9c	3.130	+ 5	2.010	0	1.579	-13	1.371	-	0.284	-	-	-	0.286	++
10	3.110	-15	2.066	- 4	1.577	-15	1.440	- 9	0.780	+23	0.180	-3	0.230	0
11a	3.111	-14	2.006	- 4	1.579	-13	1.441	- 8	0.76	+ 3	0.169	-14	0.233	+ 3
11b	3.116	- 9	2.006	- 4	1.580	-12	1.441	- 8	0.745	-12	0.171	-12	0.227	- 3
12a	3.126	+ 1	2.005	- 5	1.513	-	1.427	-20	0.749	- 8	0.176	- 7	0.230	0
12b	3.132	+ 7	2.104	++	1.526	-	1.450	+ 3	0.790	+33	0.178	- 5	0.237	- 7
12c	3.116	- 9	2.008	- 2	1.577	-15	1.450	+ 3	0.764	+ 7	0.173	-10	0.239	+ 9
12d	3.185	++	2.027	+17	1.603	+11	1.476	+29	0.752	+ 7	0.170	-13	0.236	+ 6
15	3.122	-13	1.988	-22	1.574	-18	1.438	-11	0.726	-31	0.185	+ 2	0.231	+ 1
16a	3.13	+ 5	2.02	- 8	1.62	+28	1.45	+ 3	0.76	+ 3	0.20	+17	0.225	- 5
16b	3.12	- 5	2.07	- 8	1.62	+28	1.44	- 7	0.740	-17	0.180	- 3	0.234	+ 4
Avg.	3.125		2.010		1.592		1.447		0.757		0.183		0.230	

Tool No.	Edge B A Size	A Dev.	B Size	B Dev.	VB' Size	VB' Dev.	KB Size	KB Dev.	KM Size	KM Dev.	KL Size	KL Dev.	KT Size	KT Dev.
1	2.96	-12	1.92	+ 8	1.84	+14	0.93	- 8	0.52	- 6	0.14	- 2	0.061	- 2
2a	2.95	-22	1.9	-12	1.8	-26	0.88	-	0.52	- 6	0.14	- 2	0.066	+ 5
2b	2.957	-15	1.914	+ 2	1.798	-28	0.935	- 3	0.507	-19	0.122	-20	0.066	+ 5
2c	2.954	-18	1.914	+ 2	1.804	-22	0.936	- 2	0.507	-19	0.128	-14	0.067	+ 4
3a	2.956	-16	1.916	+ 4	1.818	- 8	0.943	+ 5	0.538	+12	0.143	+ 1	0.064	+ 1
3b	2.960	-12	1.900	-12	1.820	- 6	0.935	- 3	0.540	-14	0.135	- 7	0.067	+ 6
4	2.969	- 3	1.918	+ 6	1.839	+13	0.942	+ 4	0.538	+12	0.135	- 7	0.063	0
5a	2.974	+ 2	1.910	- 2	1.808	-18	0.937	- 1	0.544	+18	0.157	+15	0.058	- 5
5b	2.972	0	1.913	+ 1	1.808	-18	0.942	+ 4	0.541	+15	0.150	+ 8	0.061	- 2
7	2.96	-12	1.91	- 2	1.83	+ 4	0.94	+ 2	0.53	+ 4	0.15	+ 8	0.060	- 3
8	2.965	- 7	1.908	- 4	1.835	+ 9	0.938	0	0.520	- 6	0.137	- 5	0.064	+ 1
9a	2.969	- 3	1.928	+16	1.851	+25	0.944	+ 6	-	-	0.126	-16	-	-
9b	3.02	+48	-	-	-	-	0.949	+11	0.492	-34	0.161	+19	0.032	-
9c	2.790	- 2	1.927	+15	1.838	+12	0.939	+ 1	0.380	-	-	-	0.081	++
10	2.970	- 2	1.910	- 2	1.834	+ 8	0.940	+ 2	0.530	+ 4	0.150	+ 8	0.060	- 3
11a	2.964	- 8	1.903	- 9	1.828	- 4	0.932	- 6	0.53	+ 4	0.123	-19	0.065	+ 2
11b	2.964	- 8	1.903	- 9	1.823	- 3	0.934	- 4	0.525	- 1	0.138	- 4	0.061	- 2
12a	2.986	+14	1.910	- 2	-	-	0.931	- 7	0.536	+10	0.172	+30	0.062	- 1
12b	3.004	+32	1.925	+13	1.844	+18	0.940	+ 2	0.511	-15	0.152	+10	0.070	+ 7
12c	2.958	-14	1.902	-10	1.823	- 3	0.943	+ 5	0.535	+ 9	0.138	- 4	0.064	+ 1
12d	3.018	+46	1.920	+ 8	1.864	+38	0.958	+20	0.554	+28	0.135	- 7	0.064	+ 1
15	2.957	-17	1.918	+ 6	1.819	- 7	0.943	+ 5	0.525	- 1	0.144	+ 2	0.063	0
16a	2.98	+ 8	1.91	- 2	1.83	+ 4	0.93	- 8	0.53	+ 4	0.15	+ 8	0.060	- 3
16b	2.969	- 3	1.77	-	1.68	-	0.942	+ 4	0.515	-11	0.142	0	0.064	+ 1
Avg.	2.972		1.912		1.826		0.938		0.526		0.142		0.063	

TABLE 2.4

IMPORTANT DEVIATIONS

Tool No.	Laboratory	Defaults On Edge A	Defaults On Edge B
2a	Aachen	VB' + KB + KM +	KB -
3a	Kapfenberg	KM +	
9b	Manchester	KT -	KT -
9c	Manchester	KB - KM - KT +	KM - KT +
12a	Torino	VB'	
12b	Torino	B + VB' -	
12d	Michigan	A +	
16b	Pittsburgh		B - VB' -

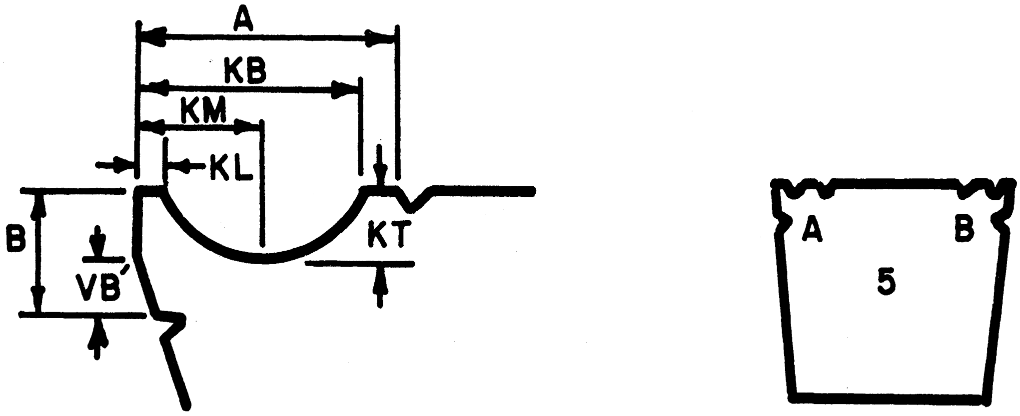

TOOL INSERT PROFILE

FIG. 2.1

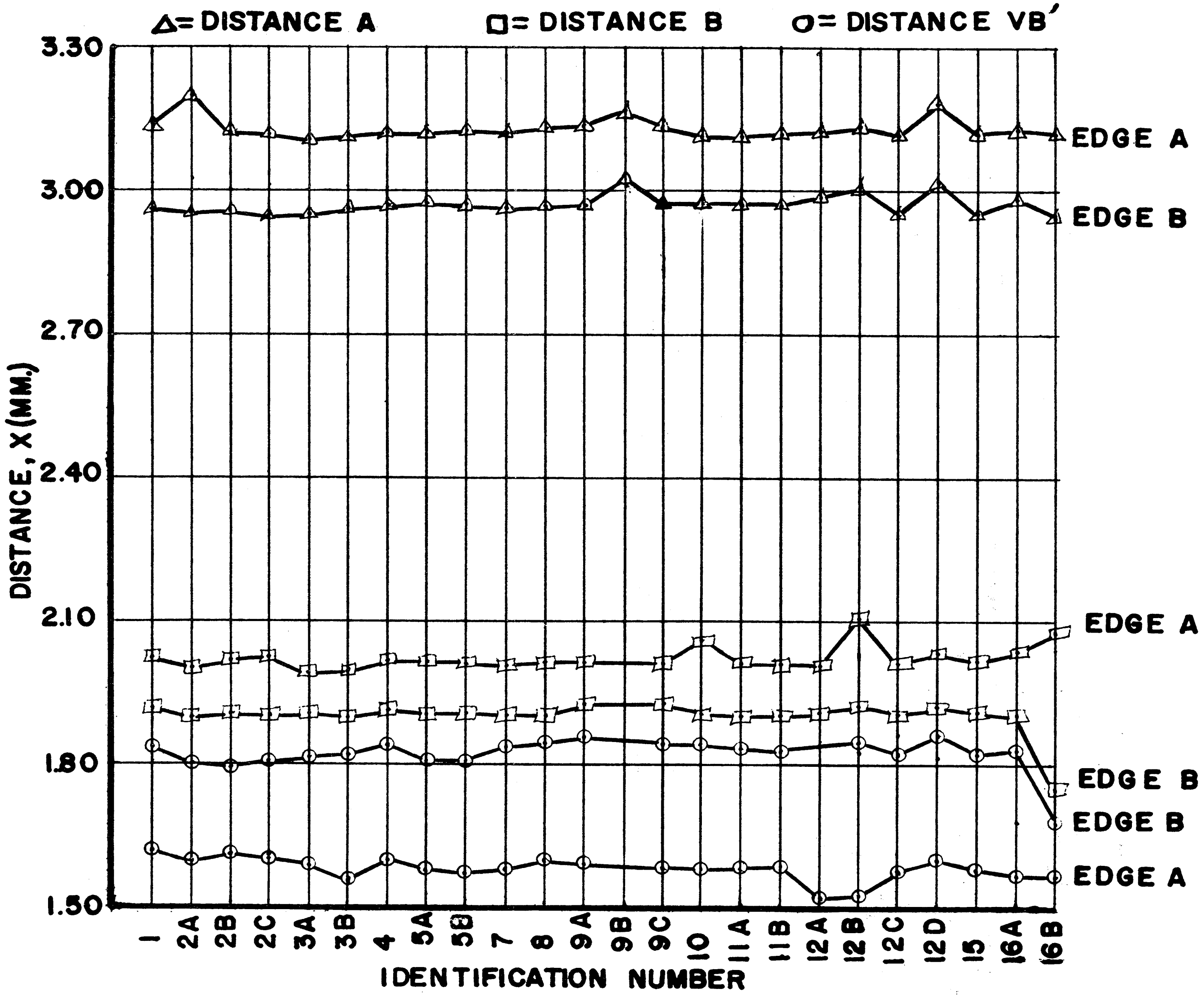

COMPARATIVE TOOL WEAR MEASUREMENTS

FIG. 2.2

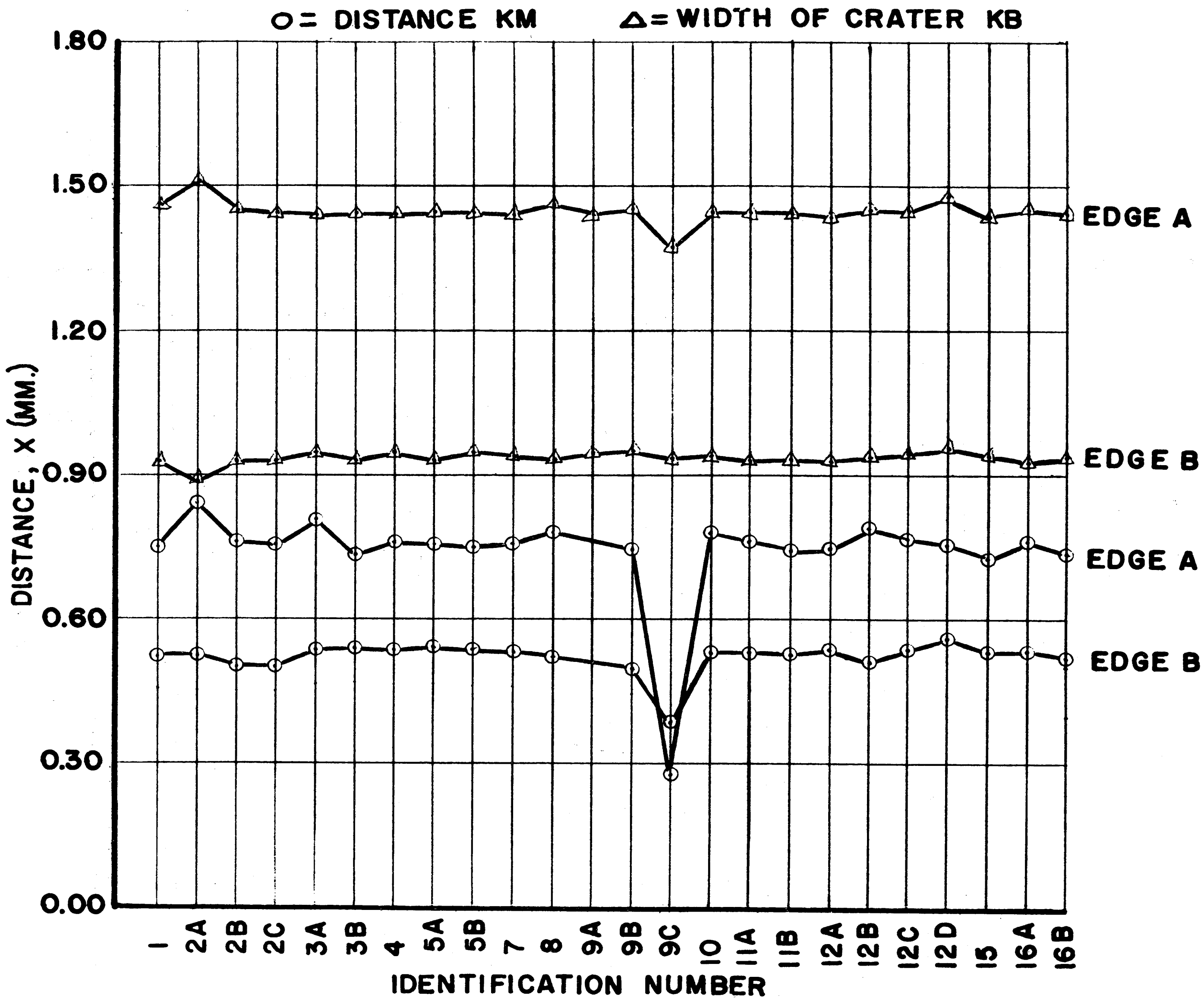

COMPARATIVE TOOL WEAR MEASUREMENTS

FIG. 2.3

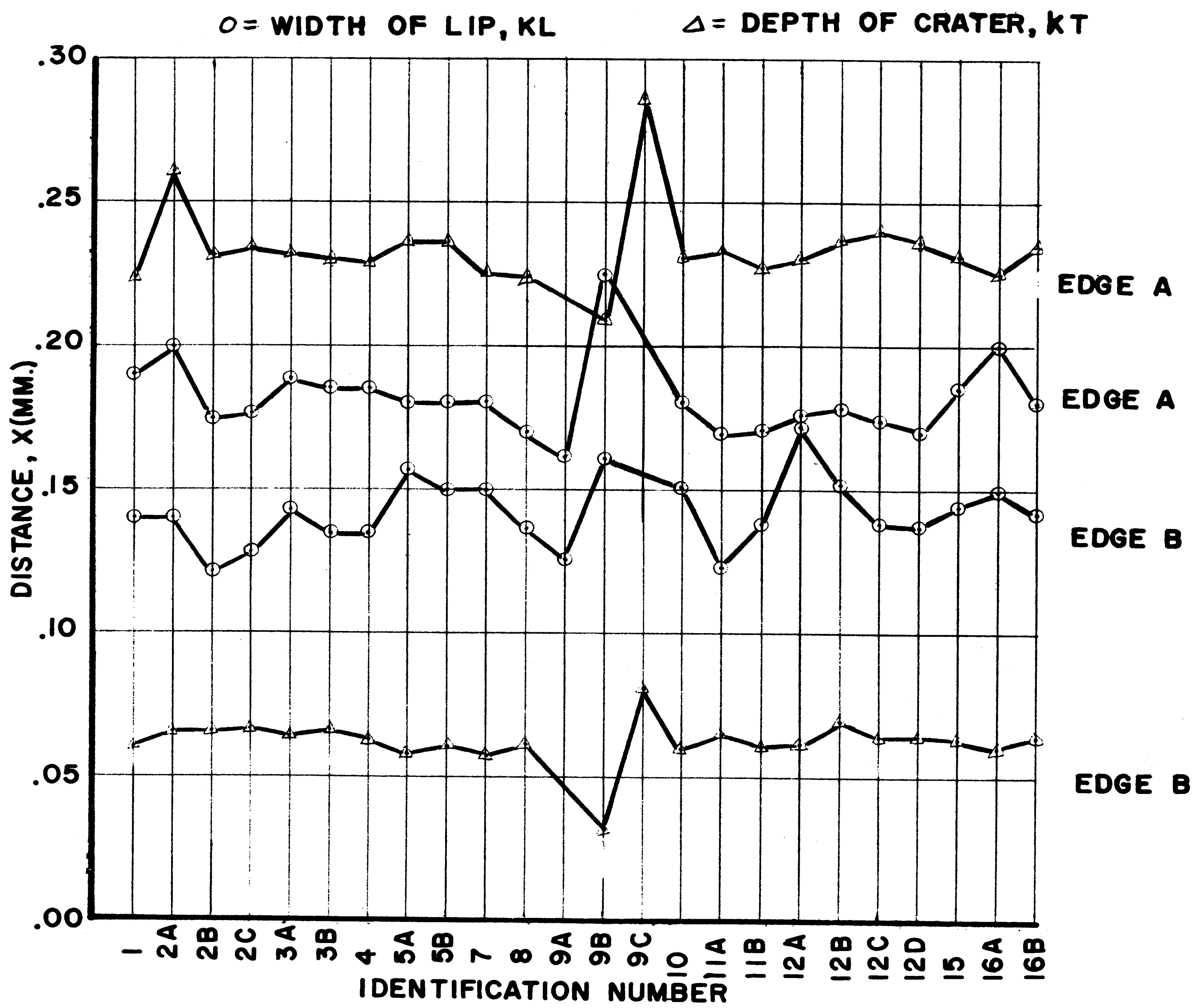

COMPARATIVE TOOL WEAR MEASUREMENTS

FIG. 2.4

PART III

INFLUENCE OF SPEED AND FEED ON FORCES, FINISH AND BUILT-UP EDGE

INTRODUCTION

Professor Pekelharing at the University of Delft undertook a voluntary study of the influence of built-up edge on surface finish using the same tools and work material being studied for the Main Program. The following information is abstracted from the working report submitted to the CIRP/OECD Committee in January, 1965.

The primary purpose of this investigation was to determine the effect of a BUE (Built-Up Edge) on the surface finish of a medium carbon steel. Also, its effects on the cutting forces at various feeds and speeds were considered. The objective was to determine the cutting conditions for obtaining the best possible surface finish on a medium carbon steel workpiece.

TEST CONDITIONS

The workpiece material was XC45 steel; Heat No. Z0648. The tool materials were standard CIRP/OECD carbide tool tips. A P10 carbide tool was used for the determination of cutting forces and surface roughness, and a P30 carbide tool for the quick stop tests. The tool geometry is as follows: $\alpha = 6$, $\gamma = 6$, $\lambda = 0$, $\chi = 70$, $\varepsilon = 90$, r = 0.8 mm (see Fig. 13 of Interim Report No. 1) and the depth of cut was kept constant at d = 3 mm. For the determination of cutting force and surface roughness, three different feeds were used (0.16 mm/rev, 0.25 mm/rev, and 0.50 mm/rev). The cutting speed was varied and the resulting force and surface roughness were measured.

RESULTS

It is evident from Figs 3-1 through 3-6 that the surface finish varies with the cutting forces required for the different tool speeds. (Note: F_z is the vertical component, F_x is the feeding or longitudinal component and F_y is the radial component for cylindrical turning operations. Also, R_1 is the conventional surface roughness produced by the secondary cutting edge parallel to the axis of rotation; R_2 is the surface roughness produced by the major cutting edge around the circumference.) Neglecting very low speeds, the cutting force increases as the speed increases until a maximum force has been reached. This occurs rather rapidly. For example, at a feed of 0.25 mm/rev (0.010 ipr) the maximum cutting force occurs at a cutting speed of 30 m/min (98 fpm). This value was found to change approximately linearly with the feed, or it can be expressed mathematically as VxS = Constant where V is the speed for maximum cutting force and S is the feed (see Figs. 3-7).

After the maximum cutting force has been reached and the speed continues to increase, the surface roughness and cutting forces taper off asymptotically as shown in the first six figures. It is therefore concluded that the feed should be large and the speed high enough to be beyond the maximum cutting force range. This, however, brings into play the economic feasibility of a decrease in tool life that is sacrificed for a good surface finish. For instance, other machining processes may be economically more desirable.

The reason that a rough surface is present at relatively low speeds and a smooth surface at high speeds is that a BUE is formed and disappears as the speed increases. Two sets of photographs were taken to illustrate this theory. The first set (Figs. 3-8 through 3-11) shows the results of some quick stops at various cutting speeds. The feed used for these tests was 0.16 mm/rev. The pictures show the cut surfaces on the shoulder of the turning cut and the undersides of the chips. The BUE is visible and increases in size as the speed increases. It begins to decrease noticeably at V = 31.5 m/min (106 fpm) until it disappears at 50 m/min (164 fpm). It should be noted that the pictures for V = 36 m/min and V = 40 m/min show carbide tool fragments that have broken off during the test. Because of the difficulty in deliberately accomplishing this they have been left in the sequence.

The second set (Figs. 3-12 through 3-14) of pictures are side angle shots that show the results of the BUE on the surface of the workpiece. At very low cutting speeds segmented chips are obtained. These chips may be considered as large individual built-up edges that have formed and parted from the tool. This behavior is clearly evident in the photograph for V = 3.5 m/min (Fig. 3-12). The result of this is a rough surface that contains a pattern of drag marks left by the BUE.

As the speed increases, the chip becomes continuous and a normal BUE is formed on the tool that acts as an increased rake angle. As a result, the cutting forces decrease. The BUE increases in size as the tool moves along the surface and acts as an extension of the tool. It extends below the regular cutting surface and as a result leaves an indentation in the surface. This continues until the BUE reaches a size such that the tool acts as a moment arm and the cutting force breaks off the BUE from the workpiece. The small forward edge which is below the surface of the tool is left on the work surface and the rest becomes part of the chip. This pattern is repeated over and over and consequently gives a uniformly torn surface. This is clearly evident in the sequence of pictures. As the speed increases further the BUE decreases and therefore a better surface finish is obtained. At V = 50 m/min no BUE is formed and a smooth surface is obtained.

CONCLUSION

The best cutting condition for a smooth surface finish is one in which the cutting speed is high enough not to produce a BUE. This varies among materials as well as with the feed. In general, it may be stated that a maximum feed should be used so that the cutting speed required to eliminate the BUE is a minimum. The exact values for each of these is different for various tool materials. There is too little of this type of information to justify attempting a more formal expression at this time.

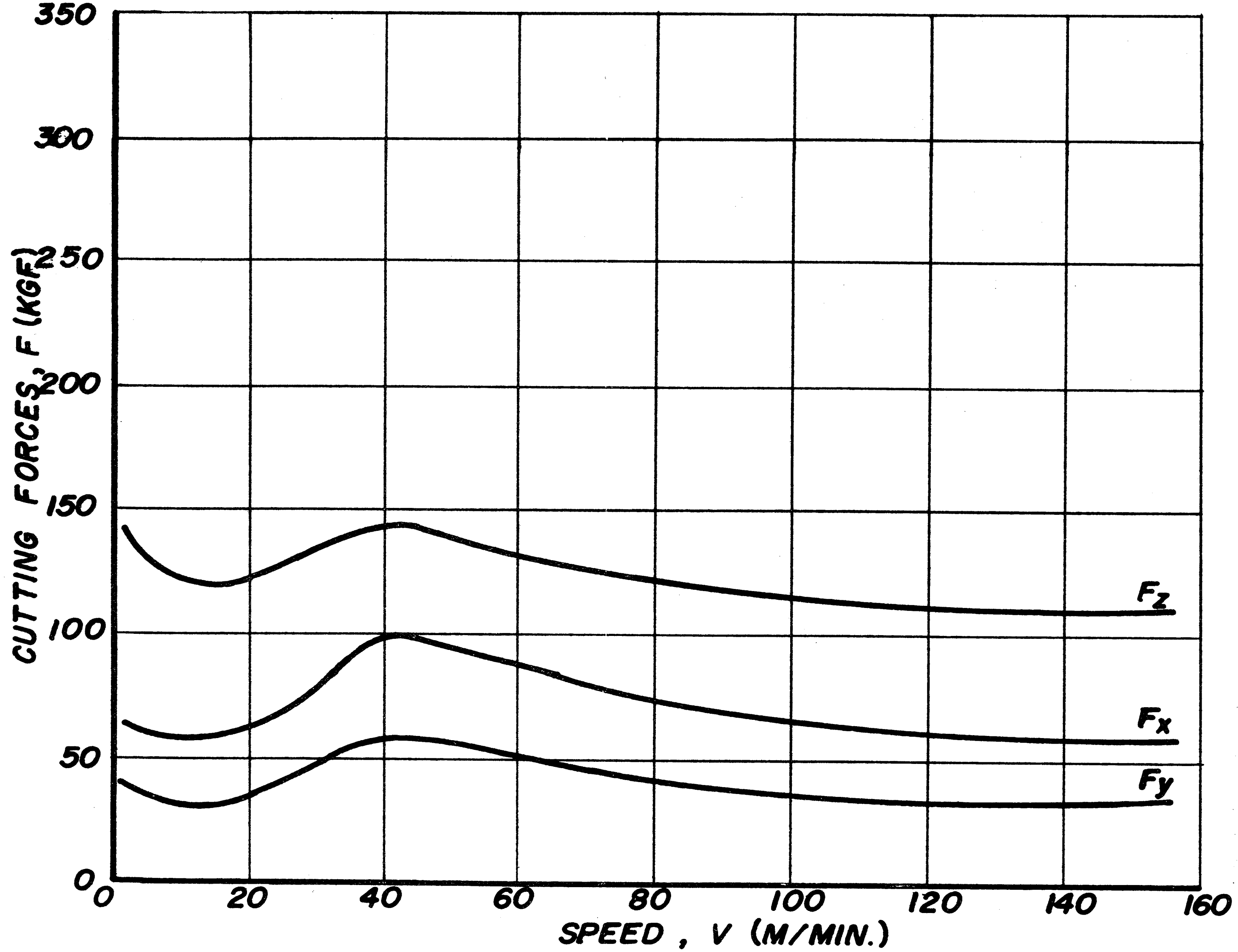

CUTTING FORCES vs SPEED

FEED = 0.16 MM/REV.

FIG. NO. 3-1

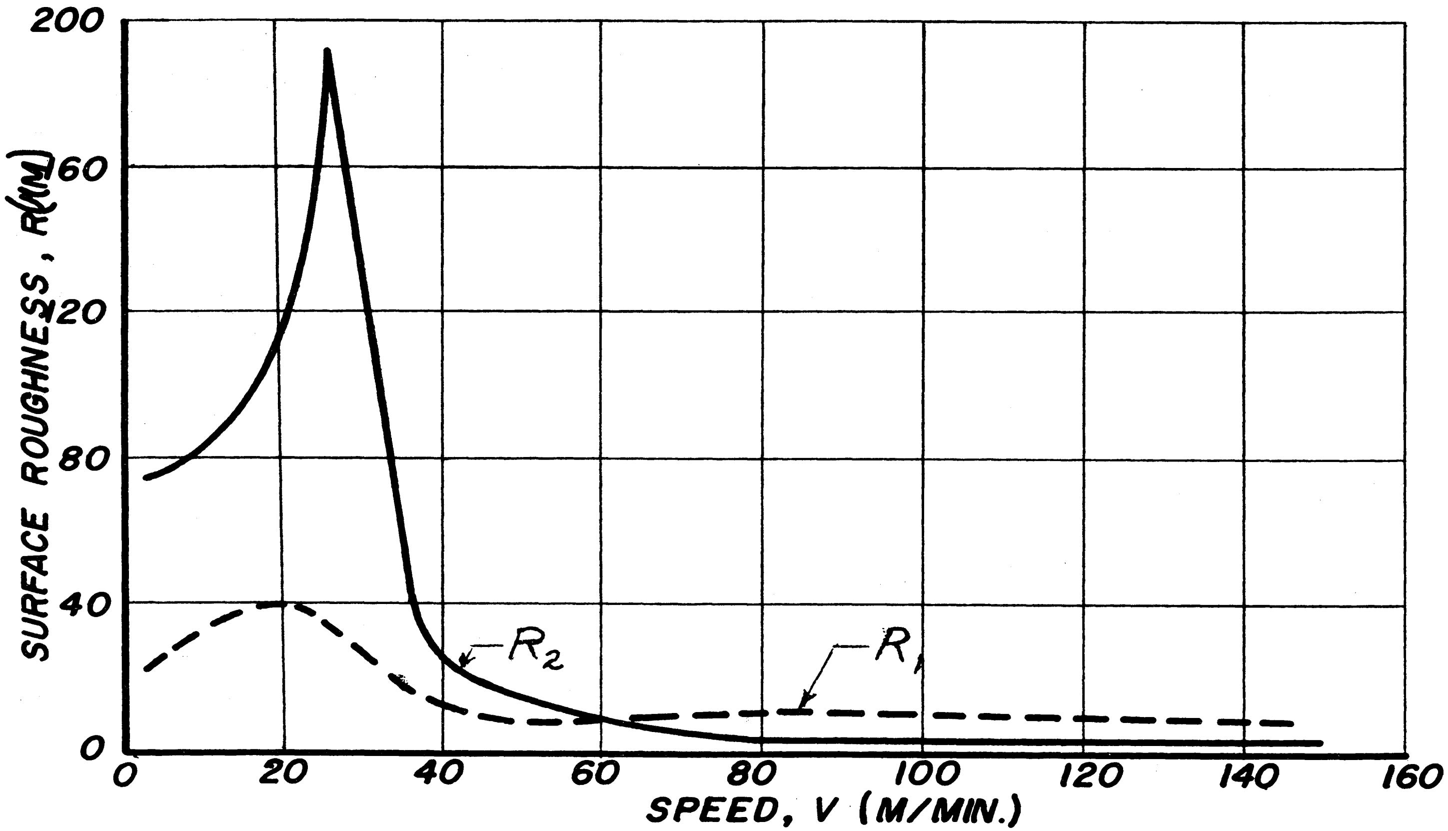

SURFACE ROUGHNESS vs SPEED
FEED = 0.16 MM/REV.

FIG. NO. 3-2

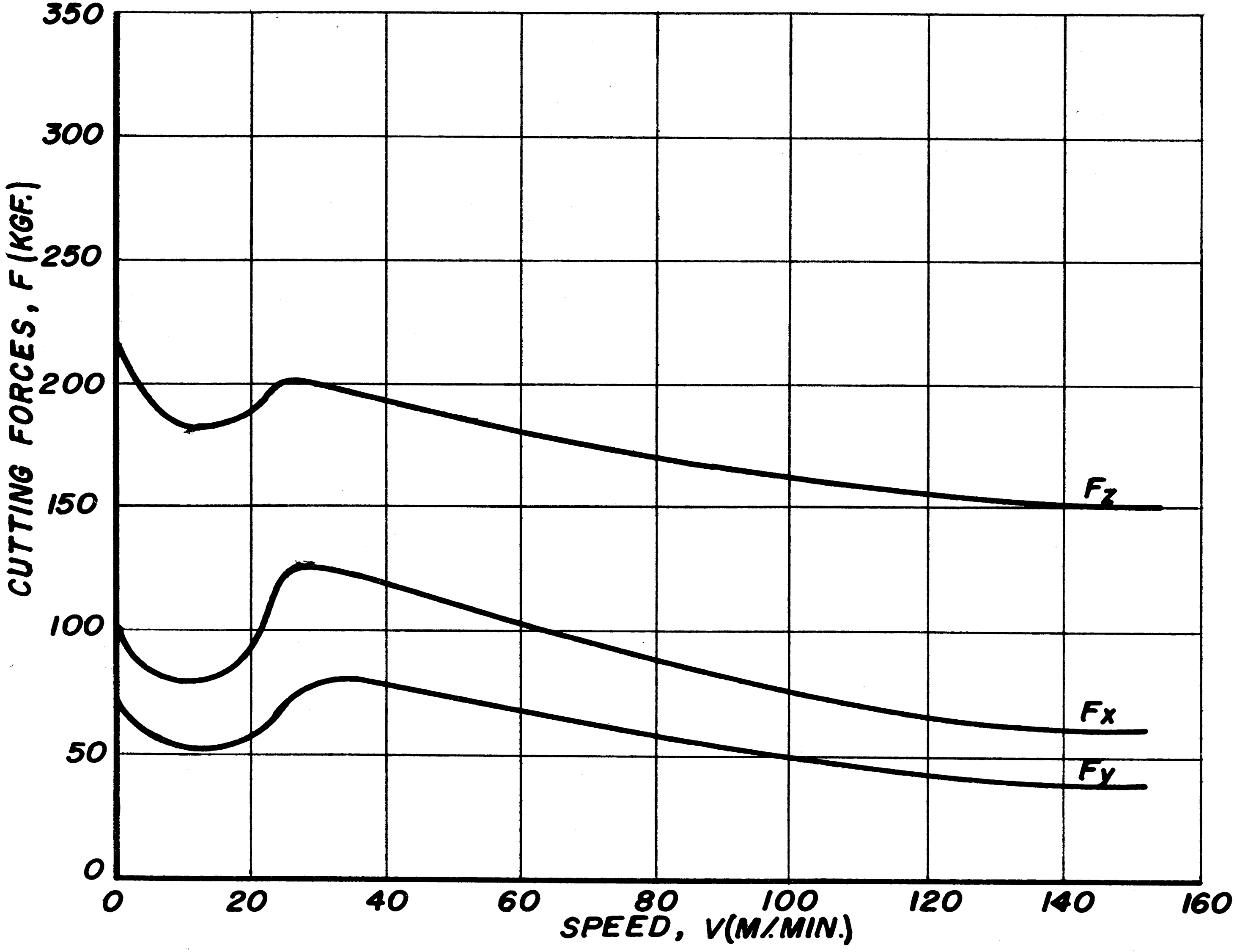

CUTTING FORCES vs SPEED

FEED = 0.25 MM/REV.

FIG. NO.3–3

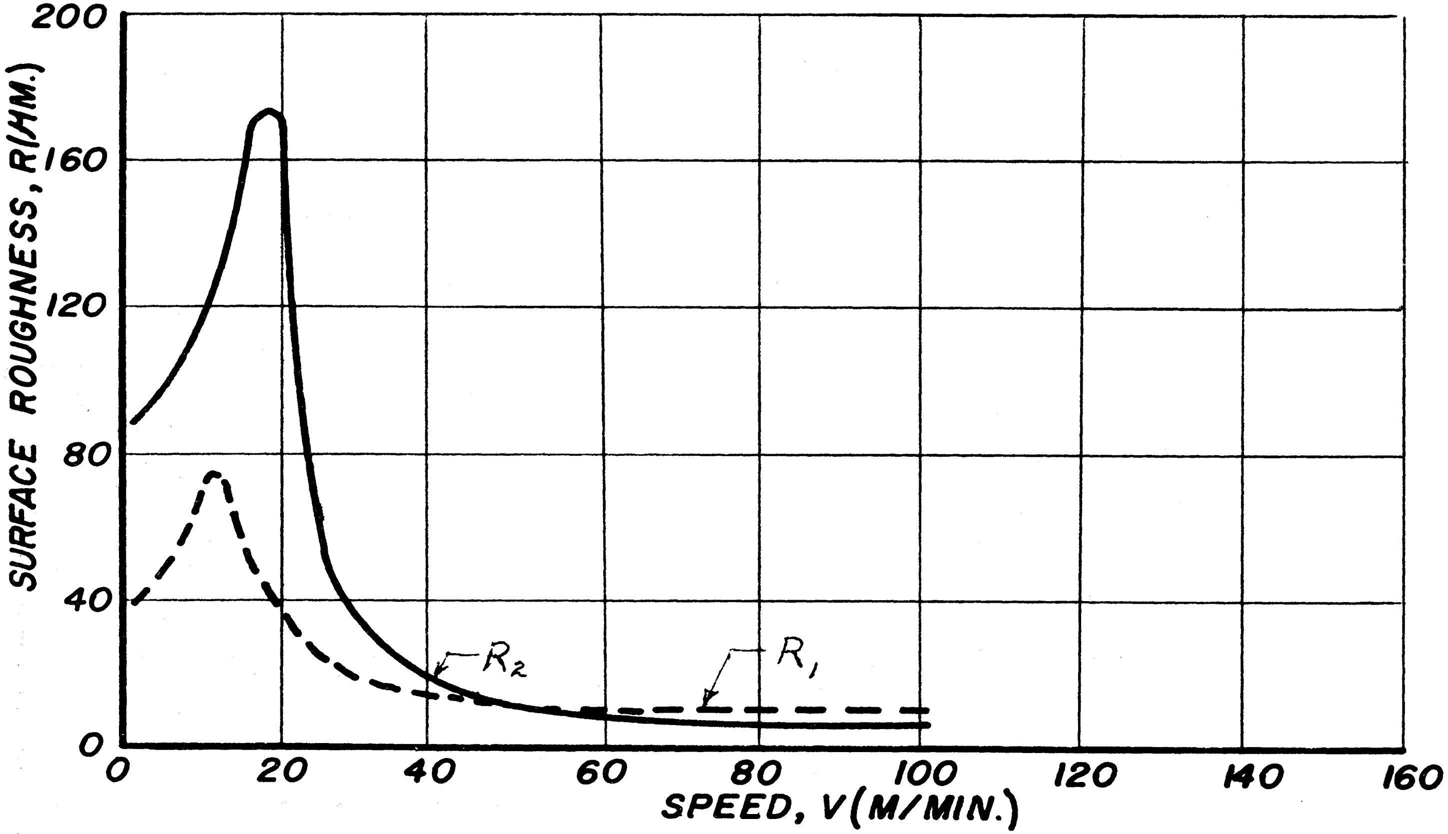

SURFACE ROUGHNESS vs SPEED

FEED = 0.25 MM/REV.

FIG. NO. 3-4

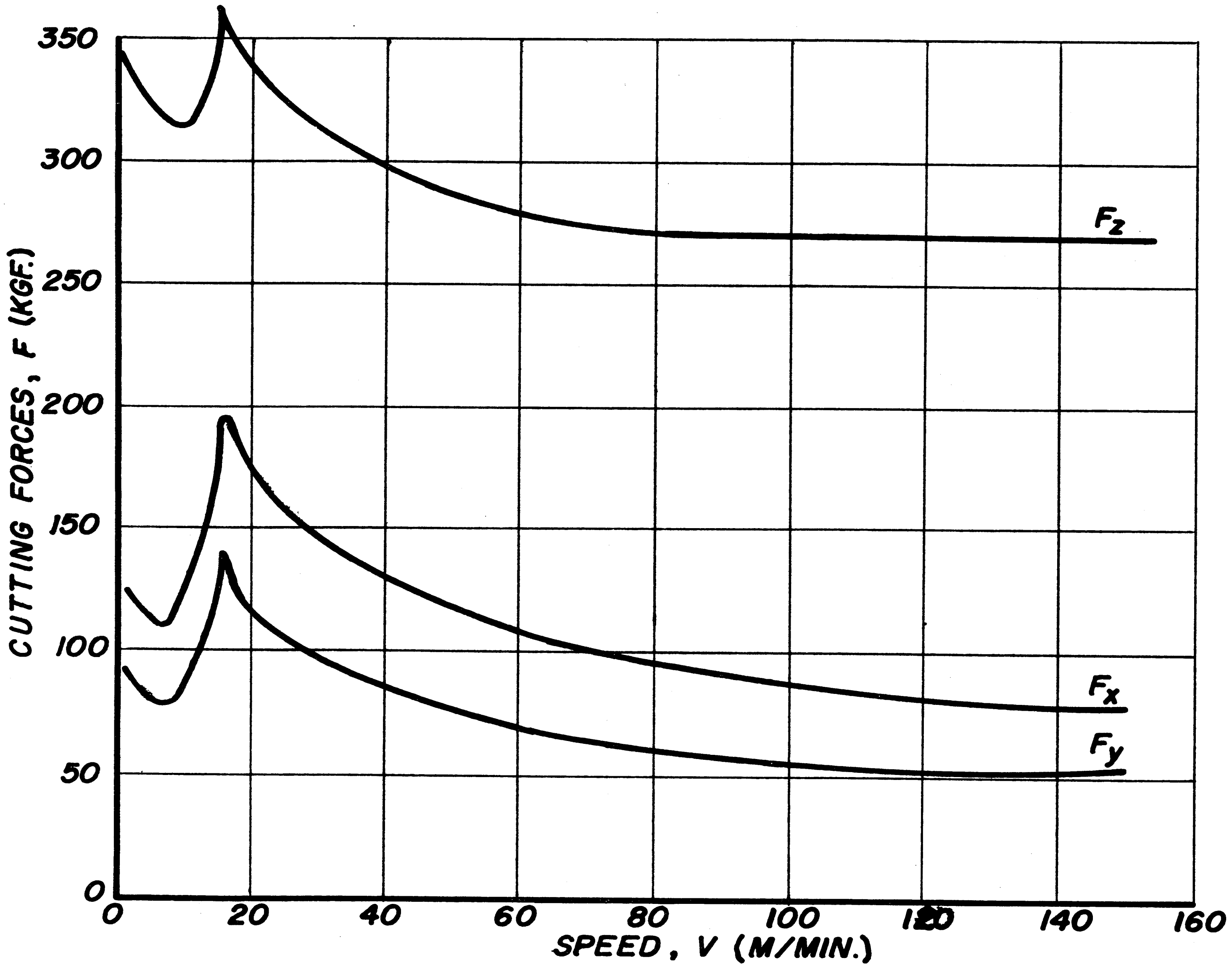

CUTTING FORCES vs SPEED
FEED = 0.50 MM/REV.

FIG. NO. 3-5

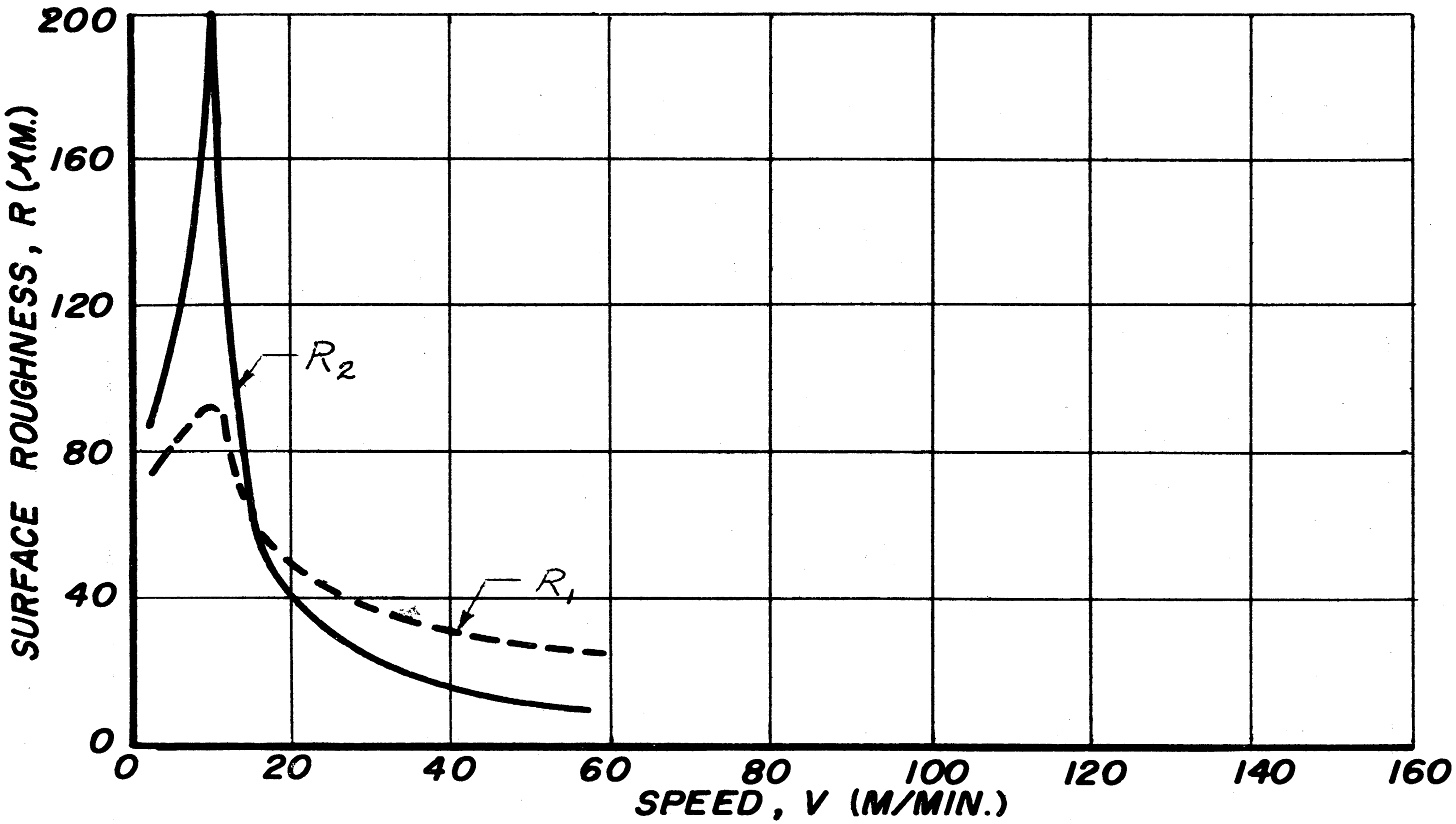

SURFACE ROUGHNESS vs SPEED

FEED = 0.50 MM/REV.

FIG. NO. 3-6

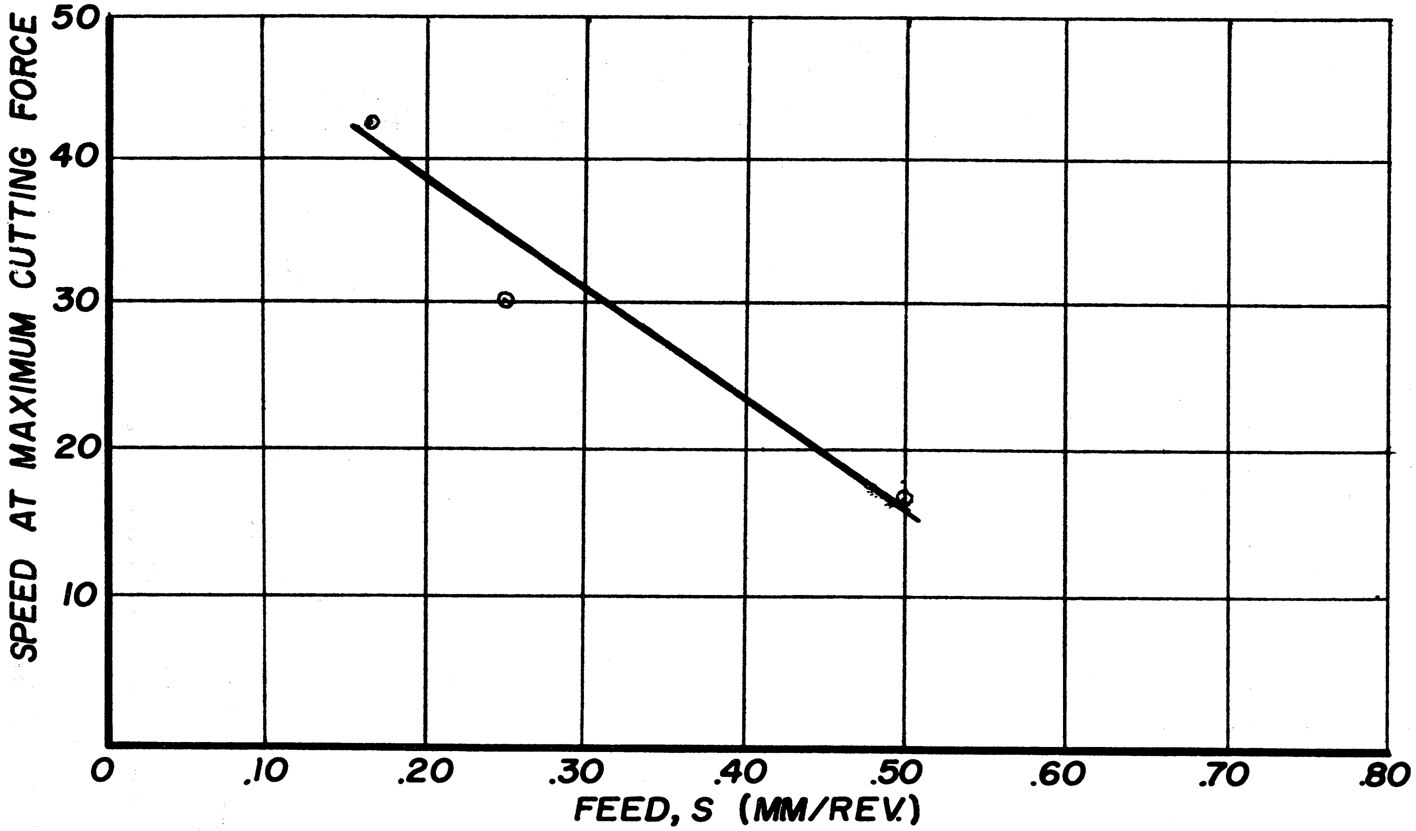

FEED vs SPEED AT MAXIMUM CUTTING FORCE

FIG. NO. 3-7

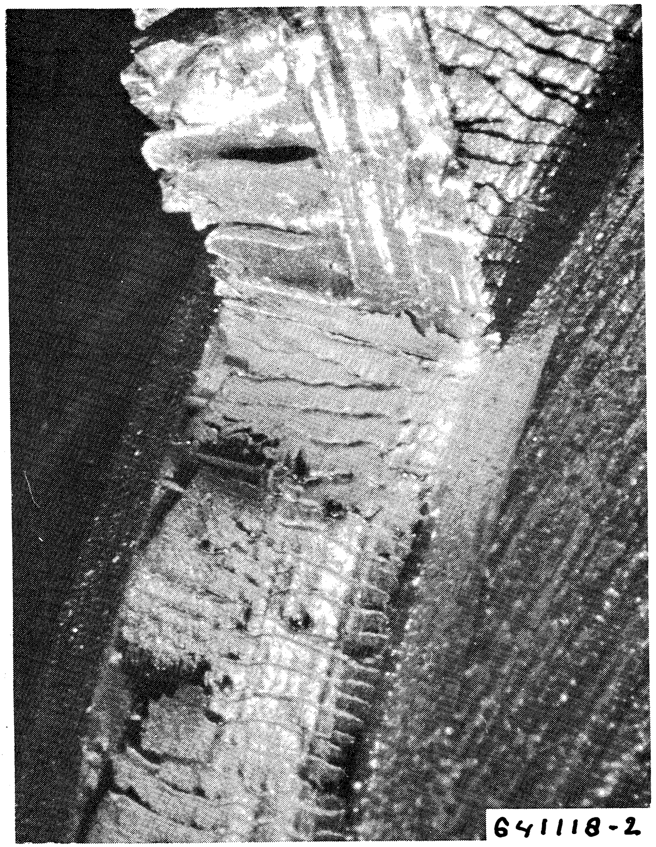

SPEED
V = 3.5 M/MIN.
= 11.5 FPM

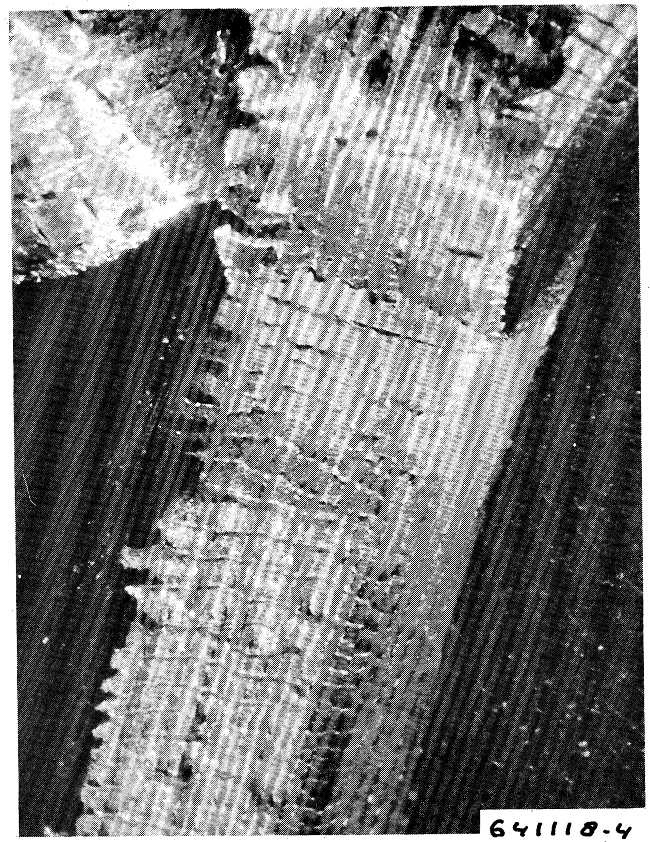

SPEED
V = 5.0 M/MIN.
= 16.5 FPM

QUICK-STOP SPECIMENS

NOTES

UNDERSIDE OF CHIP
MACHINED SURFACE

FIG. NO. 3-8

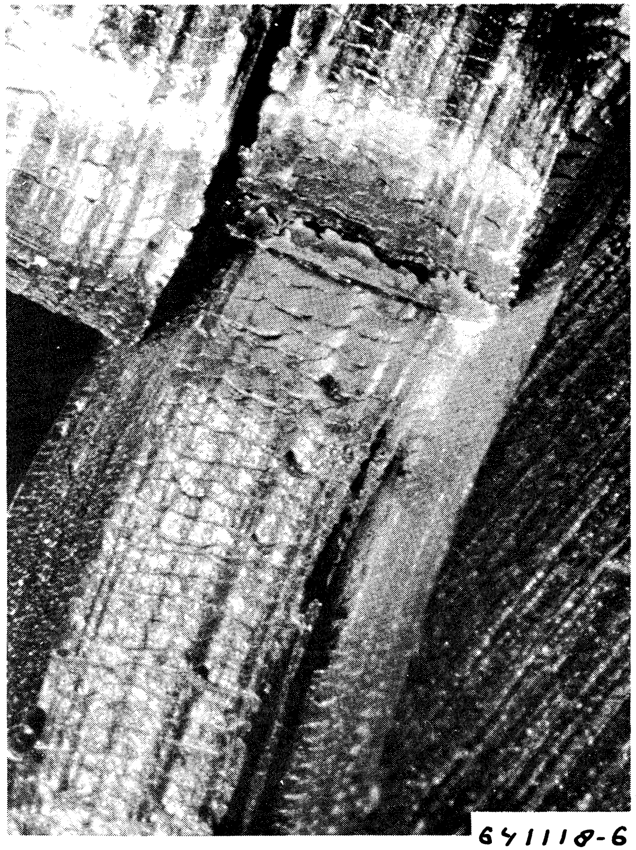

SPEED
V = 16.0 M/MIN.
= 52.5 FPM

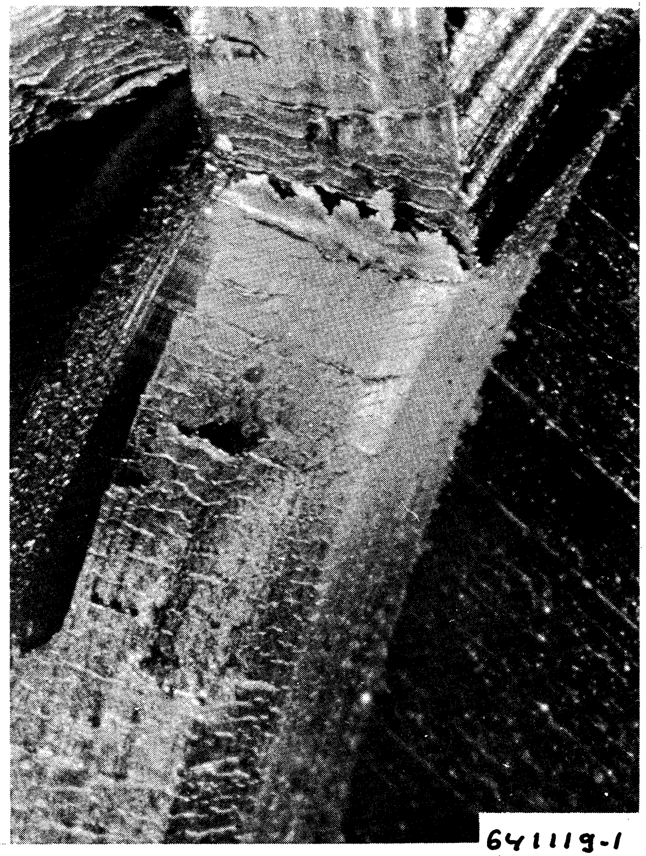

SPEED
V = 25.0 M/MIN.
= 82.2 FPM

QUICK-STOP SPECIMENS

NOTES

UNDERSIDE OF CHIP
MACHINED SURFACE

FIG. NO. 3-9

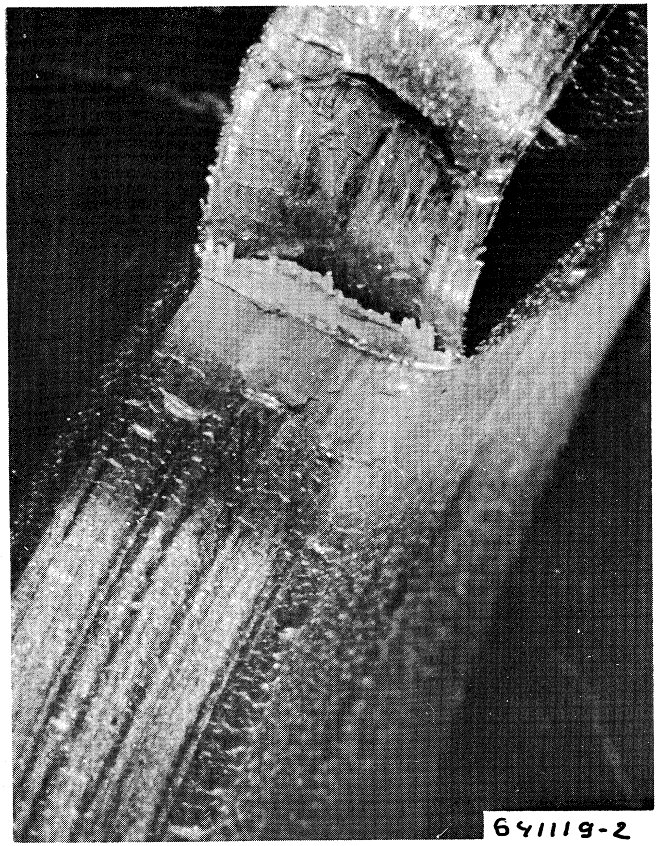

SPEED
V = 31.5 M/MIN
= 104.0 FPM

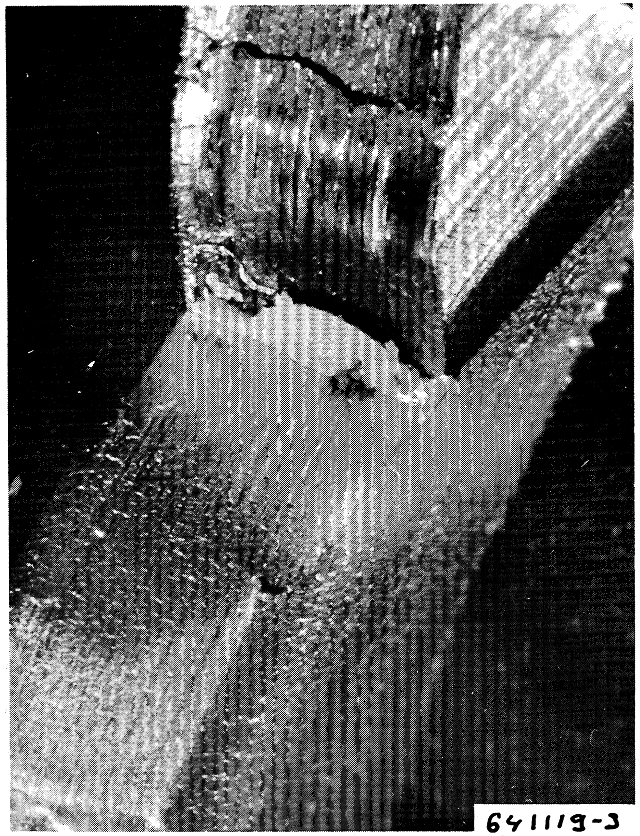

SPEED
V = 36.0 M/MIN
= 118.1 FPM

QUICK-STOP SPECIMENS

NOTES

UNDERSIDE OF CHIP
MACHINED SURFACE

FIG. NO. 3-10

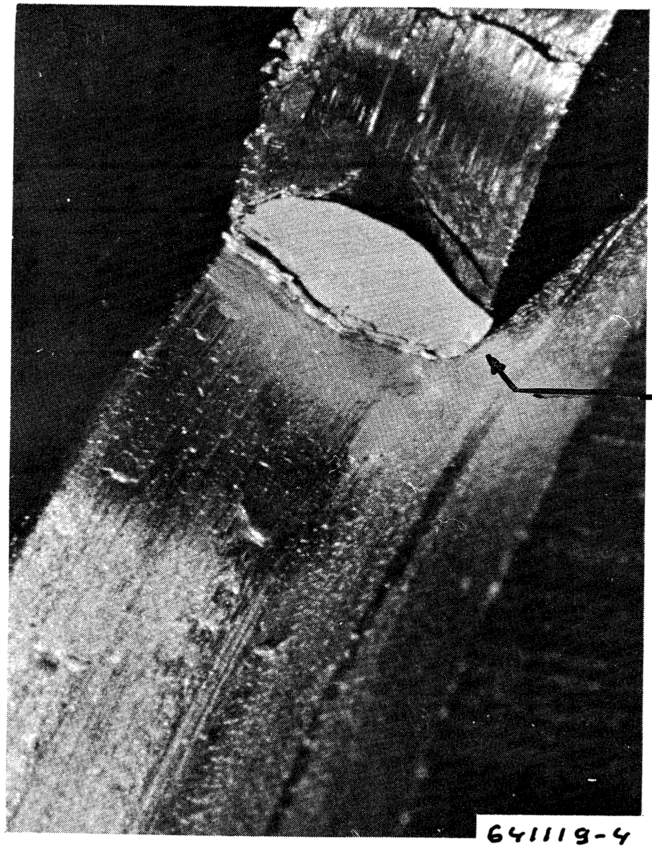

SPEED

V = 40.0 M/MIN
= 131.0 FPM

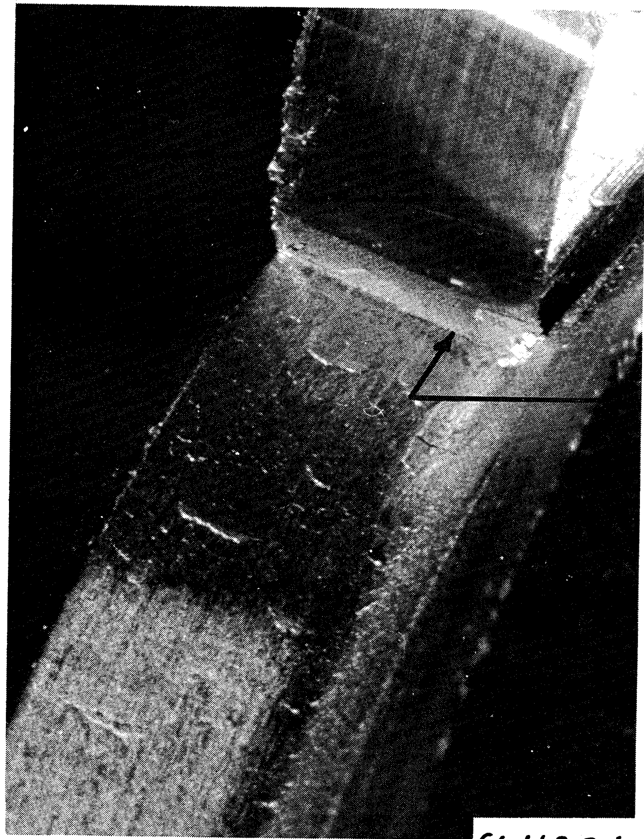

SPEED

V = 50.0 M/MIN
= 164.0 FPM

QUICK-STOP SPECIMENS

NOTES

UNDERSIDE OF CHIP
MACHINED SURFACE

FIG. NO. 3-11

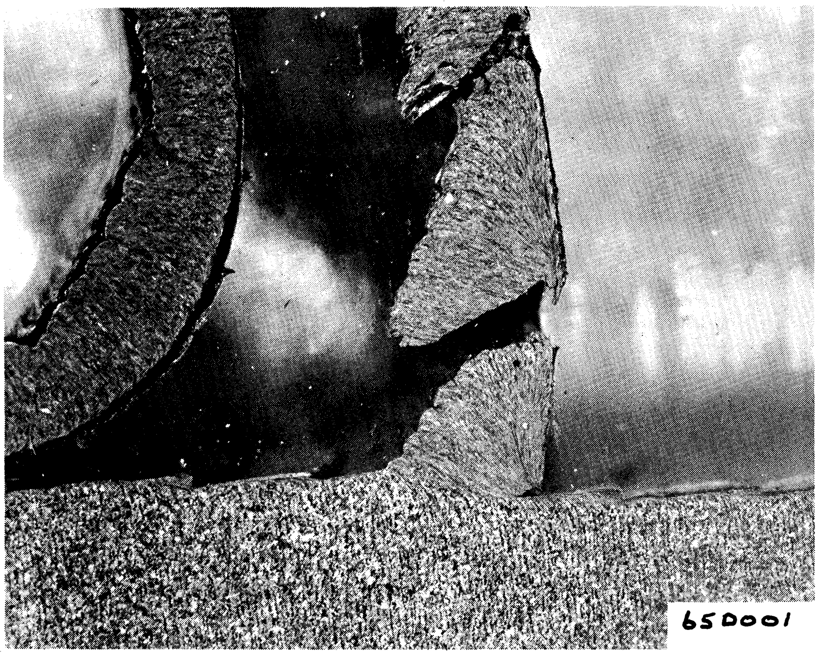

SPEED = 3.5 M/MIN.

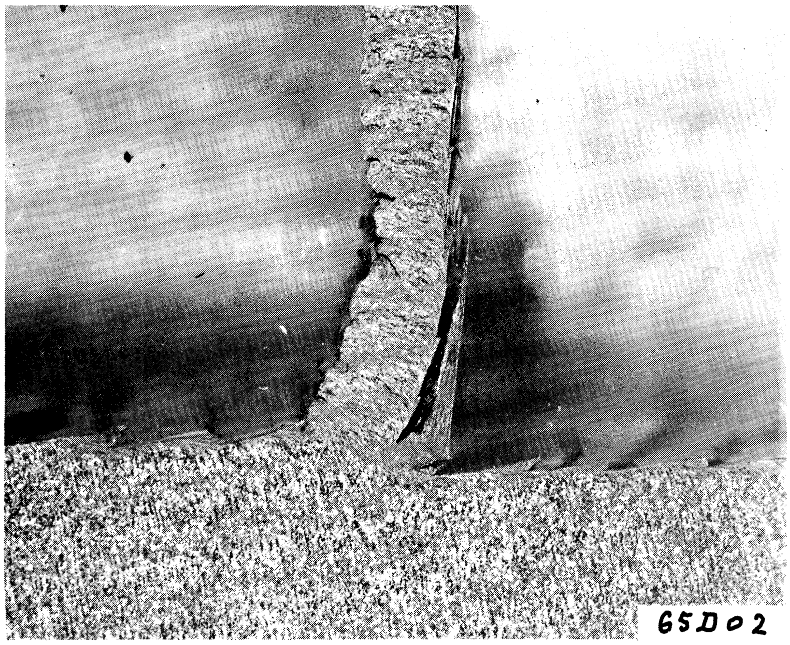

SPEED = 5.0 M/MIN.

CROSS-SECTION OF QUICK-STOP SPECIMENS

FIG. NO. 3-12

SPEED = 25.0 M/MIN.

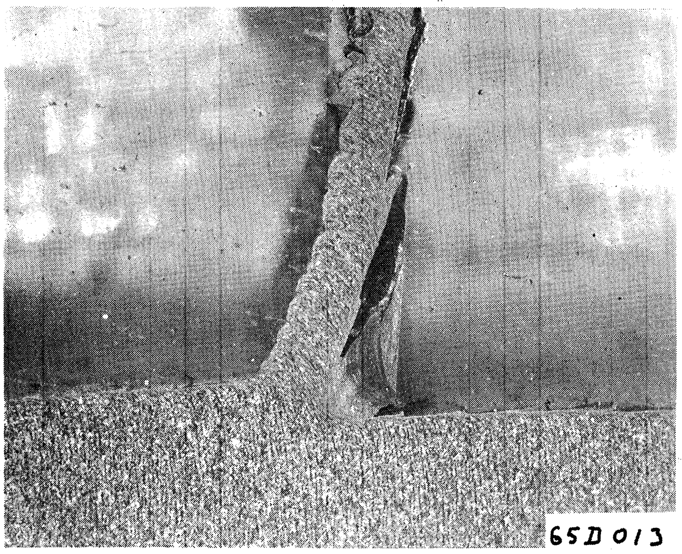

SPEED = 31.5 M/MIN.

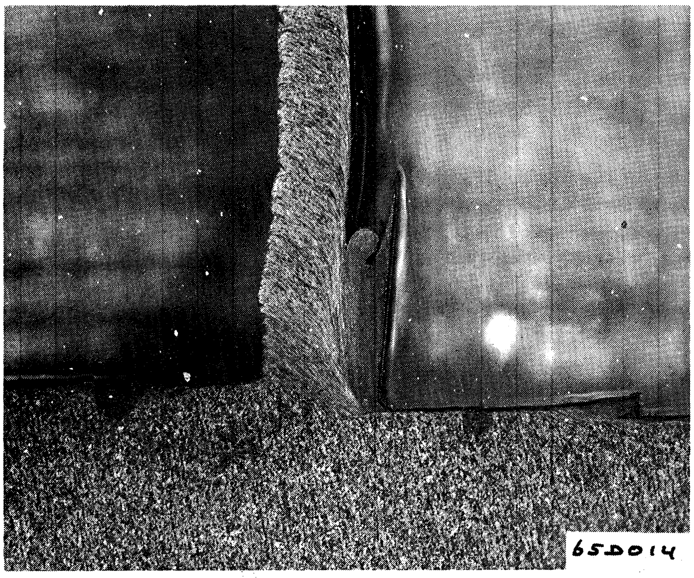

SPEED = 36.0 M/MIN.

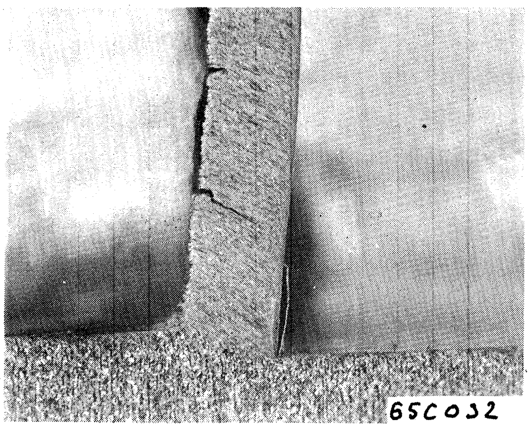

FIG. NO. 3-13

CROSS-SECTION OF QUICK-STOP SPECIMENS

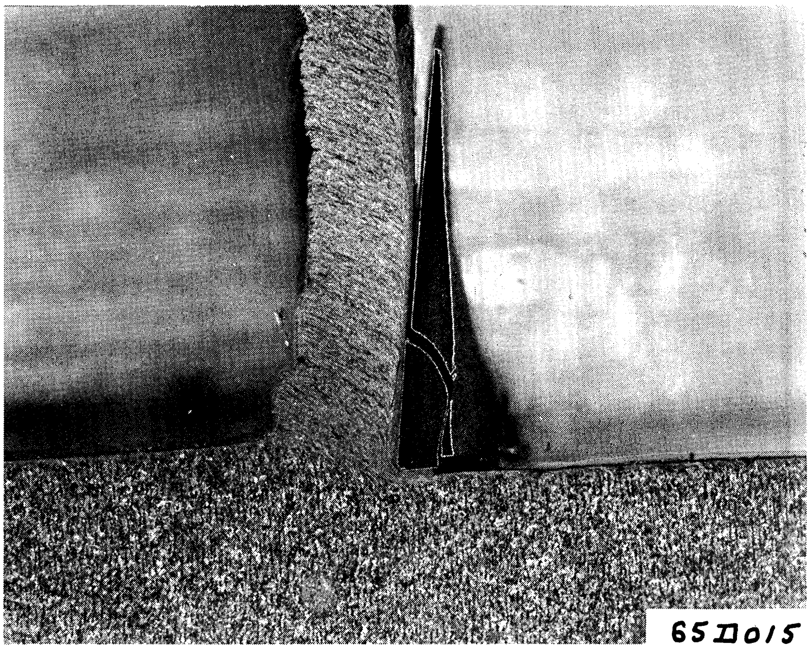

SPEED = 40.0 M/MIN.

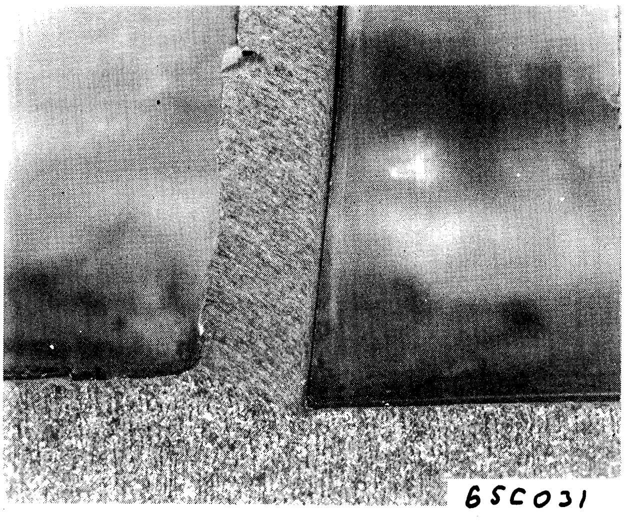

SPEED = 50.0 M/MIN.

CROSS-SECTION OF QUICK-STOP SPECIMENS

FIG. NO. 3-14

PART IV

A NEW METHOD FOR STUDYING TOOL WEAR IN FINISH MACHINING

INTRODUCTION

The University of Delft under the direction of Professor Pekelharing has specialized and concentrated extra effort in studying the problems of finish machining and has developed special techniques for this purpose. Some of these were tried on the CIRP/OECD work and tool combinations and the results along with description of techniques is given in the following abstract of a report submitted to the OECD in January, 1965.

When finish turning, the main problem is to maintain the dimensional accuracy and surface smoothness of the machined pieces within specific limits. When operating at speeds above the area where a built-up edge is formed, nose wear and groove wear of turning tools are important factors in the determination of surface conditions. No attempt is made to explain the causes of nose and groove wear except to point out that considerable research has been done in this field with varied results. One purpose of this report is to stimulate interest in a test program in which the consequences of nose wear and groove wear may be adequately studied.

THE COMPARATIVE TEST PROGRAM

A very moderate test program is suggested. It involves essentially the study of the results of tool wear on the surface roughness of the workpiece and the interaction of the resulting pattern on the tool configuration. The intent of this study is to produce results which may be used for comparison with the results of others. With this in mind, it is essential to develop an accurate means for the measurement of wear. In this particular test, a jig for holding the tool both in the lathe and under photographic equipment was made and a displacement gage was attached to the front. The tool could then be removed and replaced in the lathe at will without affecting its position. Photographs of the tool at high magnification can be taken and a single picture showing the development of the wear can be made by superimposing one upon the other (see top of Fig. 4-7).

This procedure always shows much dispersion; therefore, it is advisable to repeat the test five times so that meaningful results may be obtained. According to experience at the University of Delft, the following test conditions are best suited:

Workpiece material:	XC45 (OECD stock)
Tool Material:	carbide P10 (standard OECD tool tips)
Tool geometry:	$\alpha = 6°$, $\gamma = 6°$, $\lambda = 0°$, $\mathcal{X} = 70°$, $\mathcal{E} = 90°$, r = 0.5 mm
Cutting speed:	V = 200 m/min (655 fpm)
Feed:	s = 0.1 mm/rev (0.004 ipr)
Depth of cut:	d = 0.4 mm (0.016 in.)

DATA TO BE MEASURED

On the tool piece, there are two dimensions of primary inportance to this investigation. The first is the degree of nose wear, N (see Fig. 4-7). The second dimension is the depth of the grooves (G). The tool should show a pattern of grooves along the line of contact with the finished surface of the work. Except for the first and last ones, these grooves should have a distance equal to the feed from peak-to-peak or valley-to-valley. From these two dimensions the theoretical increase of the diameter due to the tool wear may be calculated: 2(N+G)μM (microns). On the workpiece the surface roughness is measured.

These data should be plotted up against cutting time. Figures 4-2 through 4-6 are obtained and are the results of four tests run at the aforementioned conditions. Figures 4-5 and 4-6 show the relationship between cutting time and G and N for four different kinds of steel. Three tests were run on each material.

RECOMMENDATIONS FOR THE EXECUTION OF THE TEST

A rigid lathe in a good state of maintenance is needed for these tests since the results of such tests are strongly influenced by vibrations. It was found preferable to mount the workpiece between two dead centers. A carbide tipped center is recommended for the tailstock and it is advisable to provide a bronze insert for the workpiece center hole. This should be kept well greased, since much heat is generated.

It was found that not every tool tip supplied had perfect cutting edges. Therefore it was necessary to regrind them in such a way that the nose radius was precisely 0.8 mm and the cutting edge roundness was below 5 mm as measured with the Arnoulf method.

MEASURING METHODS

In Fig. 4-7 the description of the dimensions N and G is shown. The degree of nose wear N may be measured with the aid of the instruments shown in Fig. 4-1. The depth of the grooves G may be measured with the aid of either a measuring microscope or a profile projection apparatus. Preference was indicated for photographing the profile of the tool and measuring the degree of wear afterwards on a point magnified 250 or 333 times. This gives the advantage of recording the complete profile of wear for future reference. The progression of wear may be studied on photograph assemblies as shown in Fig. 4-7. It should be noted that it is advisable to tilt the tool a small amount so that a good sharp profile is obtained (see Fig. 4-1).

The roughness (R+) of the workpiece after a certain cutting time may be determined with the aid of either a light section microscope or a tracer instrument.

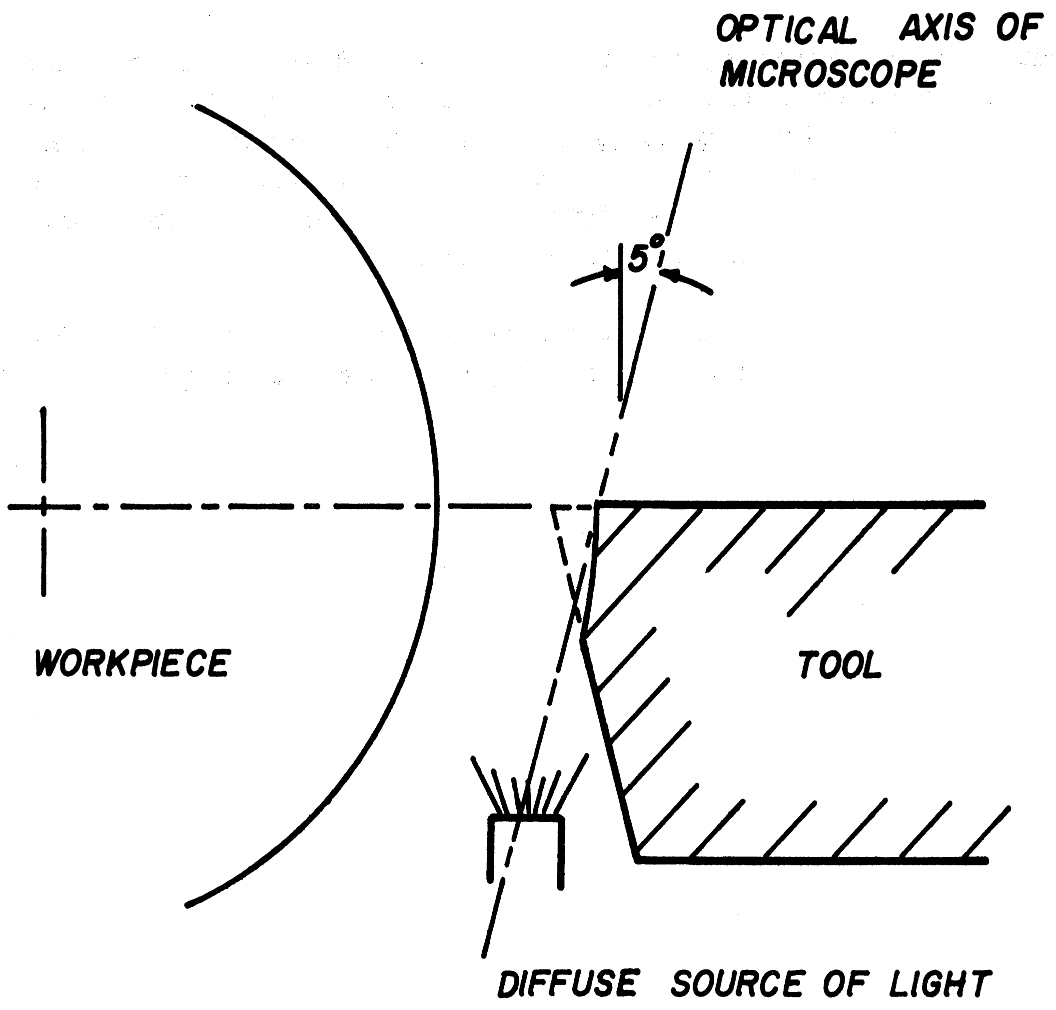

MEASURING METHOD OF GROOVE DIMENSIONS

FIG. NO. 4-1

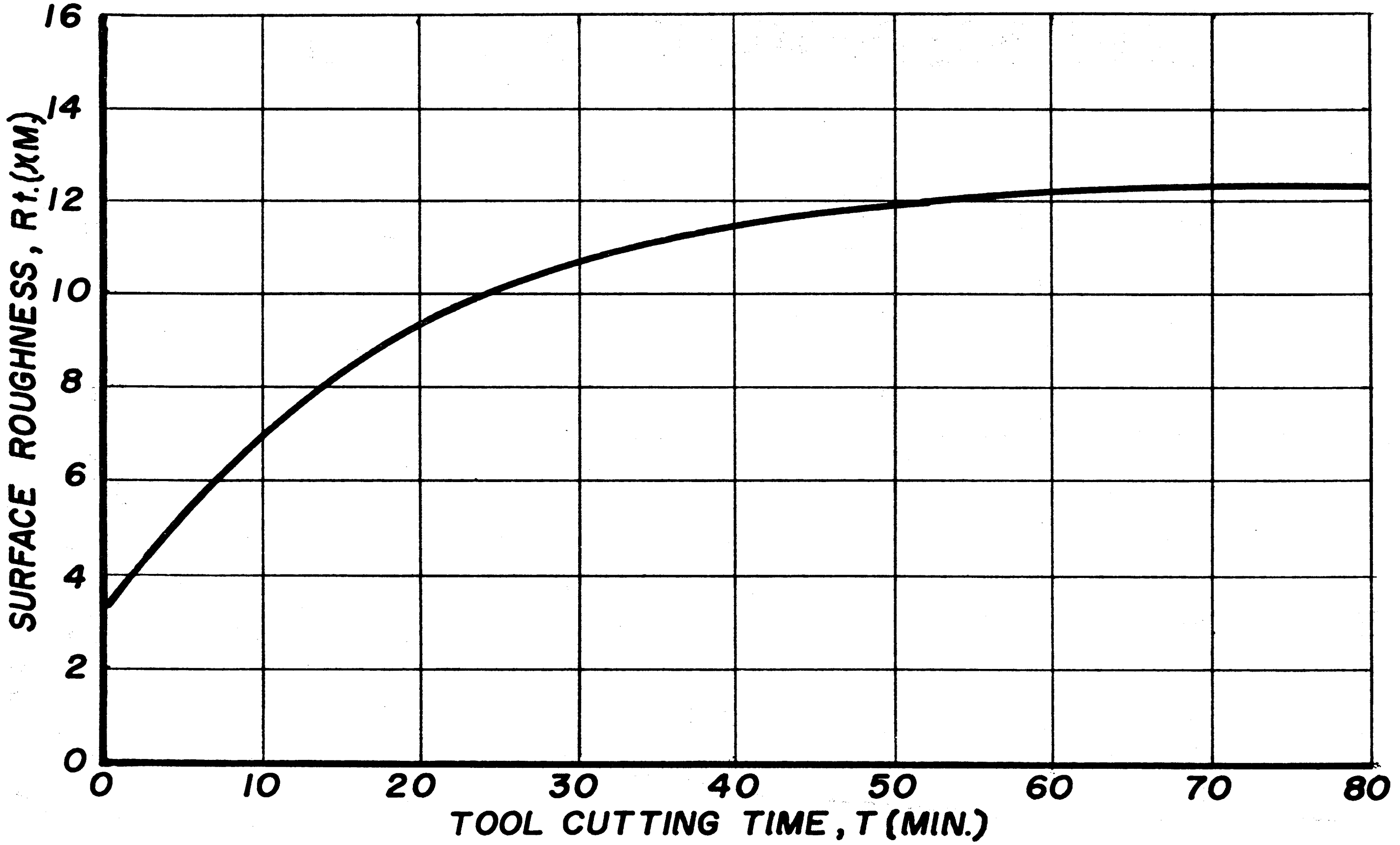

SURFACE ROUGHNESS vs CUTTING TIME

FIG. NO. 4-2

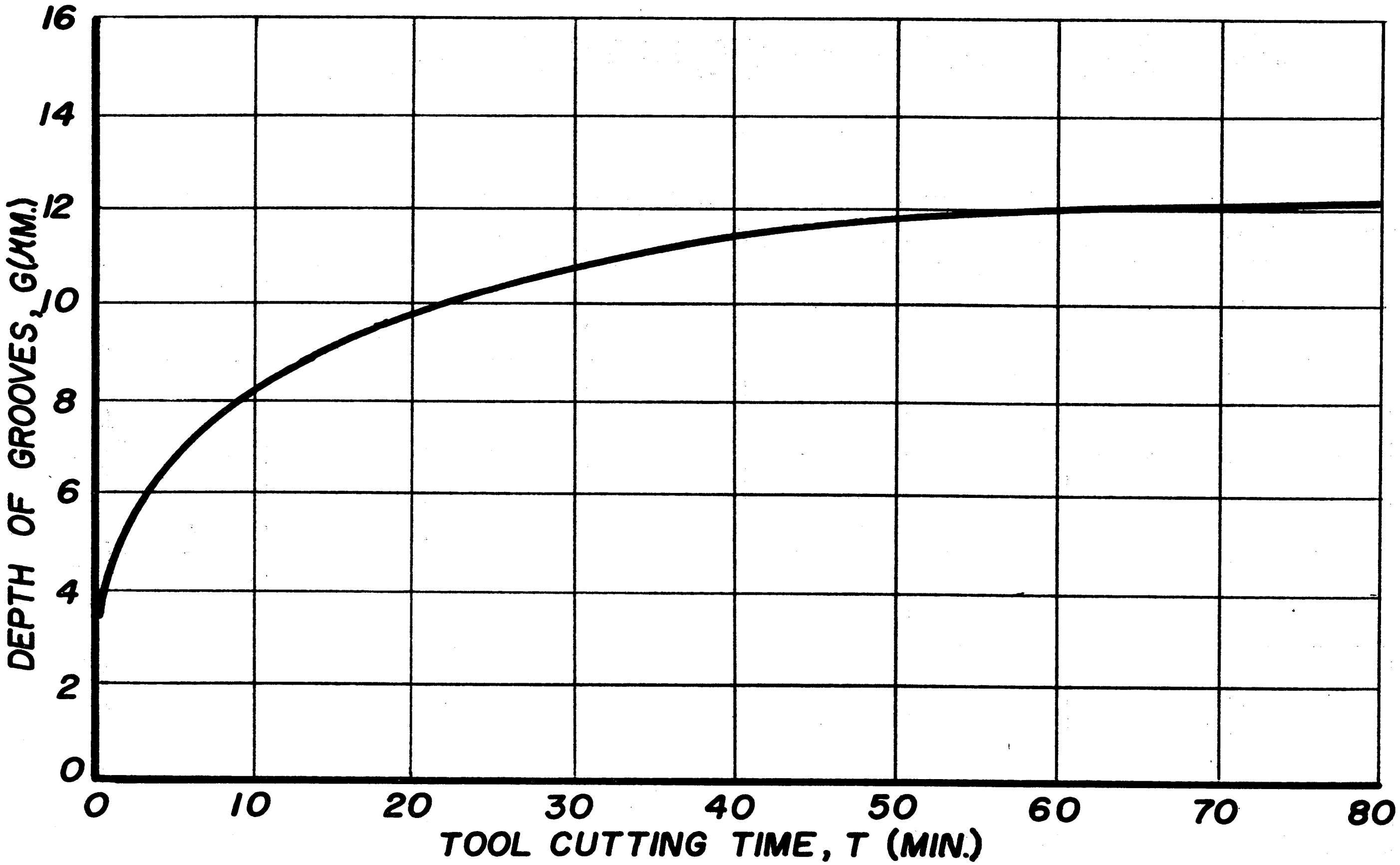

DEPTH OF GROOVES vs CUTTING TIME

FIG. NO. 4-3

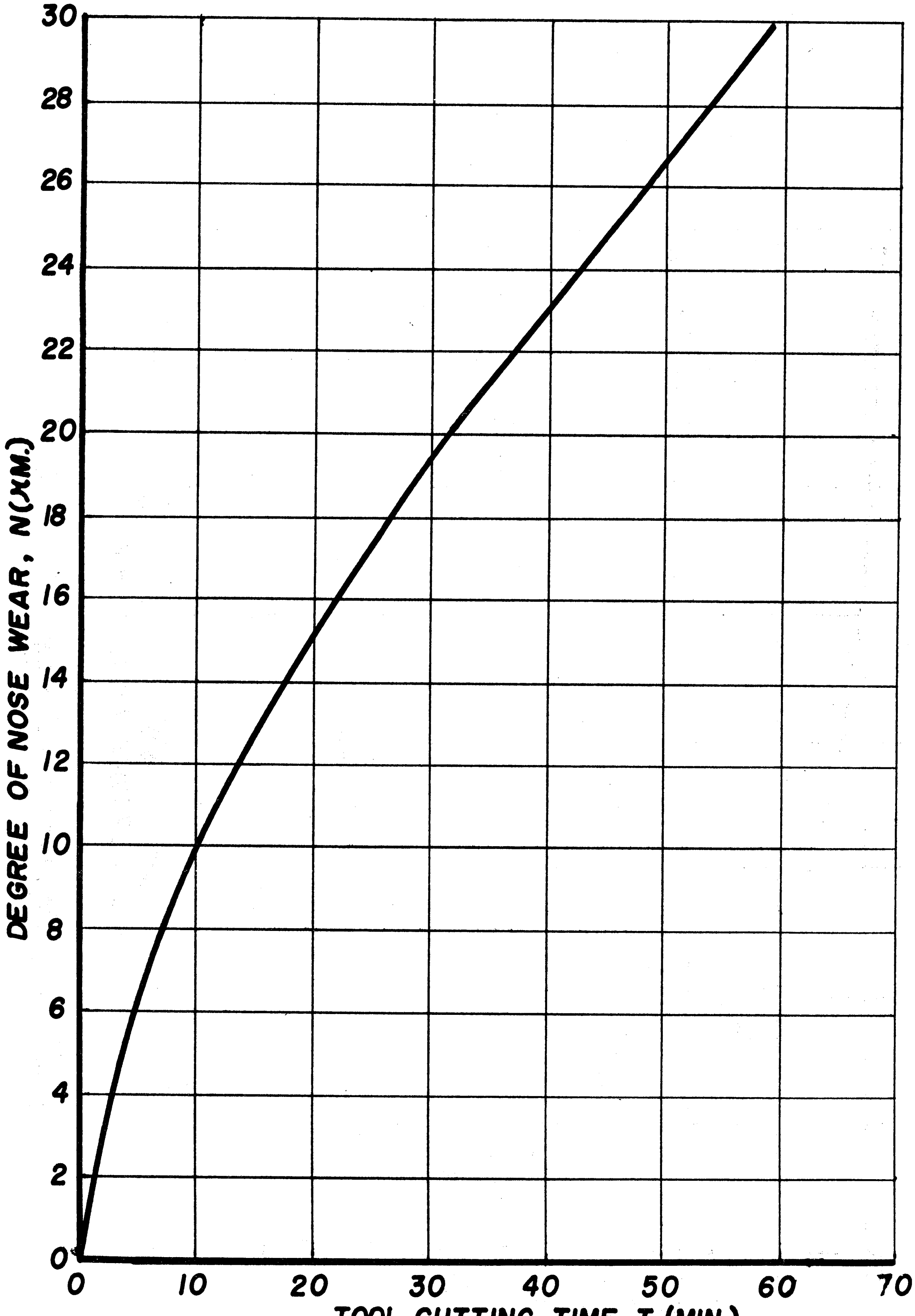

DEGREE OF NOSE WEAR vs CUTTING TIME

FIG. NO. 4-4

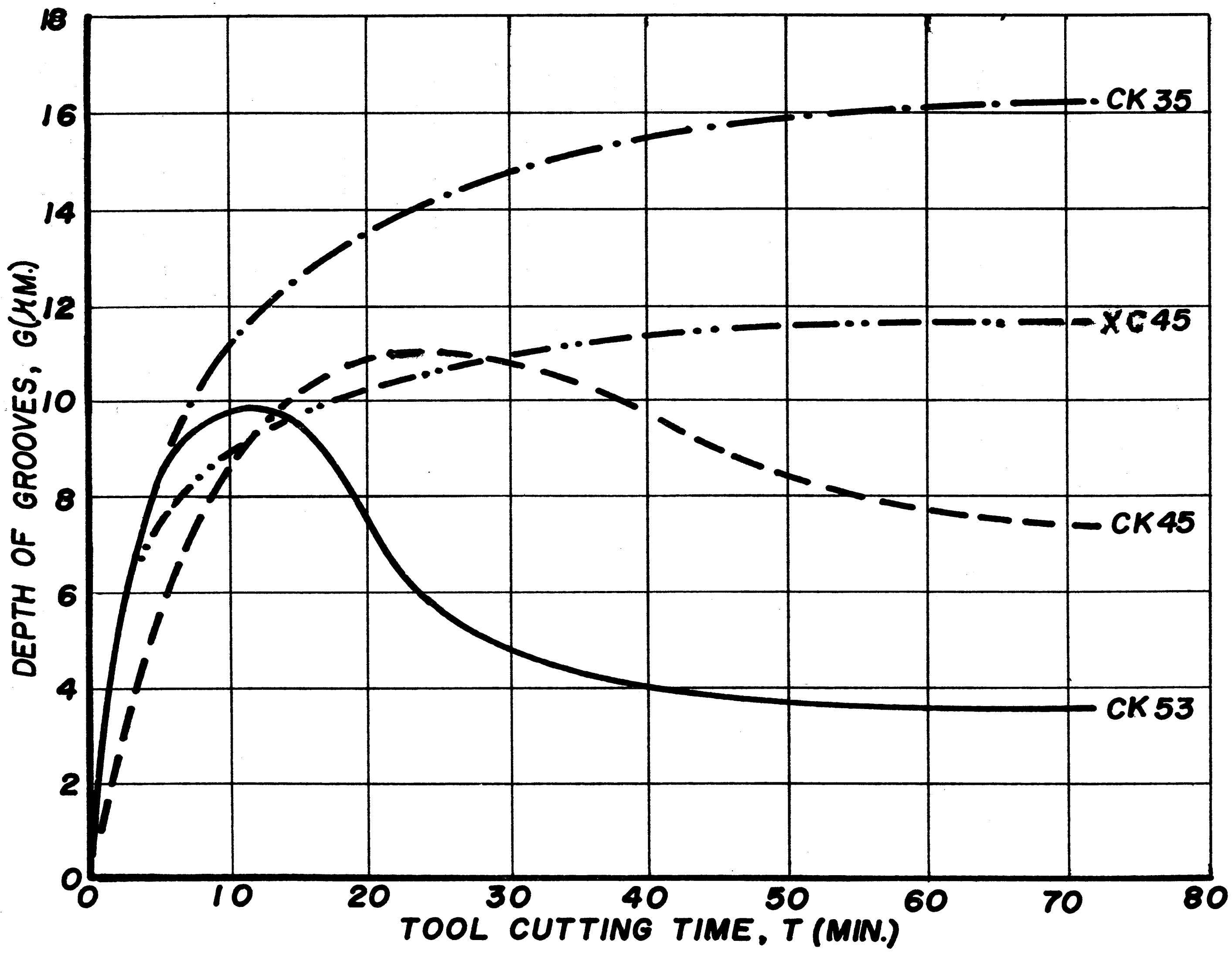

DEPTH OF GROOVES vs CUTTING TIME

FIG. NO. 4- 5

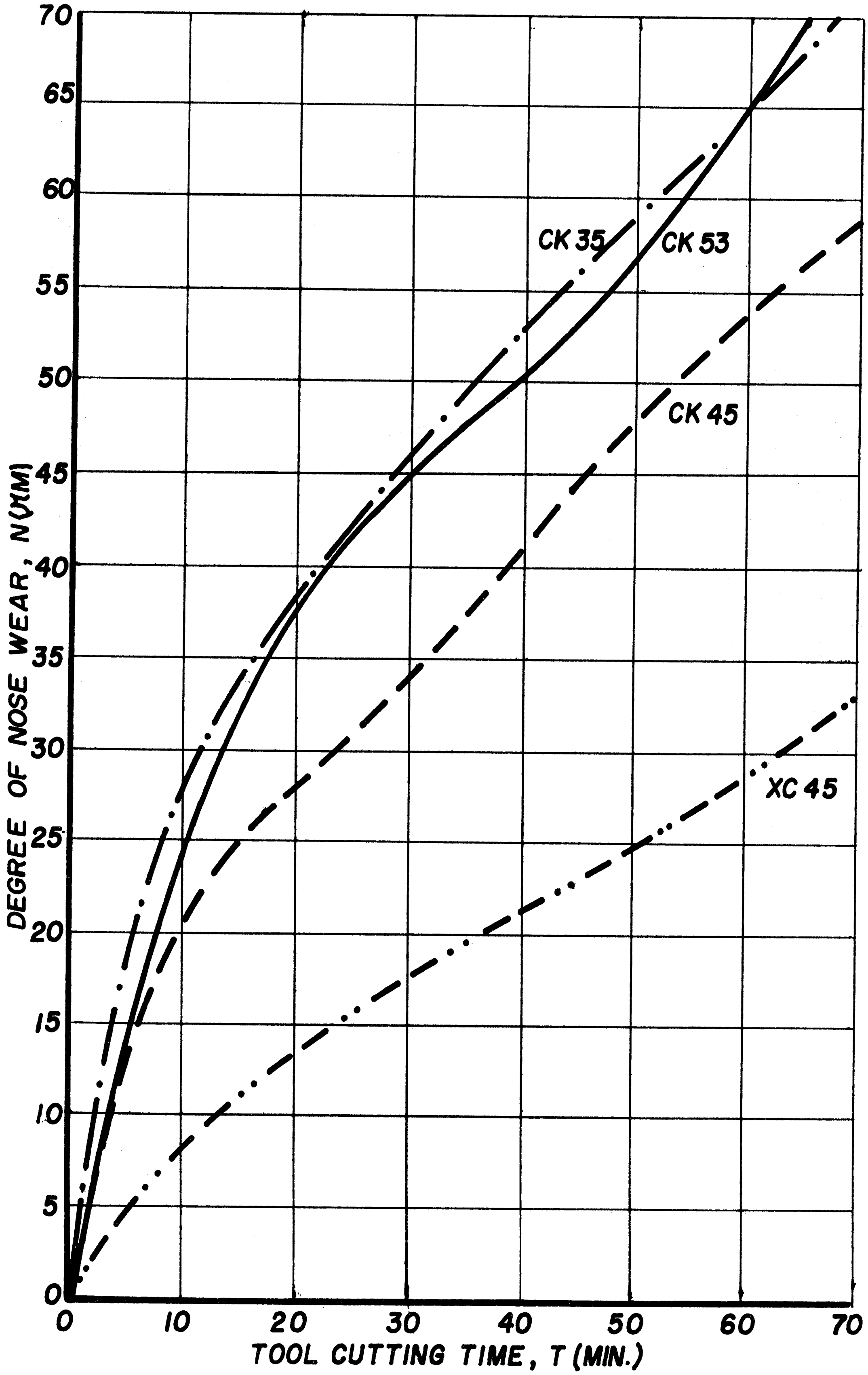

DEGREE OF NOSE WEAR vs CUTTING TIME

FIG. NO. 4-6

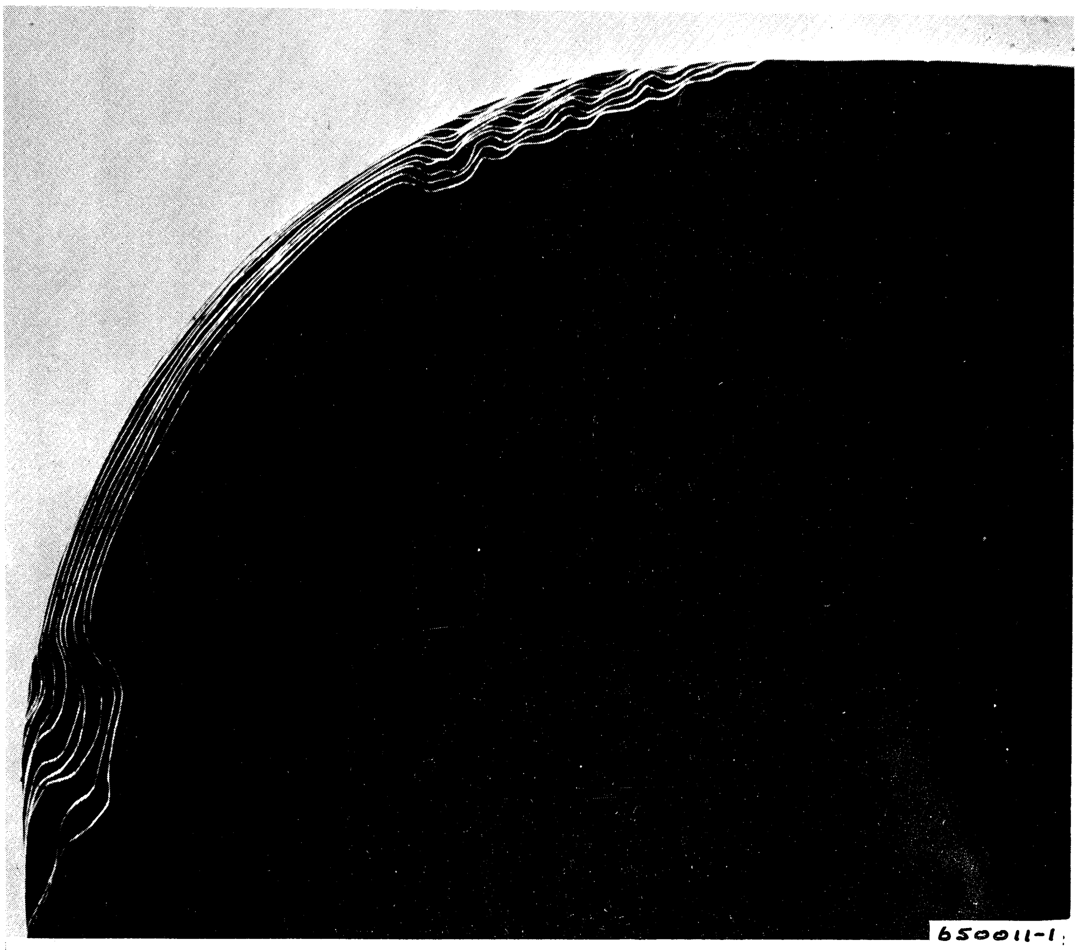

125 X MAGNIFICATION

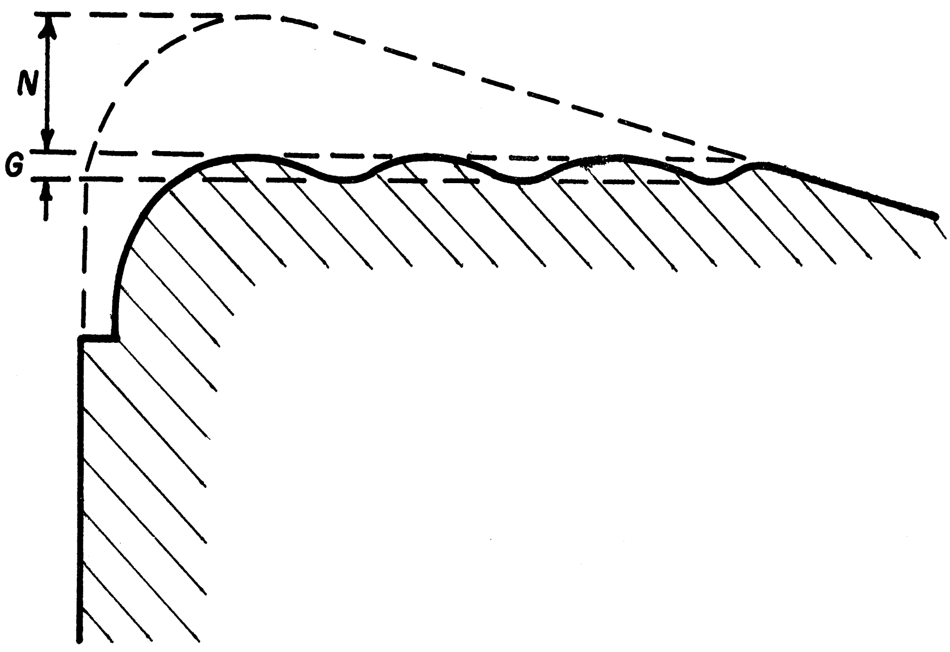

PHOTOGRAPH & SCHEMATIC OF TOOL WEAR IN FINISH MACHINING

FIG. NO. 4-7

PART V

PLASTICITY STUDY OF XC45 WORK MATERIAL (1045 STEEL)

The following is a translation and condensed summary of a report submitted by Professor Olov Svahn of Chalmers University in Goteborg, Sweden. It presents the results of an initial study of the plasticity of the XC45 work material used for Phase 1 of the CIRP/OECD program on tool wear.

No attempt has been made to correlate the results with other program data because of the lack of similar results for subsequent phases. The experimental analysis consisted of conventional tension and compression tests carried out at relatively low strain rates. Further studies at high strain rates are contemplated for later phases of the program. The following condensation is intended to document the methods and essential results for Phase 1. Results are presented only for heat No. Z0648 but it was indicated that those for heat No. Z0656 are "in acceptable agreement."

PROCEDURE AND METHOD OF ANALYSIS

The purpose of the tests was to determine true stresses and strains in the case of tensile tests and compression tests. The samples were taken from the material according to Fig. 5-1. Fifteen samples each were used for the tensile and compression tests. Dimensions of both types of specimens are shown in Fig. 5-2.

Tension (Procedure)

The tensile tests were performed in an Amelor test machine at a head speed which resulted in a strain rate of less than 0.01 per sec. All tensile samples were photographed for determination of area and waist radius as shown in Fig. 5-3. Calculations were done according to Bridgeman's method, which considers the three-dimensional state of stress at the "necked-in" area. Bridgeman's equation is

$$\sigma = \frac{P}{A} \times \frac{1}{\left(1 + \frac{2r}{a}\right) \ln \left(1 + \frac{a}{2r}\right)} \qquad \text{(V-1)}$$

where:

$$\left.\begin{array}{l} \sigma = \text{true stress} = \frac{P}{A} \times \frac{1}{K} \\ P = \text{load} \\ A = \text{effective area} \\ r = \text{neck radius} \\ a = \text{radius of sample} \\ K = \text{Bridgeman's correction factor} \end{array}\right\}$$

See Fig. 5-3 for details

Compression (Procedure)

The compression tests were performed in a Fjellman hydraulic press. Press velocity was approximately 0.1 mm/sec corresponding to a strain rate of 0.005 per sec. The compression samples were centerless ground to diameters of 9.00 ± 0.01 mm and the height H was 18.00 ± 0.01 mm. To reduce friction the end surfaces were lubricated with Molykote "Spray-Rapid." The load and displacement were continuously recorded by Offener recorders. The load transducer was calibrated on the machine. It consisted of a cylinder with 16 strain gauges attached to it. The sideplacement was given by a potentiometer. Similar instrumentation was used for the tensile tests. Some scatter of data could be expected because of the instrumentation but this was minimized by calibrating it in the testing machines.

Tension (Error Calculation)

<u>Probable Errors in Original Data</u>:

Load:	ΔP	=	± 5 kp
Diameter:	Δa	=	± 0.01 mm
Correction factor:	ΔK	=	± 0.002

The above relate to the following equation which is derived from Equation (V-1).

$$k_t = \frac{P}{\pi a^2} \times \frac{1}{K} \qquad \text{(V-2)}$$

Substitution of the probable errors into Equation (V-3) yields the probable error in the resulting stress.

$$\frac{\Delta k_t}{k_t} = \left|\frac{\Delta P}{P}\right| + \left|-\frac{2\Delta a}{a}\right| + \left|-\frac{\Delta k}{K}\right| \qquad \text{(V-3)}$$

For example, when

$$k_t = 100.2 \text{ kp/mm}^2$$
$$P = 1150 \text{ kp}$$

$$K = 1.077$$
$$2a = 3.69 \text{ mm}$$

Substitution in Equation (V-3) yields

$$\Delta k_t = 100.2 \left[\frac{5}{1150} + \frac{2 \times 0.02}{3.69} + \frac{0.002}{1.077}\right]$$

$$\Delta k_t = 1.188 \text{ kp/mm}^2 \quad 1.5 \text{ kp/mm}^2$$

Consequently the probable error in stress is less than 1.5 kilograms per square millimeter (2130 psi) or about 1.5%.

Compression (Error Calculation)

Probable Errors in Measurements:

Diameter:	Δd	=	$\pm$ 0.01 mm
Height:	Δh	=	$\pm$ 0.01 mm
Load:	ΔP	=	$\pm$ 100 kp
	(ΔP	=	$\pm$ 100 obtained because of errors in reading)

The corresponding calculations are as follows:

$$k_c = \frac{P}{A} = \frac{P}{V} \cdot h_m \qquad \text{(V-4)}$$

where:

$$A = \frac{\pi d^2}{4}$$

h_m = specimen height at the load under consideration

$$\frac{\Delta k_c}{k_c} = \left|\frac{\Delta P}{P}\right| + \left|\frac{2\Delta d}{d}\right| + \left|-\frac{\Delta h}{h}\right| \qquad \text{(V-5)}$$

for

$$k_c = 44.7 \text{ kp/mm}^2$$
$$P = 2884 \text{ kp}$$
$$d = 9 \text{ mm}$$
$$h = 18 \text{ mm}$$

Substitution yields:

$$\Delta k_c = 44.7 \left[\frac{100}{2884} + \frac{2 \times 0.01}{9} + \frac{0.01}{18}\right]$$

$$\Delta k_c = 1.68 \text{ kp/mm}^2$$

which gives a probable error of less than 2.0 kilograms per square millimeter (2840 psi) or about 4.5%.

TEST RESULTS

Sample test data are recorded in Tables 5-1 and 5-2 for tension and compression, respectively. Data points and average lines are shown for all tests on heat No. Z0648 in Fig. 5-4. From the tension results one could conclude that:

1. The material in the center zone 1 is harder than the rest.
2. Zones 2, 3, and 4 correspond fairly well.
3. Zone 4 has the least scatter while zone 3 has the largest scatter. This is probably due to the history of the material.
4. The curves have approximately the same slope and are parallel.

The compression test curves correlate well with the tensile curves considering that end friction was not taken into account. A comparison of similar data from heat No. Z0656 shows the tensile results to be in acceptable agreement but the compressive results for Z0656 are higher although the slope is the same as for Z0648. The higher value for Z0656 was thought to be due to different specimen dimensions.

No attempt has been made to interpret the results of this plasticity study in relation to tool wear because only one work material has been studied thus far and there have not been any significant differences in tool wear characteristics between the two heats of XC45 steel. Subsequent tool wear studies with different compositions and microstructures and plasticity studies at high strain rates will provide a more substantial body of information in which to search for fundamental correlation. These results will be analyzed and added to the larger body of information.

TABLE 5-1

TYPICAL TENSILE TEST DATA

Material: XC45 (steel)
Heat No.: Z0648
Sample: 1

For nomenclature see Fig. 5-3

Load kp, kg	2a Neck Diameter, mm	r Neck Radius, mm	Stress, kp/mm^2	Strain
0	4.90		0	0.000
1000	4.87		53.6	0.006
1100	4.85		59.5	0.022
1200	4.79		66.5	0.045
1300	4.74		73.7	0.069
1355	4.63	21.5	78.3	0.114
1350	4.47	16.2	83.1	0.183
1355	4.41	13.5	85.3	0.191
1340	4.33	10.8	86.6	0.244
1325	4.25	9.7	88.5	0.284
1300	4.09	7.5	93.6	0.360
1275	3.93	7.0	98.3	0.440
1245	3.88	6.5	98.4	0.470
1220	3.82	5.4	98.1	0.496
1190	3.72	4.3	99.5	0.552

TABLE 5-2

TYPICAL COMPRESSION TEST DATA

Material: XC45 (steel)
Heat No.: Z0648
Dimensions on test pieces:
Diameter: 9.00 ± 0.01 mm
Height: 18.00 ± 0.01 mm

Volume: 1145 ± 3 mm^3
Strain Rate: 0.005 s^{-1}

Instantaneous Height, mm	Load kp, kg	$k_c = P/A$, kp/mm^2	Strain
	Test 1:1		
18.00	0	0	0.0000
17.75	2961	46.9	0.0139
17.50	34.6	5212	0.0296
17.25	4239	64.6	0.0422
17.00	4858	72.0	0.0574
16.50	5610	81.0	0.0871
16.00	6263	87.5	0.1178
15.00	7174	94.0	0.1824
14.00	8085	98.8	0.2516
13.00	9072	102.9	0.3258
12.00	10211	107.0	0.4056
11.00	11463	110.1	0.4926
10.00	12906	112.6	0.5880
9.00	14614	114.8	0.6935
	Test 1:2		
18.00	0	0	0.0000
17.75	2847	44.1	0.0139
17.50	3340	51.0	0.0296
17.25	4137	62.4	0.0422
17.00	4745	70.4	0.0574
16.50	5618	81.0	0.0871
16.00	6149	85.9	0.1178
15.00	7136	93.5	0.1824
14.00	7971	97.4	0.2516
13.00	8996	102.0	0.3258
12.00	10097	105.8	0.4056
11.00	11312	108.6	0.4926
10.00	12716	111.0	0.5880
9.00	14462	113.6	0.6935

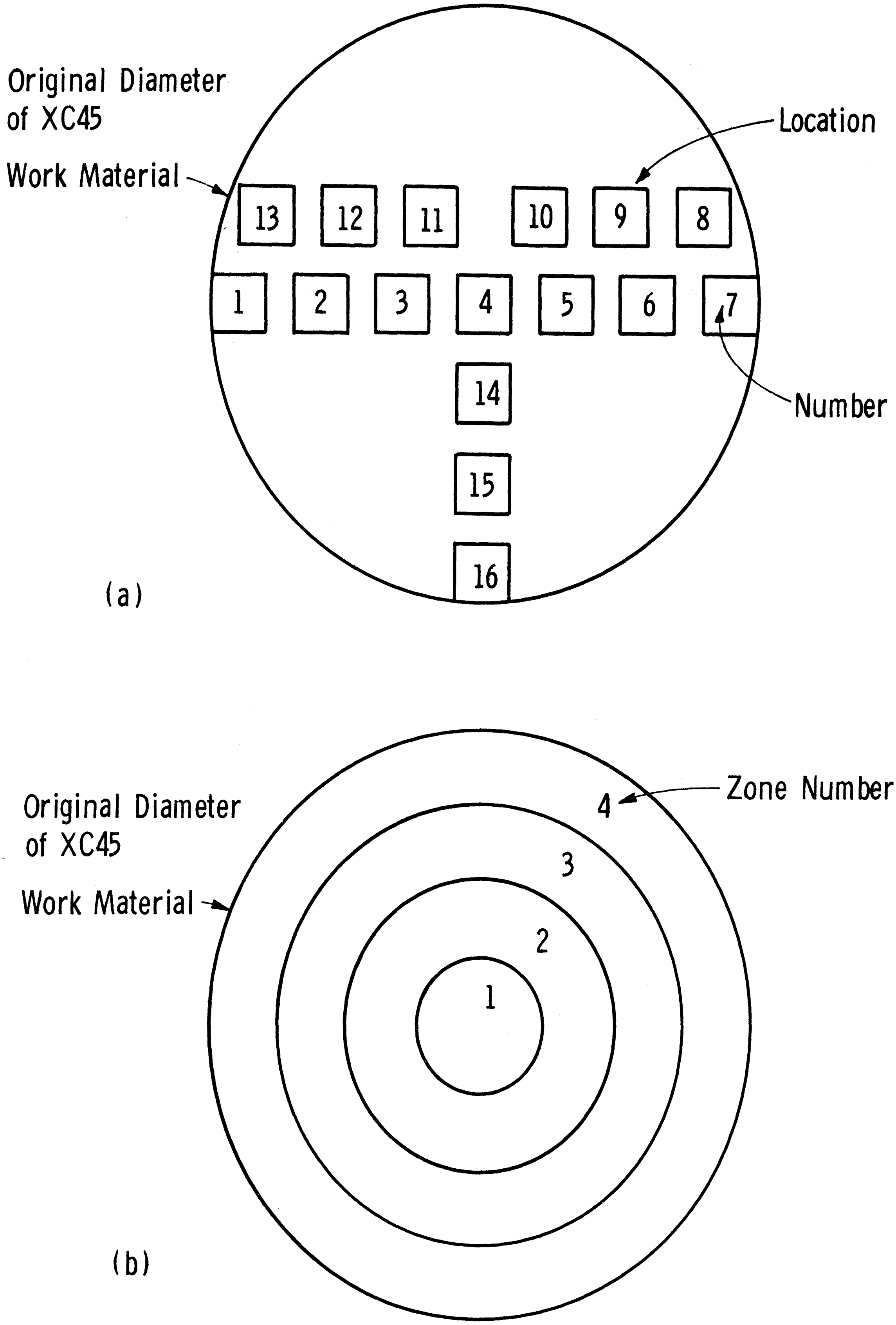

Fig. 5-1. Location of both compression and tension specimens by test number is shown in (a). Zone number is shown at (b).

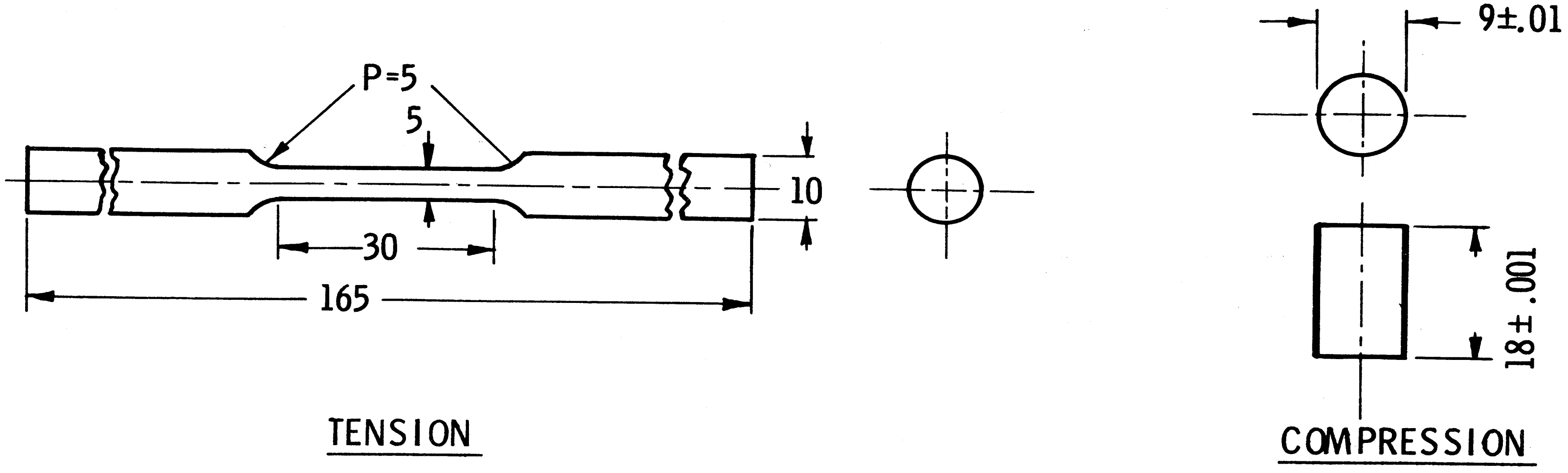

Fig. 5-2. Dimensions of test specimens. All sizes are given in mm (millimeters).

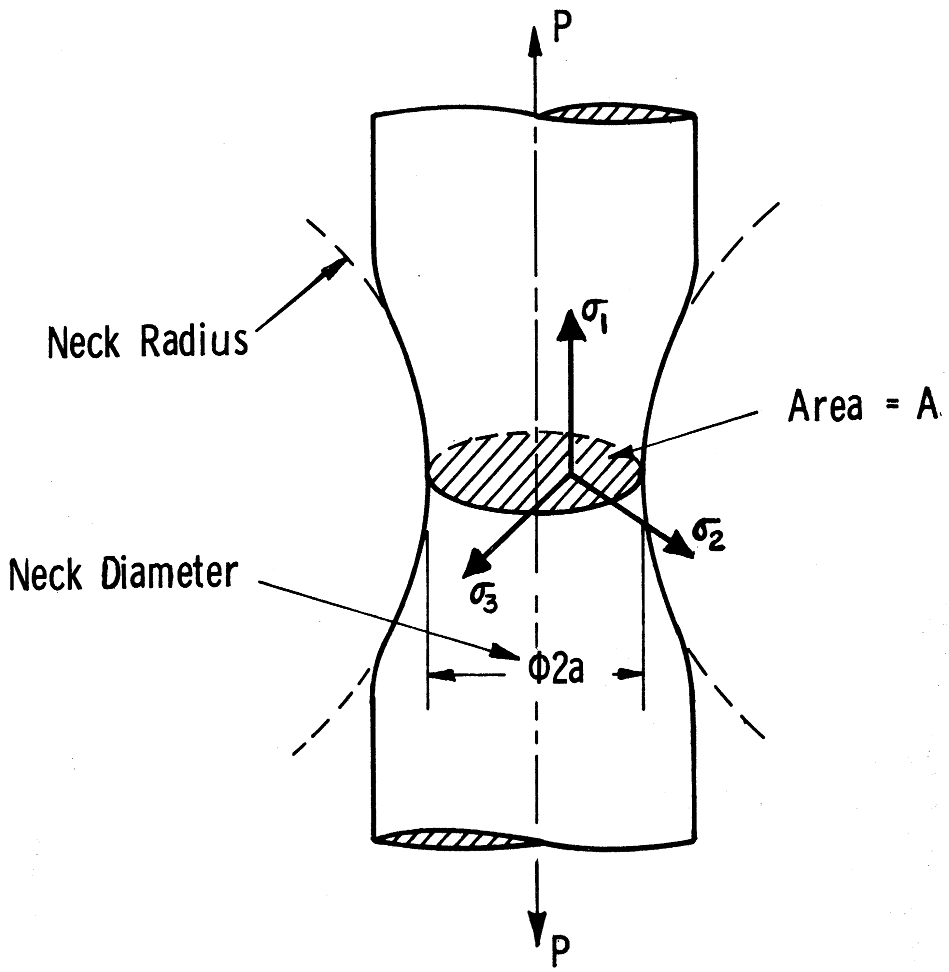

Fig. 5-3. Dimensions of strained tensile specimen.

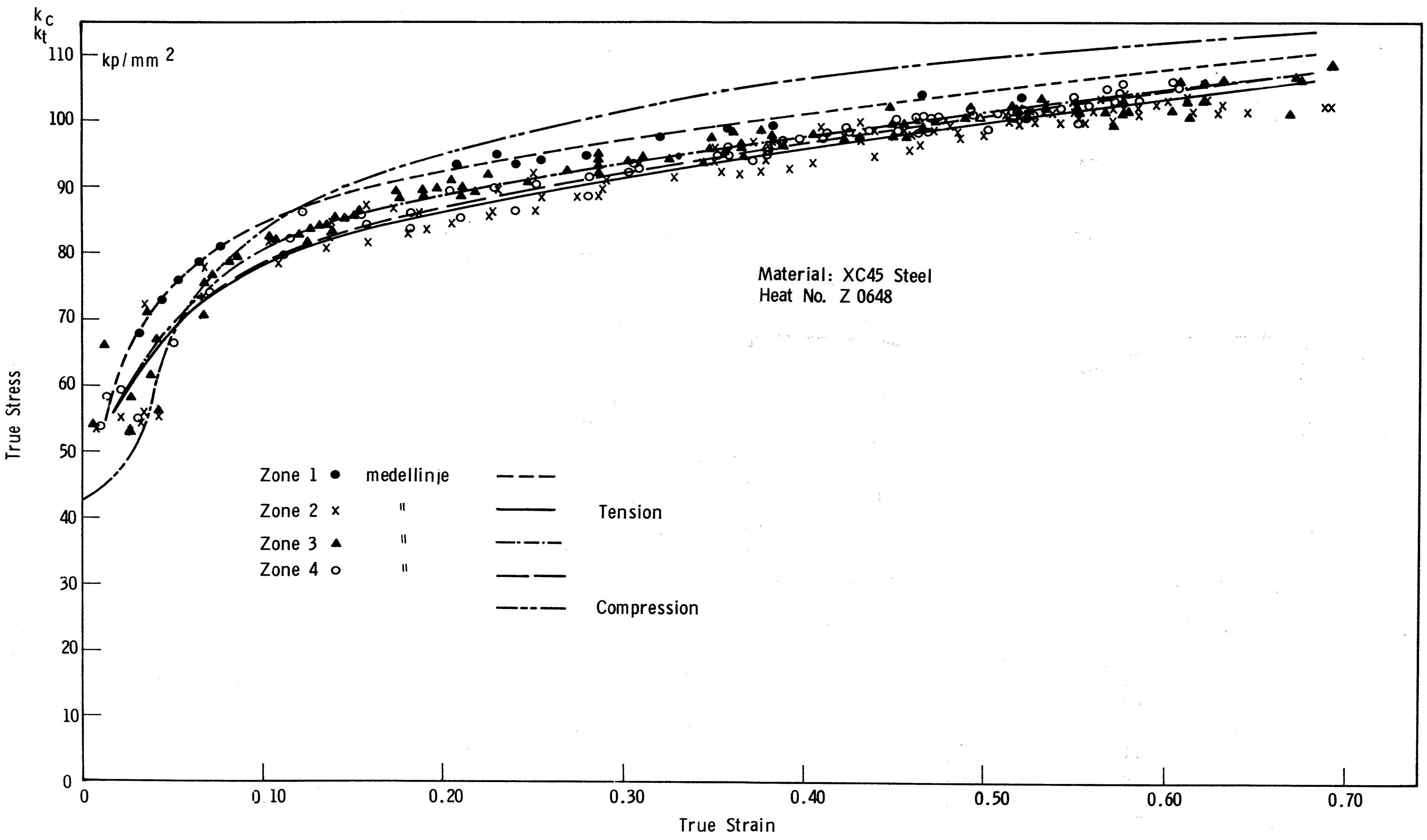

Fig. 5-4. True stress vs. true strain.

DISTRIBUTION LIST

(One copy unless otherwise noted)

AFML (MATF, F. L. Whitney) 6
WPAFB, Ohio 45433

Defense Documentation Center 20
Cameron Station
Alexandria, Virginia 22314

AFML (MAA, Mr. J. Teres)
WPAFB, Ohio 45433

AFML (MAAE)
WPAFB, Ohio 45433

AFML (MAAM, Librarian)
WPAFB, Ohio 45433

AFML (MAX, Dr. Lovelace)
WPAFB, Ohio 45433

Hq., USAF (AFSPPI, Mr. Joe Joers)
Washington, D.C. 20330

SEG (RTD)
SEPIE
WPAFB, Ohio 45433

SEG (RTD)
SEPIR
WPAFB, Ohio 45433

FTD (TDEWP)
WPAFB, Ohio 45433

Commander
Army Research Office
Arlington Hall Station
Arlington, Virginia 22210

U. S. Army Production Equipment Agency
Rock Island Arsenal
Rock Island, Illinois
Attn: Manufacturing Technology Division,
AMXPE-MT

Army Materials Research Agency
Watertown 72, Massachusetts
Attn: S. V. Arnold

Chief, Bureau of Naval Weapons
Department of the Navy
Industrial Division
Washington, D.C. 20013
Attn: Industrial Readiness Branch
(PID-2)

U. S. Naval Research Laboratory
Washington, D.C. 20390
Attn: Code 6383

Defense Metals Information Center
Battelle Memorial Institute
505 King Avenue
Columbus, Ohio 43201
Attn: Library

Scientific & Technical Information
Facility
P. O. Box 5700
Bethesda, Maryland 20014
Attn: Technical Library,
RQT-16448

National Academy of Sciences
National Research Council
Materials Advisory Board
2101 Constitution Avenue, N.W.
Washington, D.C. 20418

Adamas Carbide Corporation
Market & Passaic Streets
Kenilworth, New Jersey
Attn: A. J. Fisher, Director
Research and Engineering

Aerojet-General Corporation
P. O. Box 296
Azusa, California
Attn: K. F. Mundt
Vice President of Manufacturing

AiResearch Manufacturing Company
9851 Sepulveda Boulevard
Los Angeles, California 90009
Attn: Technical Library

Alfred University
College of Ceramics
Alfred, New York
Attn: Dr. Philip H. Crayton

Allegheny Ludlum Steel Corporation
Research Center
Breckenridge, Pennsylvania
Attn: P. R. Borneman
Chief Research Metallurgist

Commander
Watervliet Arsenal
Watervliet, New York
Attn: Mr. George Hohenstein
Production Methods

AVCO Corporation
Lycoming Division
Main Street
Stratford, Connecticut
Attn: Superintendent
Manufacturing and Engineering

Battelle Memorial Institute
505 King Avenue
Columbus, Ohio 43201
Attn: Mr. Francis W. Boulger, Chief
Metalworking Research Division

Bell Aircraft Corporation
Niagara Falls Airport
Buffalo 5, New York
Attn: R. W. Varrial, Manager
Product Engineering

Bendix Corporation
Research Laboratories Division
Southfield, Michigan
Attn: Ronald M. Centner

The Boeing Company, Headquarters
P. O. Box 3707
Seattle 24, Washington
Attn: B. K. Bucey, Director
Research and Development

The Boeing Company, Headquarters
P. O. Box 3707
Seattle 24, Washington
Attn: L. Pickerell, Manager

Carborundum Company
P. O. Box 337
Niagara Falls, New York
Attn: Dr. E. Dow Whitney

Carnegie Institute of Technology
Pittsburgh 13, Pennsylvania
Attn: Dr. M. C. Shaw, Head
Department of Mechanical
Engineering

Chicago Latrobe
411 W. Ontario Avenue
Chicago 10, Illinois
Attn: D. J. Kallio, Chief Engineer

Cincinnati Milling & Grinding Machines
4701 Marburg Avenue
Cincinnati, Ohio 45209
Attn: Dr. M. Eugene Merchant

Cincinnati Milling & Grinding Machines
4701 Marburg Avenue
Cincinnati, Ohio 45209
Attn: Gerald W. Long
Production Development Department

Cincinnati Milling & Grinding Machines
4701 Marburg Avenue
Cincinnati, Ohio 45209
Attn: Dr. Richard L. Kegg
Physical Research Department

Cleveland Twist Drill Company
1242 E. 49th Street
Cleveland 14, Ohio
Attn: D. D. Burdett, Vice President
Manufacturing and Engineering

Cleveland Twist Drill Company
1242 E. 49th Street
Cleveland 14, Ohio
Attn: R. D. Lesher, Research Engineer
Research Laboratory Dept. 106

Crucible Steel Company of America
P. O. Box 7257
Pittsburgh 13, Pennsylvania
Attn: E. J. Dulia, Manager
Product Research

Curtiss-Wright Corporation
Metals Process Division
P. O. Box 13
Buffalo, New York
Attn: R. A. Kaprelian, General Manager

Douglas Aircraft Company, Inc.
3855 Lakewood Boulevard
Long Beach 8, California
Attn: O. L. Rumble, Tooling Manager

Douglas Aircraft Company, Inc.
3855 Lakewood Boulevard
Long Beach 8, California
Attn: J. S. Sempres
Production Development Manager

Firth Sterling, Inc.
Carbide Division
3115 Forbes Avenue
Pittsburgh, Pennsylvania
Attn: T. G. Barnes, Vice President

Fairchild Stratos Corporation
Aircraft and Missiles Division
Hagerstown 10, Maryland
Attn: L. B. Carroll, Manager
Tool Manufacturing and Design

Fairchild Stratos Corporation
Aircraft and Missiles Division
Hagerstown 10, Maryland
Attn: A. D. Jairett, Manager
Tool Engineering and Manufacturing

Firth Loach Metals, Inc.
Buttermilk Hollow Road
McKeesport, Pennsylvania
Attn: W. J. Loren, President

Ford Motor Company
20000 Rotunda Drive
Dearborn, Michigan
Attn: Dr. V. F. Zackay, Director
Research and Engineering Center

Ford Motor Company
20000 Rotunda Drive
Dearborn, Michigan
Attn: Dr. M. Huminik
Research and Engineering Center

Ford Motor Company
20000 Rotunda Drive
Dearborn, Michigan
Attn: Scientific Laboratory
Ceramics and Glass Department

General Dynamics/Astronautics
San Diego 12, California
Attn: D. Weisinger

General Dynamics/Ft. Worth
Grants Lane
Ft. Worth, Texas
Attn: F. A. Fuhrer, Chief
Manufacturing Engineering

General Electric Company
Large Jet Engine Department
Cincinnati, Ohio 45215
Attn: Guy Bellows, Manager
Manufacturing Engineering Research Laboratory

General Electric Company
1 River Road
Schenectady 5, New York
Attn: Dr. W. W. Gilbert, Manager
Machine Division

General Motors Corporation
General Motors Technology Center
Detroit, Michigan
Attn: H. D. Hall, Director
Manufacturing Development

Goodyear Aerospace Corporation
Tool Research and Development
Akron 15, Ohio
Attn: R. J. Moldovon

Greenfield Tap & Die Company
Sanderson Street
Greenfield, Massachusetts
Attn: R. S. Harper
President and General Manager

Greenfield Tap & Die Company
Sanderson Street
Greenfield, Massachusetts
Attn: S. Sinclair, Director of Research
Engineering Department

Grumman Aircraft Engineering Corporation
Bethpage, L.I., New York
Attn: W. J. Hoffman, Vice President
Manufacturing Engineers

Grumman Aircraft Engineering Corporation
Bethpage, L.I., New York
Attn: Mrs. Sara T. Moxley, Director
Technical Info File, Pl. 12

Heald Machine Company
10 New Bond Street
Worcester 6, Massachusetts
Attn: Dr. R. S. Hahn
Research Engineer

Hughes Aircraft Company
Florence and Teals
Building 15, Mail Station H-155
Culver City, California
Attn: W. W. Lampkin
Vice President of Manufacturing

IIT Research Institute
10 W. 35th Street
Chicago, Illinois 60616
Attn: F. C. Holtz, Senior Metallurgist
Metallurgical Engineering

Kennametal, Inc.
700 Lloyd Avenue
Latrobe, Pennsylvania
Attn: W. L. Kennecott, Vice President

Kearney & Trecker Corporation
11000 Theodore Trecker Way
Milwaukee, Wisconsin
Attn: W. C. Beverung
Assistant Sales Manager

Landis Tool Company
Waynesboro, Pennsylvania
Attn: H. E. Balsiger, Chief Engineer

Latrobe Steel Company
Latrobe, Pennsylvania
Attn: C. R. Wendell, Manager
Metallurgical Services and
Tool Steels

LTV-Vought Aeronautics Division
P. O. Box 5907
Dallas, Texas 75222
Attn: W. W. Wood

Lockheed Aircraft Corporation
California Division
2555 N. Hollywood Way
Burbank, California
Attn: Robert L. Vaughn

Lockheed Georgia Company
86 S. Cobb Drive
Marietta, Georgia
Attn: W. P. Frech
Manufacturing Engineering

The Marquardt Corporation
16555 Saticoy Street
Van Nuys, California
Attn: Director of Manufacturing

The Martin Company
Baltimore 3, Maryland
Attn: Chief Librarian
Engineering Library

Naval Ordnance Test Station
China Lake, California
Attn: Dr. B. Langenecker

DISTRIBUTION LIST (Continued)

Professor Walter Backofen
Department of Metallurgy
Massachusetts Institute of Technology
77 Massachusetts Avenue
Cambridge, Massachusetts

Professor Nathan H. Cook
Room 35-132
Massachusetts Institute of Technology
77 Massachusetts Avenue
Cambridge, Massachusetts

McDonnell Aircraft Corporation
P. O. Box 516
St. Louis 66, Missouri
Attn: A. F. Hartwig
Chief Industrial Engineer

McDonnell Aircraft Corporation
P. O. Box 516
St. Louis 66, Missouri
Attn: Central Files Department 110

Metcut Research Associates, Inc.
3980 Rosslyn Drive
Cincinnati, Ohio 45209
Attn: Dr. Michael Field, President

Mr. Leslie L. Gould, Staff Metallurgist
Materials Advisory Board
National Academy of Sciences
2101 Constitution Avenue, N.W.
Washington, D.C. 20418

National Science Foundation
Office of International Science Activities
Washington, D.C. 20550
Attn: Dr. Philip W. Hemily, Deputy Head

National Science Foundation
Office of International Science Activities
Washington, D.C. 20550
Attn: Mr. Ray W. Mayhew, Head
International Organizations Staff

National Science Foundation
Office of International Science Activities
Washington, D.C. 20550
Attn: Mr. Paul A. Roessler, Staff Associate
International Organizations Staff

National Twist Drill Company
6841 N. Rochester Road
Rochester, Michigan
Attn: C. J. Oxford, Director of Research

Department of the Navy
Bureau of Naval Weapons
Material Division
Washington 25, D.C.
Attn: Thomas F. Kearnes

North American Aviation, Inc.
Rocketdyne Division
6633 Canoga Avenue
Canoga Park, California
Attn: Joe Foreman

North American Aviation, Inc.
Rocketdyne Division
6633 Canoga Avenue
Canoga Park, California
Attn: E. C. Haynie, D/520

North American Aviation, Inc.
Space and Information Systems Division
12214 Lakewood Boulevard
Downey, California
Attn: L. E. Gatzek, D/098

Northrop Corporation
Norair Division
1001 W. Broadway
Hawthorne, California
Attn: V. L. Boland

Northrop Corporation
Norair Division
1001 E. Broadway
Hawthorne, California
Attn: R. R. Nolan

Pennsylvania State University
207 Old Main Building
University Park, Pennsylvania
Attn: Professor A. O. Schmidt
Industrial Engineering

Pratt & Whitney Aircraft Company, Inc.
East Hartford 8, Connecticut
Attn: R. A. Foisie, Product Engineering

Pratt & Whitney Aircraft Company, Inc.
East Hartford 8, Connecticut
Attn: R. Stoner, Supervisor
Methods Development Section

Purdue University
Lafayette, Indiana
Attn: Professor O. D. Lascoe
Industrial Engineering

Republic Aviation Corporation
Farmingdale, L.I., New York
Attn: A. Kastelowitz
Director of Manufacturing Research

Rohr Aircraft Corporation
P. O. Box 878
Chula Vista, California
Attn: B. F. Raynes
Executive Vice President

Ryan Aeronautical Company
3701 Harbor Drive
San Diego 12, California
Attn: J. P. Orr

Sandia Corporation
Sandia Base
Alburquerque, New Mexico
Attn: E. P. Quigley, Supervisor
Manufacturing Processes
Development Division 2565

Society of Carbide Engineers
718 Finley Road
Lombard, Illinois
Attn: William Pelger

Solar Aircraft Company
Facilities Division
San Diego 12, California
Attn: J. A. Logan, Manager

Mr. K. W. Stalker
Lake Layetteville Road
Springdale, Arkansas 72764

Thompson-Ramo-Wooldridge, Inc.
23555 Euclid Avenue
Cleveland 17, Ohio
Attn: E. J. Hayes

Tungsten Alloy Manufacturing Company
65-67 Colden Street
Newark, New Jersey

Union Twist Drill Company
Research and Development Department
Monroe Street
Athol, Massachusetts

United Aircraft Corporation
400 Main Street
E. Hartford 8, Connecticut

Sikorsky Aircraft Division
United Aircraft Corporation
N. Main Street
Stratford, Connecticut
Attn: W. S. Nochisaki

Sikorsky Aircraft Division
United Aircraft Corporation
N. Main Street
Stratford, Connecticut
Attn: A. Sperber

United Greenfield Corporation
411 W. Ontario
Chicago 11, Illinois
Attn: Woodrow Tichy, Vice President

University of California
Los Angeles, California
Attn: Professor M. A. Simon

University of California
Los Angeles, California
Attn: Reno Cole

University of California
Bancroft Way
Berkeley 8, California
Attn: Professor E. G. Thomsen
Industrial Engineering

University of Cincinnati
Cincinnati, Ohio
Attn: Professor L. Doty
Mathematics Department

DISTRIBUTION LIST (Continued)

University of Cincinnati
Cincinnati, Ohio
Attn: Professor Hans Ernst

University of Cincinnati
Cincinnati, Ohio
Attn: Dr. J. R. Lemon
Engineering College

University of Cincinnati
Cincinnati, Ohio
Attn: Dr. I. Morse
Engineering College

University of Cincinnati
Cincinnati, Ohio
Attn: Dr. Frank Tse

University of Dayton
Research Institute
Dayton, Ohio 45409
Attn: G. J. Roth

University of Denver
Denver Research Institute
Denver 10, Colorado
Attn: Robert Venuti
Research Metallurgist

University of Illinois
Department of Mechanical Engineering
Urbana, Illinois
Attn: Professor K. J. Trigger

University of Illinois
Department of Mechanical Engineering
Urbana, Illinois
Attn: Dr. B. F. Von Turkovich

University of Wisconsin
Madison, Wisconsin
Attn: Professor J. C. Bollinger

Valeron Corporation
Valenite Metals Division
31100 Stephenson Highway
Madison Heights, Michigan

Dr. L. C. Hamaker
Vice President of Technology
Vanadium-Alloys Steel Company
Latrobe, Pennsylvania

Vascoloy-Ramet Corporation
800 Market Street
Waukegan, Illinois
Attn: Dr. F. H. Driggs

Vitro Corporation of America
Chemistry and Arc Department
200 Pleasant Valley Way
West Orange, New Jersey
Attn: Dr. Stanley Grand

Wendt-Sonis Company
10th and Collier Streets
Hannibal, Missouri
Attn: T. V. Hilt, General Manager

Weldon Tool Company
3000 Woodhill Road
Cleveland 14, Ohio
Attn: W. C. Bergstrom

Westinghouse Electric Corporation
Aviation Gas Turbine Division
Kansas City, Missouri
Attn: D. C. Goldberg
Manager of Metallurgy

Westinghouse Electric Ccrporation
Aviation Gas Turbine Division
Kansas City, Missouri
Attn: E. C. Sedlack
Manager of Manufacturing

Professor S. A. Tobias
Mechanical Engineering Department
The University of Edgbaston
Birmingham 15, England

Professor-Dr.-Ing. F. Eisele
Institut fur Werkzeugmaschinen
und Betriebswiessnschaften
Technische Hochschule Muenchen
Muenchen 2
Arcisstrasse 21, Germany

Professor-Dr.-Ing. H. Optiz
Laboratorium fur Werkzeugmaschinen
und Betriebslehre
Technische Hochshule Aachen
Aachen
Wuellnerstrasse, Germany

Adamas Carbide Corporation
Kenilworth, New Jersey 07033
Attn: E. L. Dreyer, President

Carmet Company
1515 Jarvis Avenue
Ferndale, Michigan 48220
Attn: C. H. Toensing, Director
Technical Services

VR/Wesson Company
800 Market Street
Waukegan, Illinois 60086
Attn: R. L. Brogan, Vice President

Newcomer Products, Inc.
P.O. Box 272
Latrobe, Pennsylvania 15650
Attn: J. Kozusko

Vermont American Corporation
500 East Main Street
Louisville 2, Kentucky
Attn: John D. Knox, Manager
Multi Metals Division

Metal Carbides Corporation
6001 Southern Boulevard
Youngstown, Ohio 44512
Attn: R. T. Beeghly

Sandvik Steel, Inc.
1702 Nevins Road
Fair Lawn, New Jersey
Attn: D. P. Cameron